

UCLA

UCLA Electronic Theses and Dissertations

Title

Ligand Substituent Effects on Redox-Switchable Polymerization Catalysts

Permalink

<https://escholarship.org/uc/item/3476j2wn>

Author

Alexander, Laughlin

Publication Date

2018

Peer reviewed|Thesis/dissertation

UNIVERSITY OF CALIFORNIA

Los Angeles

Ligand Substituent Effects on Redox-Switchable Polymerization Catalysts

A thesis submitted in partial satisfaction
of the requirements for the degree Master of Science in chemistry

By

Alexander Lewis Laughlin

2018

© Copyright by

Alexander Lewis Laughlin

2018

ABSTRACT OF THE THESIS

Ligand Substituent Effects on Redox-Switchable Polymerization Catalysts

By

Alexander Lewis Laughlin

Master of Science in Chemistry

University of California, Los Angeles, 2018

Professor Paula Loredana Diaconescu, Chair

Plastic pollution necessitates the need for new sustainable polymer technologies. Such materials are accessible via the construction of biobased materials and biodegradable microstructural engineering. Such motifs can be rationally synthesized via redox-switchable catalysis, which exhibits orthogonal reactivity towards various monomers. In this vein, this work aims to ascertain ligand substitution as a modality of control over the orthogonal reactivity. By investigating a set of substituents on a phosphine ligand scaffold with varied electron-donating and electron-withdrawing effects, an investigation into the electronic properties of such catalysts is undertaken. Synthesis and characterization of one variant of the yttrium complexes of interest is presented, as well as its reactivity in ring-opening polymerizations. These findings are compared to previous work with another yttrium analogue. Essentially, no ligand substitution effect was found, but reactivity toward an additional orthogonal monomer was discovered.

The thesis of Alexander Lewis Laughlin is approved.

Richard B. Kaner

Hosea Martin Nelson

Paula Loredana Diaconescu, Committee Chair

University of California, Los Angeles

2018

TABLE OF CONTENTS

Abstract	ii
List of Figures, Tables, Charts, and Schemes	v
Nomenclature	viii
Acknowledgements	ix
Chapter 1. Introduction	1
Chapter 2. Research Methods and Results	26
2 A. Syntheses of Catalysts	29
2 B. Redox Stability of 3-YO'Bu	29
2 C. Depolymerization and Polymer Analysis	29
2 D. Solvent Effects	32
2 E. Polymerizations with 3-YO'Bu	33
2 F. Lewis Acidity	36
2 G. Alkoxide Ligand	38
Chapter 3. Experimental	39
2 A. Synthesis of 1,1'-diazidoferrocene (A)	39
2 B. Synthesis of 2-(<i>tert</i> -butyl)-6-(diphenylphosphaneyl)-4-methoxyphenol (B)	41
2 C. Synthesis of 2-(<i>tert</i> -butyl)-6-(diphenylphosphaneyl)-4-fluorophenol	42
2 D. Synthesis of 3-YOtBu	43
2 E. Redox Stability	45
2 F. Polymerizations with 3-YO'Bu	45
Appendix	46
References	83

LIST OF FIGURES, EQUATIONS, TABLES, CHARTS, AND SCHEMES

Scheme 1-1 : PLA-based plastic paradigm _____	3
Figure 1-1: Examples of polymer tacticity _____	5
Equation 1-2: Number average molecular weight (M_n), where N_i is the number of molecules with mass M_i _____	5
Equation 1-2: Weight average molecular weight (M_w), where N_i is the number of molecules with mass M_i _____	6
Equation 1-3: Polydispersity index (PDI) _____	6
Scheme 1-2: Mechanism of Ziegler-Natta catalysis, converting ethylene into polyethylene _____	8
Figure 1-2: Most common PLA polymerization catalysts _____	8
Scheme 1-3: Mechanism of Lewis acid catalyzed ROP _____	8
Table 1-1: Summary of PLA polymerizations with various catalysts _____	9
Table 1-2 Mechanical properties of various isomeric forms of PLA _____	10
Figure 1-3: PLA tacticities and microstructures _____	11
Scheme 1-5: Switchable polymerization catalysis switching between two active, orthogonal states _____	13
Scheme 1-6: Light-stimulated switchable polymerization catalysis _____	14
Scheme 1-7: Heat-stimulated switchable polymerization catalysis _____	15
Scheme 1-8: Pressure-stimulated switchable polymerization catalysis _____	16
Scheme 1-10: Allosteric modulation of polymerization catalysis _____	17
Scheme 1-11: Redox-switchable polymerization catalysis published by the Long group _____	18

Scheme 1-12: Redox-switchable polymerization catalysis published by the Diaconescu group _____	19
Figure 1-3: Synthesis of block copolymers via redox-switchable Catalysis _____	20
Figure 1-4: Lewis acidity spectrum, showing a switch domain. Selectivity can be achieved within a switch domain. Oxidation moves catalyst along spectrum to the right; reduction shifts catalyst to the left. _____	21
Figure 1-5: Lewis acidity spectrum showing two adjacent switch domains. This configuration permits orthogonal reactivity of monomers 1 and 2. _____	21
Scheme 1-13: Redox switching at the active metal center _____	22
Figure 1-5: Salfen proligand _____	23
Figure 1-6: Ligand substitutions of yttrium phosfen catalysts _____	24
Scheme 2-1: Synthesis of 1,1'-diazidoferrocene _____	27
Scheme 2-2: Synthesis of 2-(tert-butyl)-6-(diphenylphosphaneyl)-4-methoxyphenol _____	27
Scheme 2-3: Synthesis of 2-bromo-6-(tert-butyl)-4-fluorophenol _____	27
Scheme 2-4: Synthesis of 3-YO'Bu _____	28
Scheme 2-5: synthesis of 2-YO'Bu _____	28
Scheme 2-6: Intermolecular transesterification _____	30
Scheme 2-6: Intramolecular transesterification _____	30
Figure 2-1: Example of a monomodal GPC trace _____	32
Figure 2-2: Example of a monomodal GPC trace _____	32
Chart 2-1: Lactide polymerization in benzene _____	33

Chart 2-2: Lactide polymerization in benzene _____	33
Table 2-1: Polymerization assay _____	34
Table 2-1: Contrasting polymerization rates _____	35
Figure 3-1: 1-InOPh _____	37

NOMENCLATURE

δ	chemical shift
LA	<i>L</i> -lactide
BBL	β -butyrolactone
CL	ϵ -caprolactone
SO	styrene oxide
CHO	cyclohexene oxide
Et ₂ O	diethyl ether
Fc	mono-substituted ferrocenyl
ⁿ BuLi	<i>n</i> -butyllithium
DCM	dichloromethane
NMR	nuclear magnetic resonance
TBE	1,1,2,2-tetrabromoethane
THF	tetrahydrofuran
TMEDA	N,N,N',N'-tetramethylethylenediamine

ACKNOWLEDGMENTS

Without the endless support of my family, I could not have been afforded the opportunity to explore. Science, although one of the most important and noble pursuits of my life, nevertheless takes time and money – both of which I have not had to worry about. I have as good of parents as one can imagine.

Professor Diaconescu has gone to bat for me for the past four years. She not only provided a platform for me to make mistakes, but also attentive counsel and guidance, so that those mistakes would be parlayed into learning. She consistently encouraged me to become involved with seminars, conferences, and to become a part of the scientific community – read the literature, be weary of intuition, think like a scientist... I have an immense respect for her and her inspirational story.

Soohik (James) Rho and Dr. Jonathan Brosmer both worked with me directly in the laboratory. Jon taught me technique, while intermittently dancing to deep house electronic music; I am convinced that there is no one better to party with in the greater Los Angeles area. Not only did Jon insist on having a great time, but he worked smart and hard as well. He taught me an invaluable lesson about life balance. James and I have worked together on the same project, he tackled another variation of the yttrium phosphene catalyst. I taught him what I knew in the beginning, but he quickly became autonomous thereafter. He is smart, hardworking, and great to work with.

There are many people I have not mentioned in detail (Dr. Mark Abubekrov, Dr. Stephanie Quan, to name a few), but I thank all who have spent time with me in the Diaconescu group.

CHAPTER 1. INTRODUCTION

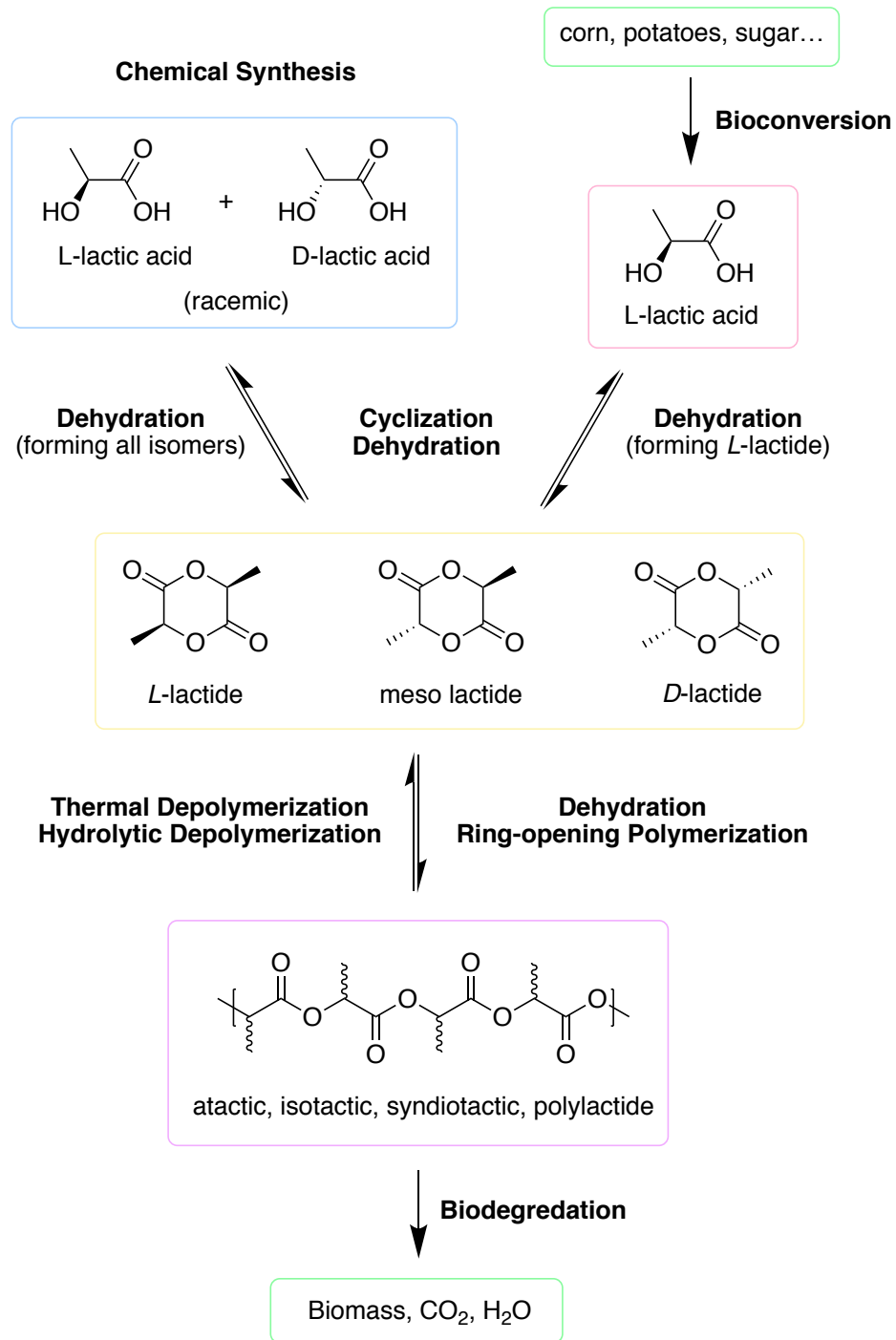
Plastic pollution persists as an ever-worsening threat to the natural environment and human health (1-8). The lure of cheap, petroleum-based commodities has manifested in approximately 8.3 billion metric tons of virgin plastic on Earth; of which, only 9% has been recycled (3). The remaining 7.6 billion metric tons has been released into the environment (3). This leakage has resulted in pervasive microplastics in all forms of terrestrial bodies of water (including drinking water) (5), an amassed 1.6 million km² area of oceanic waste (The Great Pacific Garbage Patch, approximately the size of Alaska) (6), one of the greatest threats to the survival of oceanic mammals (7), and potential human health complications (8).

A plausible remediation of the open, plastic carbon-cycle would be the synthesis of replacement materials, possessing not only the appeals of current plastics, but also the capacity to degrade into innocuous products (within environmentally-benign timeframes) or the capacity to degrade into recyclable products, closing the loop entirely. These degradation phenomena, ideally, would be facilitated by organisms and therefore circumvent the need for energy-demanding purification processes. Furthermore, plastics derived from non-petroleum feedstocks attenuate oil-dependent economies and the geopolitical conflicts associated with them. Plastics that satisfy both aforementioned criteria are deemed *biodegradable* and *biobased*, respectively (9). Starch, polyhydroxybutyrate (PHB), and polylactide (PLA) are quintessential plastics that are both biodegradable and biobased (10).

Polylactide, the polymeric form of lactide, is a promising candidate for the replacement of current petroleum-based plastics. Its materials properties are analogous to polystyrene (PS), which is produced annually on a megaton scale (11-14). PLA degrades via hydrolytic depolymerization, thermal depolymerization (both of which result in the reformation of reusable, monomeric lactide),

or through enzyme-catalyzed degradation (resulting in biomass) (13). Lactide feedstock is currently available at about 2\$ per kilogram, which is within an economically viable regime (14). Already, markets exist for polylactide-based plastic. Nature Works commodified the first synthetic polymer products made from renewable resources (22) and Cargill Dow LLC developed a cheap, solvent free continuous process for the production of PLA. This process uses corn-derived dextrose and natural fermentation to synthesize *L*-lactide as feedstock (Controlled Ring-Opening Polymerization of Lactide and Glycolid). Microbial fermentation accounts for a majority of industrial lactic acids synthesis, because it results in 98-99% purity of *L*-lactic acid (11). Chemical synthesis, however, results in a racemic mixture (11). In animals, *L*-lactic acid is formed from pyruvate during anaerobic metabolism; *D*-lactic acid, however, is not found in natural fermentation processes, and therefore can be deleterious to metabolism (11).

A complete life cycle of polylactide plastics is shown in Scheme 1-1. A more sustainable plastic paradigm may be characterized by the following steps. Bioconversion can be utilized to convert unused, animal or food waste into *L*-lactic acid via fermentation by microorganisms. Thereafter, dehydration results in the cyclization of *L*-lactic acid, forming *L*-lactide. Various ring-opening polymerization techniques can synthesize commodity polylactide. Finally, polylactide waste can be managed by natural biodegradation processes, resulting in water, carbon dioxide, and biomass.



Scheme 1-1: PLA-based plastic paradigm

Materials properties of polymers are parameterized by their molecular weight, polydispersity, tacticity, monomer sequence, and polymer chain ends (15). For instance, increasing the molecular weight of polymers quickly increases melting temperature, viscosity, and tensile strength (15). Another physical property affected by the microstructure of polymers is toughness. Toughness is defined as the amount of energy that can be absorbed by a material before the point of fracture and is an important property in materials engineering. Tensile strength, another commonplace parameter in materials engineering, is the maximum amount of stress a material can endure before fracture.

Tacticity – the stereochemistry of macromolecules – dictates the degree of crystallization of polymer materials (15). Three common forms of tacticity are shown in Figure 1-1 below: isotactic – substituents distributed on the same side, syndiotactic – alternating distribution of the substituents, and atactic – randomly distributed substituents. The more stereoregularity polymers possess, the more efficient their packing; this, in turn, increases the propensity for crystallization (15). The formation of microcrystalline domains increases the tensile strength and glass transition temperature of the material (15). Thus, materials properties can be rationally designed by altering the microstructure of the polymer's tacticity.

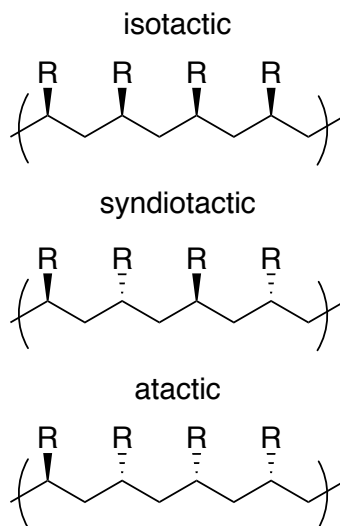


Figure 1-1: Examples of polymer tacticity

Many phenomena involving polymers are statistical; a distribution of molecular weight is always obtained during polymer synthesis (15). A measure of this distribution is the polydispersity index (PDI). It is calculated by the weight average molecular weight divided by the number average molecular weight. The equations describing the polydispersity index, the weight average molecular weight, and number average molecular weight are shown below in equations 1-1 through 1-3. Greater control over the homogeneity of the size of synthesized polymers corresponds to a lower PDI. All colligative properties of polymers are affected by the polymers dispersity (15), thus the PDI of a polymer mixture is an important synthetic parameter to consider. Manipulating the PDI of a polymer mixture is another way to rationally design material properties for a specific application.

$$M_n = \frac{\sum_i M_i N_i}{\sum_i N_i}$$

Equation 1-1: Number average molecular weight (M_n),

where N_i is the number of molecules with mass M_i

$$M_w = \frac{\sum_i M_i^2 N_i}{\sum_i N_i}$$

Equation 1-2: Weight average molecular weight (M_w),

where N_i is the number of molecules with mass M_i

$$PDI = \frac{M_w}{M_n}$$

Equation 1-3: Polydispersity index

Another important variable that serves as a method of control over the physical and chemical properties of polymeric material is the polymer chain ends. Chain ends can react after polymerization. Therefore, chain ends are important in chemical stability of the material (15). Succeeding reactions can be planned, however. For instance, polymers can be synthesized with ends that can subsequently be tethered to other facets after polymerization has occurred. An example is the attachment of polymers with thiol chain ends to modify gold surfaces (35).

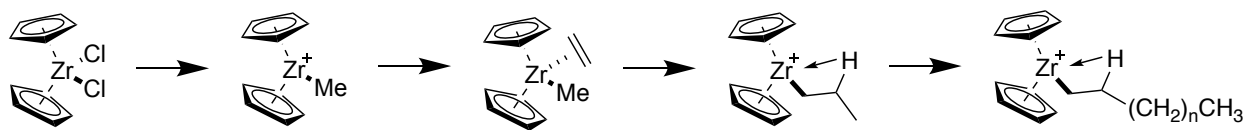
The dependence of polylactide's biodegradability and material properties on molecular weight, polydispersity, tacticity, monomer sequence, and polymer chain ends have been articulated (14). Although comparable to PS in terms of strength and Young's modulus, PLA nevertheless suffers from both a low glass transition temperature and low toughness (16). All of the aforesaid parameters are subtended by polymer synthesis, and organometallic catalysis provides the most control over these ends (14, 22).

Although the use of plastics dates back as far as 1600 B.C.E., when Mesoamericans were using natural rubber, it was not until the twentieth century that the first fully synthetic plastic was made.

Bakelite or polyoxybenzylmethylenglycolanhydride was the first fully synthetic polymer (36). Furthermore, the advent of organometallic polymerization catalysis, also discovered during the twentieth century by Karl Ziegler and Giulio Natta, paved the way for current plastic markets and current microstructural engineering strategies, which use organometallic catalysts. Ziegler-Natta catalysts, for which both Karl Ziegler and Giulio Natta received the Nobel Prize in 1963, remains one of the most important industrial reactions today, producing 15 million tons of polypropylene and polyethylene annually (37).

Organometallic polymerization catalysis afforded synthetic chemists the ability to produce high density polyethylene (high molecular weights with low PDI's) at temperate conditions, as well as stereoregular polymers (37). As stated previously, control over stereoregularity and molecular weight provides a modality to design the physical properties of the resultant polymeric materials. It is because organometallic catalysis provided an efficient method to design materials uniquely fit for a given application that plastics have become one of the most important materials of the modern era.

Two classes of Ziegler-Natta catalysts exist: homogenous and heterogeneous (37). Homogenous catalysis is defined by systems in which the substrate and catalysts are in the same phase. In heterogeneous catalysis the substrate and catalysts are in different phases. Homogenous Ziegler-Natta catalytic systems have been thoroughly developed for hafnium, titanium, and zirconium (37). A prototypical Ziegler-Natta catalyst is a zirconium metallocene complex (shown in Scheme 1-2) The initial, cationic, zirconium species is generated from a Cp_2ZrCl_2 precatalysts. This dichloride species is subsequently activated with methylaluminoxane (MAO), generating a methylated metallocenium ion. This species, in turn, coordinates to ethene, whereupon continual iterations of migratory coordination and migratory insertion generate polyethylene.



Scheme 1-2: Mechanism of Ziegler-Natta catalysis, converting ethylene into polyethylene

A technological advent, similar to the petroleum-based plastic revolution influenced by the work of Ziegler and Natta, may be possible by advancing organometallic chemistry towards the synthesis of PLA. The most common industrial catalysts used today for lactide polymerization are tin(II) octanoate, aluminum(III) *iso*-propoxide, and zinc(II) lactate (Figure 1-2); these complexes serve as Lewis acids and undergo the following mechanism (Scheme 1-3): monomer coordination to the metal center (i), insertion via nucleophilic addition of an alkoxy group on the carbonyl carbon (ii), oxygen-acyl bond cleavage, resulting in ring-opening of the lactide (22). A summary of both catalysts and the resulting materials properties can be found in Tables 1 and 2 (18).

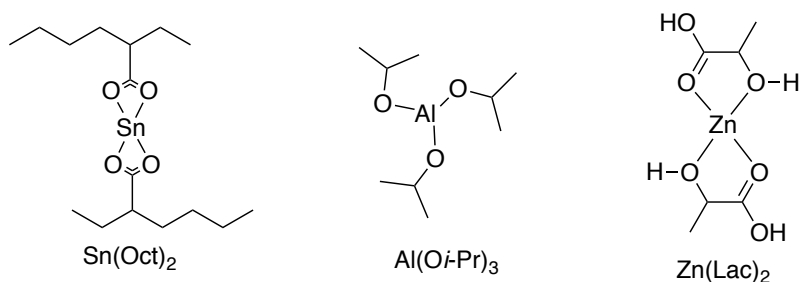
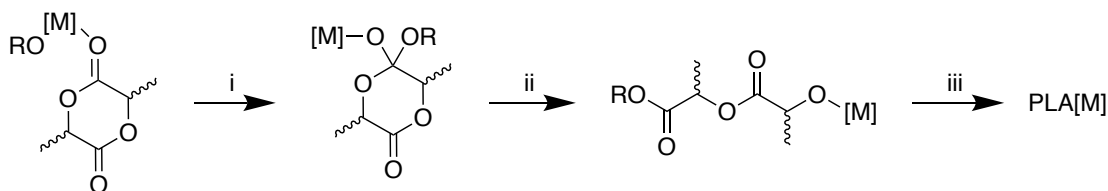


Figure 1-2: Most common PLA polymerization catalysts



Scheme 1-3: Mechanism of Lewis acid catalyzed ROP

Catalyst	Polymer	Solvent	Temperature	Reaction time	Molecular weight
Al(Oi-Pr) ₃	D,L-PLA	toluene	70-100 °C	100 hrs.	M _n ~ 90,000
Al(Oi-Pr) ₃	L-PLA	toluene	70-100 °C	100 hrs.	M _n ~ 90,000
Sn(Oct) ₂	D,L-PLA	alcohols	200 °C	20 min	M _n ~ 200,000
Sn(Oct) ₂	L-PLA	alcohols	130 °C	2-72 hrs.	M _n ~ 250,000
Sn(Oct) ₂	L-PLA	no solvent	180 °C	7 min.	M _n ~ 91,000
Zn(Lac) ₂	D,L-PLA	no solvent	140 °C	96 hrs.	M _n ~ 200,000

Table 1-1: Summary of PLA polymerizations with various catalysts

Stannous octanoate is particularly optimized for lactide polymerization. It is commercially available and has been accepted as a food additive by the Food and Drug Administration (22). As can be viewed in Table 1-1, stannous octanoate polymerizes both stereoisomers of lactide into polymers of high molecular weights within short time frames. Of importance for industry, is the fact that lactide polymerization using stannous octanoate can be performed without solvent, as purification of material is costly on large industrial scales.

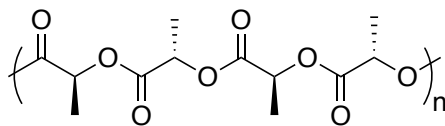
Although stannous octanoate is the most active and efficient catalyst, tin compounds invariably arouse toxicity concerns. Thus, attempts towards modifying aluminum and zinc catalysts have been conducted (22). Zinc, already present in human physiology, is principally of interest with respect to physiological compatibility; aluminum is not intrinsically a part of human physiology and may be associated with a risk for Alzheimer's disease. Yttrium and lanthanum alkoxides have also shown robust reactivity towards ROP; both initiators are much more active than aluminum alkoxides.

Polymer	Molecular Weight	Glass transition temperature	Melting temperature	Tensile strength	Elongation at Break
L-PLA	50,000	54 °C	170 °C	1400 MPa	6.0 %
L-PLA	100,000	58 °C	159 °C	3000 MPa	3.3%
L-PLA	300,000	59 °C	178 °C	3250 MPa	2.0 %
D,L-PLA	107,000	51 °C	-	1950 MPa	6.0 %
D, L-PLA	550,000	53 °C	-	2350 MPa	5.0 %

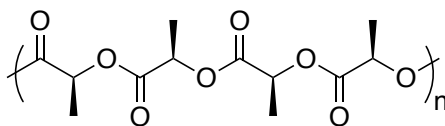
Table 1-2: Mechanical properties of various isomeric forms of PLA

Poly lactide is observed in four isomeric forms: isotactic, syndiotactic, heterotactic (in which alternation of substituents occurs in pairs), and atactic (38). Examples of these PLA microstructures are shown in Scheme 1-4. Table 1-2 provides insight into the effects of microstructure on material properties. D,L-PLA, atactic polylactide synthesized from a racemic mixture of *D*-lactide and *L*-lactide, has a substantially lower tensile strength than L-PLA, which is stereoregular. This can be attributed to the packing of microdomains within the material, as described previously. Moreover, a discernable, positive correlation can also be seen between molecular weight and tensile strength. The glass transition temperature, an important parameter for PLA's use in food packaging, also follows the same trend: positive correlation with stereoregularity and molecular weight. Finally, elongation at break is a measure of the elasticity of a polymer. Elongation at break is a measure of plasticity of a material; it is the percentage increase in length at the point of fracture. Molecular weight and stereoregularity are both negatively

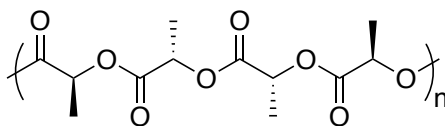
correlated with elongation at break. These phenomena are also the result of increased crystallinity within the polymers (15). Crystalline domains are harder and are easy to fracture – less plastic.



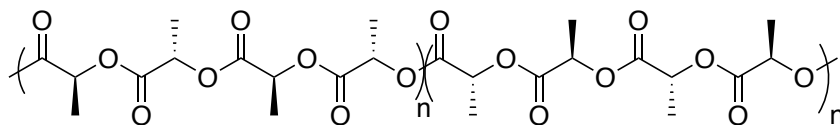
isotactic L-PLA



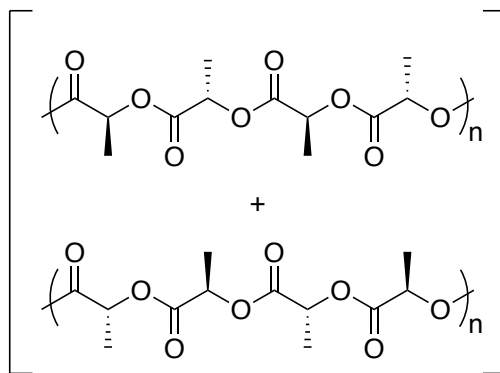
syndiotactic



heterotactic



stereoblock of PLA

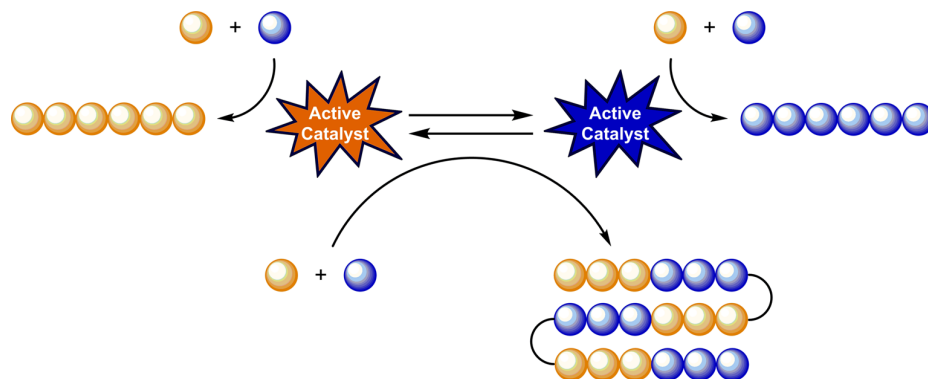


stereocomplex of L-PLA and D-PLA

Figure 1-3: PLA tacticities and microstructures

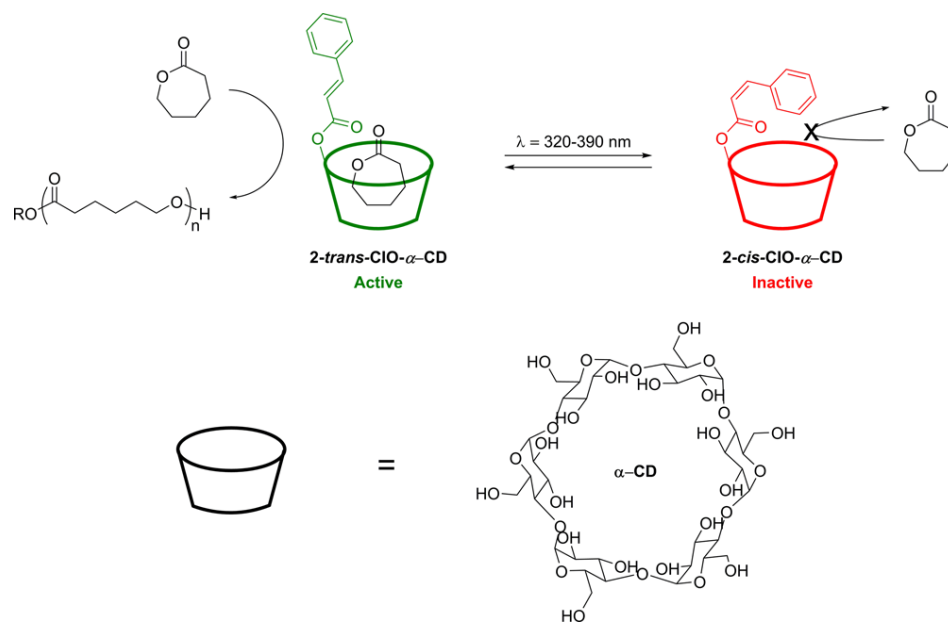
Additional methods of altering the materials properties of PLA include block copolymerization and stereocomplexation. Stereocomplexation shown in Scheme 1-4, forms strong intermolecular forces, as a result of the complimentary packing of two stereoisomeric forms of PLA (38). Block copolymerization (Scheme 1-5) –alternating segments (“blocks”) of different monomers or alternating blocks of differing tacticity – also avails the modification of PLA’s material properties (19-21). An accompanying module to block copolymerization is the potential of block copolymers to self-assemble (Polylactide (PLA)-based amphiphilic block copolymers: synthesis, self-assembly, and biomedical applications); this is particularly useful in biomedical applications, such as drug delivery.

Block copolymers can be synthesized by many synthetic routes, namely, the sequential addition of various monomers to living or immortal catalytic systems (24). Nevertheless, these systems fail to meet the synthetic feasibility of increasingly complex microstructures (24); switchable catalysis has the potential, in principle, to serve as a methodology to challenge these limitations. Discovering catalytic systems that interact orthogonally towards different monomers affords a platform for the synthesis of block copolymers – changes in catalytically active states result in the addition of various monomers to a growing polymer chain (Scheme 1-5). These changes can be affected by various stimuli: light, heat, current, pressure, or the addition of chemical species that perturb the catalyst (24).



Scheme 1-5: Switchable polymerization catalysis switching between two active, orthogonal states (Reprinted with permissions (24))

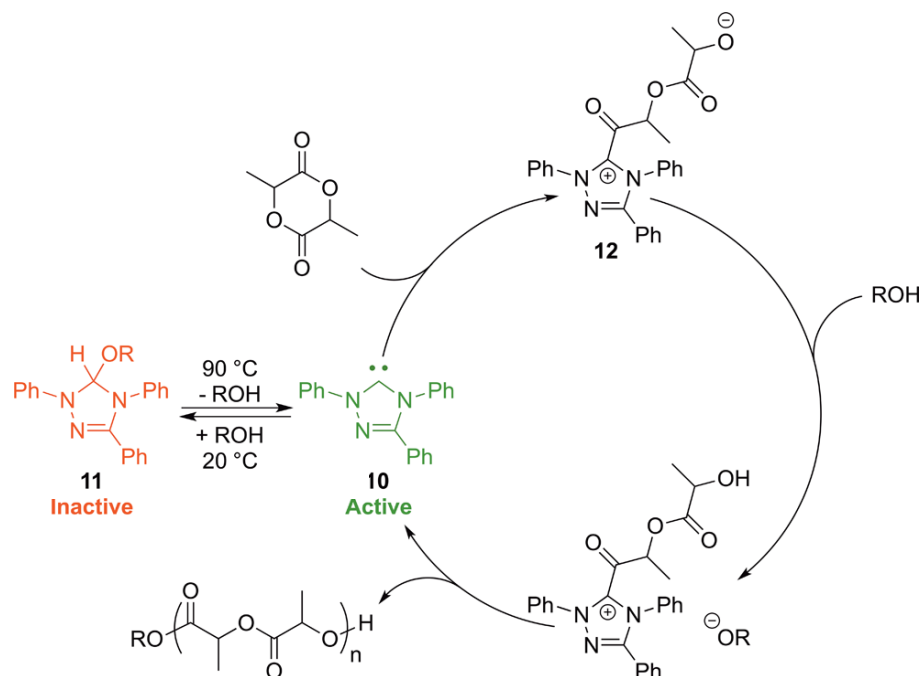
An example which uses light as a stimulus to switch a catalyst between “on” and “off” states is shown in Scheme 1-6. *Cis/trans* photoisomerization, affected by UV irradiation, switches a 2-O-trans-cinnamoyl- α -cyclodextrin (2- trans-CIO- α -CD, Scheme 6) organocatalyst between “on” and “off” states of δ -valerolactone (VL) ROP (24). Harada and co-workers showed that the guest-host dynamic in this system efficiently polymerized VL only in the catalysts active state: isomerization changed the sterics such that catalysis could occur in the *trans* isomer, but not in the *cis* isomer. The use of an organocatalyst in lieu of metal-based catalysts is beneficial, because it avoids the use of toxic metals. Using light as a stimulus is beneficial, as the energy of light required for typical transformations of the sort required is noninvasive. However, using radiation does have the downfall of requiring specific photosensitizers for a given system; this can result in synthetic complexity.



Scheme 1-6: Light-stimulated switchable polymerization catalysis

(Reprinted with permissions (24))

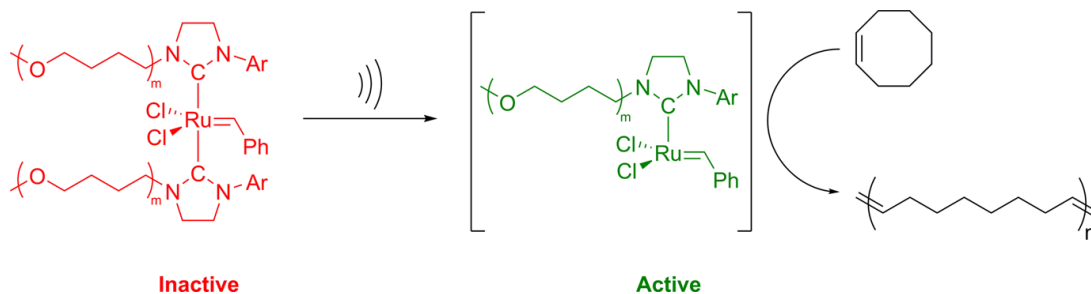
An example in which heat is used as a stimulus to switch a ROP catalyst can be shown in Scheme 1-7. In this system, heating of a modified triazole resulted in the elimination of an alcohol and the formation of a N-heterocyclic carbene (NHC), which was active in ROP of lactide (24). The reformation of the inactive precatalyst could be achieved by cooling the reaction down to 20 °C. At lower temperatures the NHC reacted with the alcohol to generate the inactive, triazole precatalyst. Heat is advantageous as a stimulus for switching, because changing the temperature of a solution can be accomplished easily. However, not only is designing systems that are responsive to thermal changes challenging, but also many energetic pathways are available at elevated temperatures, which increase the complexity of designing such systems.



Scheme 1-7: Heat-stimulated switchable polymerization catalysis

(Reprinted with permissions (24))

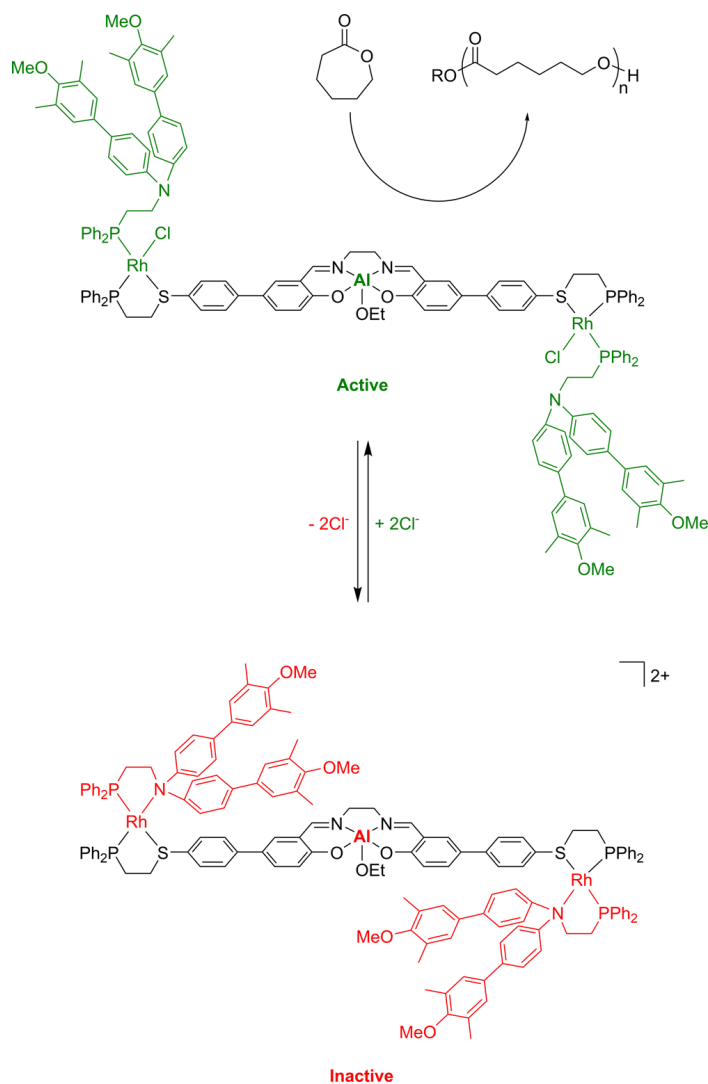
Ring-opening metathesis polymerization (ROMP) is an important polymerization technique that is capable of polymerizing a large array of monomers with good functional group tolerance (40). The polymerization occurs via an olefin metathesis mechanism, for which Yves Chauvin, Robert H. Grubbs, and Richard R. Schrock won the Nobel prize in 2005. Scheme 1-8 below represents a system, wherein an inactive ROMP catalyst is mechanochemically activated (24). Sijbesma *et al.* showed that ultrasonication resulted in a dissociation of one of the N-heterocyclic carbene ligands, thereby opening the coordination sphere. ROMP of cyclooctene followed with high conversion.



Scheme 1-8: Pressure-stimulated switchable polymerization catalysis

(Reprinted with permissions (24))

Lastly, an example of allosteric control over a ROP aluminum(III) catalyst was presented by Mirkin and co-workers (24). This reversible inhibition was made possible by exploiting Le Chatelier's principle: increasing the concentration of chloride ions would thermodynamically drive the dissociation of the amine facets of bidentate phosphinoamine ligands at two distal rhodium(I) moieties. This change in denticity resulted in large rearrangements in the complex's configuration, freeing the active catalytic site from an otherwise sterically hindered bulk. Both activation and deactivation were made possible, either by the addition of chloride ions or NaBAr^F (which would abstract the chloride ions from the rhodium(I) centers). Although an elegant example of switchable catalysis, the advancement of this type of technique requires complex synthetic consideration.

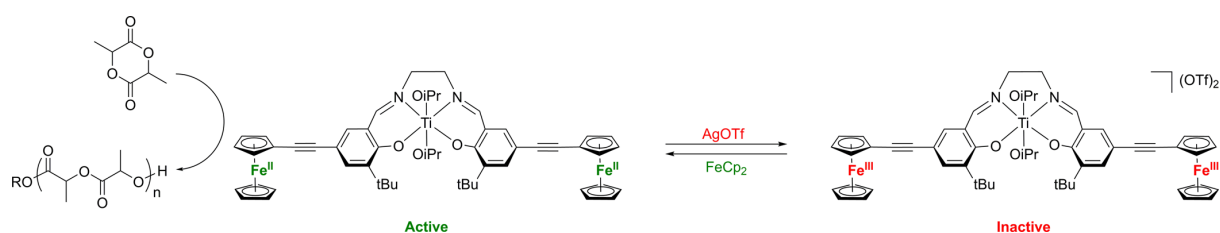


Scheme 1-9: Allosteric modulation of polymerization catalysts

(Reprinted with permissions (24))

Redox control over ring-opening polymerization (ROP) was first demonstrated by Long *et al* (24). when they discovered, in 2006, that a titanium ring-opening polymerization catalyst, tethered to a doubly ferrocene-substituted salen ligand, showed a thirtyfold decrease in the lactide polymerization rate constant upon oxidation of the ferrocene moiety via the addition of silver triflate (23, 24; Scheme 1-10). This type of modulation is referred to as substitutionally inert, redox

activity. There exists three forms of redox-active ligands: substitutionally inert, hemilabile, and fully-releasing (41). Hemilabile and fully-releasing redox-active ligands, upon oxidation, open coordination sites for catalysis to occur, thus affording redox modulation over reactivity. Substitutionally inert redox-active ligands, operate by perturbing the electron density at the metal center. Upon oxidation of the ligand scaffold, the resultant positive charge imbues electrophilicity at a proximate, ligated metal, resulting in a change of reactivity. This type of alteration in reactivity, found for instance by the Long group, can also be considered as the result of the increased Lewis acidity at the titanium(IV) center, exerted upon by the oxidized ferrocenyl units; this increase in Lewis acidity renders the catalyst inactive.



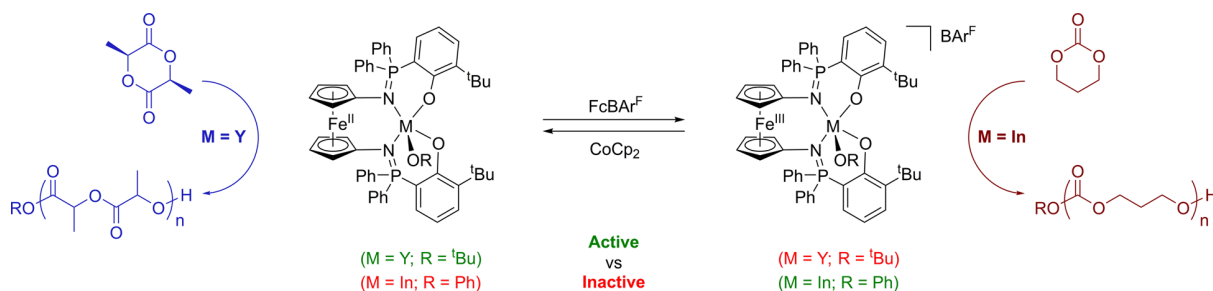
Scheme 1-10: Redox-switchable polymerization catalysts published by the Long group.

(Reprinted with permission (24))

The structure and synthesis of ferrocene places it as a uniquely proficient choice for a redox-active ligand moiety. Not only is ferrocene cheap, but it is chemically inert, soluble in organic solvents, and electrochemically reversible. Ferrocene's stability arises kinetically and thermodynamically: an eighteen-electron count, along with three-dimensional aromaticity, imbues exceptional stability, and the bulky cyclopentadienyl rings saturate the coordination sphere of iron(II). Its electrochemistry is characterized by a one-electron Nernstian couple, and its redox

potential is not dependent upon the medium within which the electrochemistry takes place; this makes ferrocene a very important internal standard in inorganic electrochemistry (42, 43).

In this vein, Diaconescu *et al.* demonstrated in 2011 that control over lactide ROP could be exerted, similar to the system put forth by the Long group, by incorporating ferrocene into a different ligand framework. However, not only was their yttrium phosfen (1,10-di(2-*tert*-butyl-6-diphenylphosphiniminophenoxy)ferrocene) complex less reactive upon oxidation by ferrocenium tetrakis(3,5-bis(trifluoromethyl)phenyl) borate (FcBAR^F), but it showed contrariwise modulation of reactivity towards trimethylene carbonate (24, 26; Scheme 1-11). Furthermore, a metal dependence was demonstrated that inverted the system's reactivity when indium was substituted for yttrium.

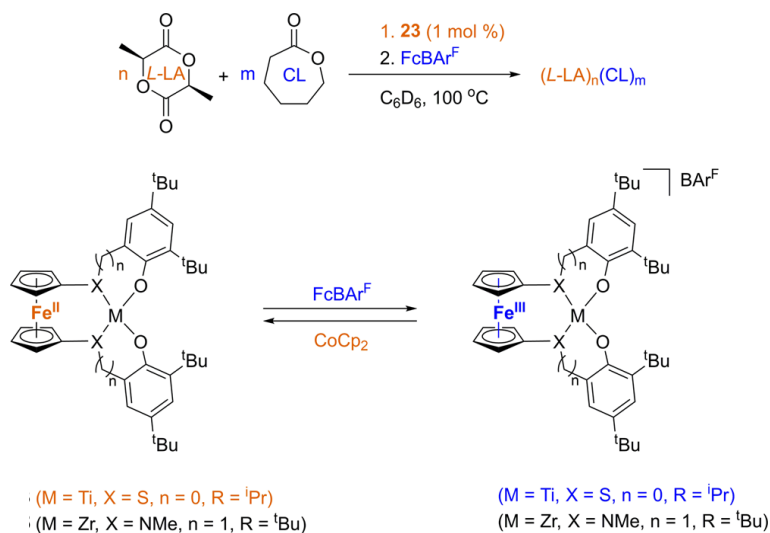


Scheme 1-11: Redox-switchable polymerization catalysis published by the Diaconescu group

(Reprinted with permission (24))

Two other systems, incorporating ferrocene into the ligand scaffold, were reported by the Diaconescu group; one of which actually enabled a one-pot synthesis of a block copolymer of LA and CL (24). This catalyst used titanium(IV) as the active metal center. The principle of selectivity was the same as before: by switching *in-situ* between oxidation states of the ferrocene backbone, a change in Lewis acidity and reactivity of the catalyst was affected. A zirconium (IV) analogue

was employed towards ROP catalysis and failed to show selectivity upon oxidation and reduction. This phenomenon was ascribed to zirconium(IV)'s greater Lewis acidity upon oxidation than the Lewis acidity in its reduced state.



Scheme 1-12: Synthesis of block copolymers via redox-switchable catalysis

(Reprinted with permissions (24))

All of these experiments on redox-switchable polymerization catalysts allude to the hypothesis that these systems operate within a margin of Lewis acidity of the metal center that can serve as a modality of switching. If a catalyst is too reactive, then it will indiscriminately polymerize any monomer. Conversely, if a catalyst is not reactive enough, then no monomers will be polymerized. However, there exists a domain within a spectrum of Lewis acidity that can serve as a site of switching (Figure 1-3) for a given monomer. Outside these domains, redox chemistry is unable to affect whether or not polymerization occurs. Within these domains, “on” and “off” states are present at opposing ends. Moreover, these “switch domains” are monomer specific. One-pot block copolymerization can therefore be considered as two adjacent switch domains, each

domain corresponding to different monomers (Figure 1-4). For instance, upon oxidation, the Lewis acidity of a catalyst may be shifted from an “on” end of one domain to an “on” end of another. An example was given by Diaconescu and coworkers: oxidation of the titanium(IV) catalyst shown above (Scheme 1-11) shifted its Lewis acidity towards the right from the “on” end of the *L*-lactide switch domain, to the “on” end of CL’s switch domain. Orthogonality of these two monomers occurred because the “on” end of LA presides at the “off” end of CL.



Figure 1-3: Lewis acidity spectrum, showing a switch domain. Selectivity can be achieved within a switch domain. Oxidation moves catalyst along spectrum to the right; reduction shifts catalyst to the left.

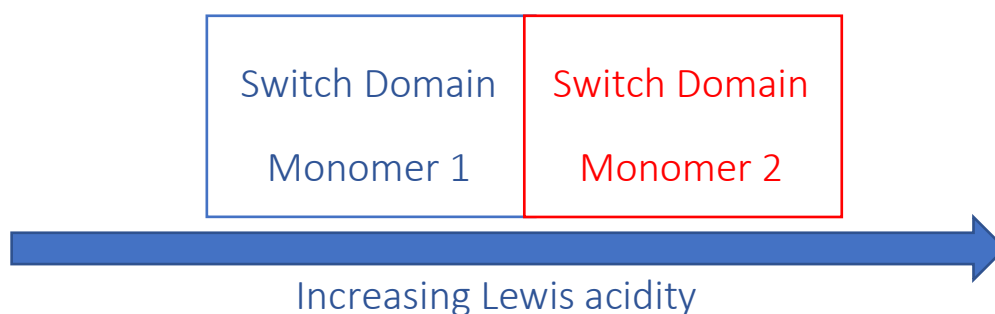
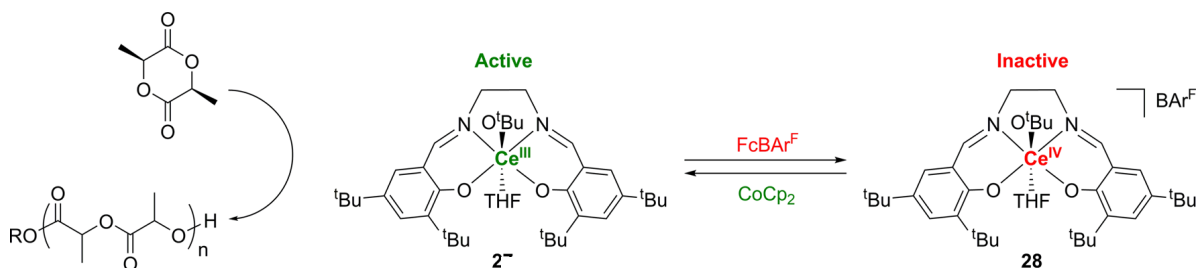


Figure 1-4: Lewis acidity spectrum showing two adjacent switch domains. This configuration permits orthogonal reactivity of monomers 1 and 2.

It is important to note that the results found by both the Long group in 2006 and the Diaconescu group in 2011, regarding the decrease in activity upon oxidation of ROP catalysts, prove that an increase in Lewis acidity can also cause inactivity. In other words, “on” states are not always to right of “off” states on a spectrum of Lewis acidity. This, at first, may seem nonintuitive, because stronger Lewis acidity usually results in greater activity. However, Diaconescu *et al.* hypothesis that the situation is more complex: alkoxide migration and ring opening may actually be hindered by greater electrophilicity at the metal center of the catalyst. It is plausible that the alkoxide ligand is coordinated too strongly for migration to occur. Thus, an “off” state of LA’s switch domain is to the right of an “on” state on a spectrum of Lewis acidity.

Redox switching can also occur at the catalytic center (24). Oxidation of a cerium(III) salen complex by ferrocenium BAr^{F} led to inactivity in the ROP of lactide. Once cobaltocene is added to a solution of the inactive cerium (IV) catalyst and lactide, the complex is reduced and the polymerization initiates. Because two modalities of redox switching are possible, an interesting lacuna exists for the possibility of several switches presiding on one catalyst. For example, if both redox events are accessible, the synthesis of a catalyst with redox activity not only at the metal center but also at the ferrocene moieties incorporated into the ligand scaffold would lead to catalysts that can be switched by two different external triggers.



Scheme 1-13: redox-switching at the active metal center

(Reprinted with permissions (24))

The phosfen ligand design arose out of an attempt to investigate the electrochemistry of a Schiff base ancillary ligand: 1,10-di(2,4-bis-*tert*-butyl-salicylimino)ferrocene or salfen (ref, Figure 1-5). This work found that the substitution of the salfen scaffold with an iminophosphorane group resulted in a more facile oxidation event. The seminal work performed by Arnold *et al.* in 2001, in which the salfen ligand was introduced, reported on the effect that various R and R' groups had on the solubility of the resulting complexes. This is an important variable in polymerization dynamics and can therefore affect the polymer materials properties (44). The iminophosphorane facet provides an additional site for various substitution, in order to curtail the solubility of the catalyst to optimize polymerization dynamics – matching the solubility of the catalyst to the optimized solvent for a given polymerization.

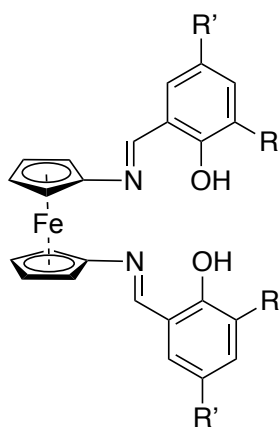


Figure 1-5: Salfen proligand

A corollary to the 2011 Diaconescu findings is to investigate the effects of ligand substitution on ROP catalysis. Changes in the phosfen ligand presumably affect the electron density at the metal center that performs catalysis; this, in principle, could serve as an additional platform of control over the polymerization of block copolymers. In other words, ligand substitution effects may be able to shift ROP catalysts along the aforementioned spectrum of Lewis

acidity (Figure 1-3). This would allow catalysts to be designed specifically to the switch domains of a given set of monomers.

Herein, the synthesis and reactivity of a modified yttrium phosphen complex, substituted by a methoxy group ortho to the phenoxide moiety, are investigated. It is feasible that these modifications can serve as an additional mode of control, perhaps posing the catalyst orthogonally reactive towards different sets of monomers. By changing this facet to an array of electron-withdrawing/electron-donating groups, an analysis of the modulation of Lewis acidity of the metal center can be made, in addition to possibly achieving monomer selectivity in redox switchable ROP.

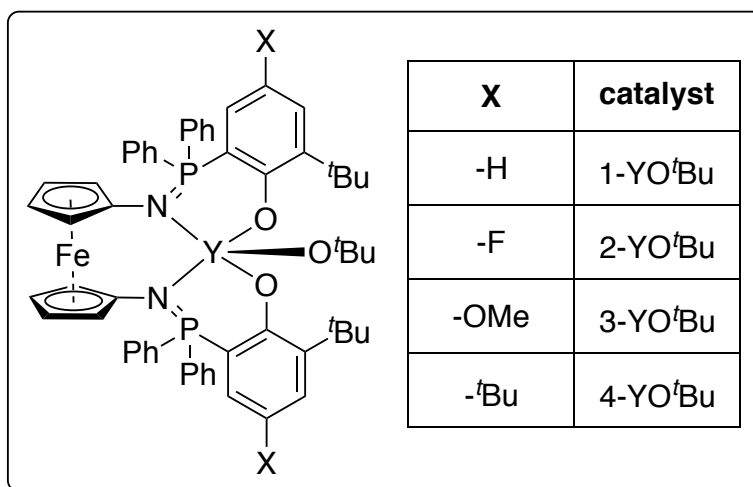


Figure 1-6: Ligand substitutions of yttrium phosphen catalysts

Figure 7 shows the yttrium complex of interest and the ligand modifications aside the respective names. It is important to note that alterations of the ligand at X can affect solubility and synthetic ease. **1-YO^tBu** is the parent complex studied in 2011 (Diaconescu *et al.*, 26). The substitutions were chosen as a spectrum of electronegativity: methoxy as the most electron

donating, *tert*-butyl next, hydrogen as a neutral reference, and, finally, fluorine as an electron-withdrawing substituent.

Chapter 2. Research Methods and Results

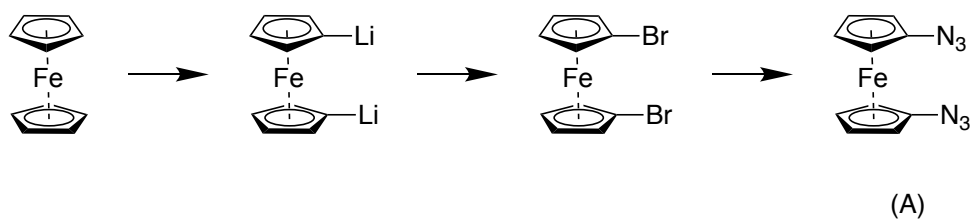
The questions that this work addresses can be asked in the following ways: do electron-donating/electron-withdrawing effects via substitution on the phosfen ligand scaffold effect the Lewis acidity of the catalytic metal center? If so, what outcomes do these substitutions spell for ROP catalysis? To answer these questions, the kinetics of ROP with the various phosfen catalysts can be juxtaposed. Therefore, a facile way to provide evidence for this inquiry is to synthesize and characterize **1-YO'Bu**, **2-YO'Bu**, **3-YO'Bu**, and **4-YO'Bu**, then gather and contrast polymerization data for each. The results of such procedures and discussions thereof are given in the following subchapters.

Subchapter 2 A. Syntheses of Catalysts

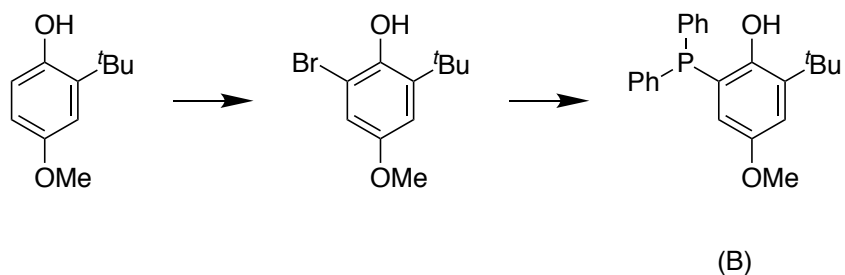
Attempts to synthesize both **2-YO'Bu** and **3-YO'Bu** were made. Both the syntheses of **2-YO'Bu** and **3-YO'Bu** are convergent, involving Staudinger reactions with 1,1'-diazidoferrocene (**A**) at the nexuses with 2-(*tert*-butyl)-6-(diphenylphosphaneyl)-4-fluorophenol (**C**) and 2-(*tert*-butyl)-6-(diphenylphosphaneyl)-4-methoxyphenol (**B**), respectively. The successful syntheses carried out in this work, the syntheses of **3-YO'Bu** and **C**, are shown in Schemes 2-1 through 2-4. **2-YO'Bu** was not isolated, but **C** – a precursor of **2-YO'Bu** – was synthesized and characterized via ^1H , ^{31}P , and ^{19}F NMR spectroscopy (Appendix). **3-YO'Bu** was successfully synthesized, characterized by ^1H NMR, and ^{31}P NMR (Appendix).

Although **3-YO'Bu** was isolated, the salt metathesis of **3-YCl** and potassium *tert*-butoxide was performed many times without success. The failed attempts resulted in either no reaction or an unknown red precipitate that was insoluble in THF, C_6D_6 , and DCM; therefore, NMR spectra were unobtainable. Ensuring that the reaction was carried out at $0\text{ }^\circ\text{C}$, as well as ensuring that

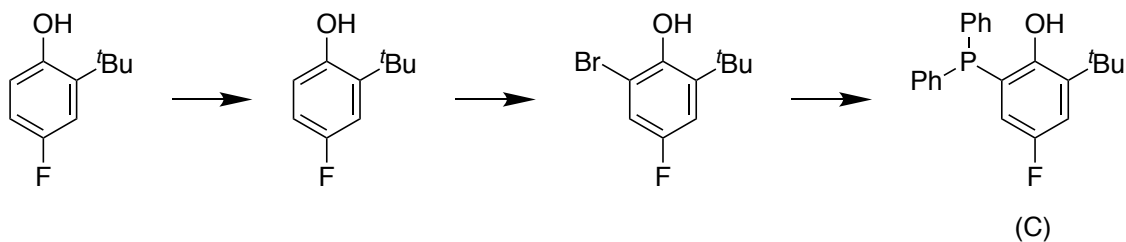
KO^tBu was added slowly, prevented the synthesis of this unknown red solid. High purity of **3-YCl** and KO^tBu was also imperative for the synthesis of **3-YO^tBu**. KO^tBu needed to be freshly sublimed, and, if **3-YCl** was not extracted well and washed with hexanes, then no reaction would occur. It is important to note that whatever impurity was responsible for this result was NMR silent. However, an additional extraction with toluene and washing with hexanes would allow for the isolation of **3-YO^tBu**.



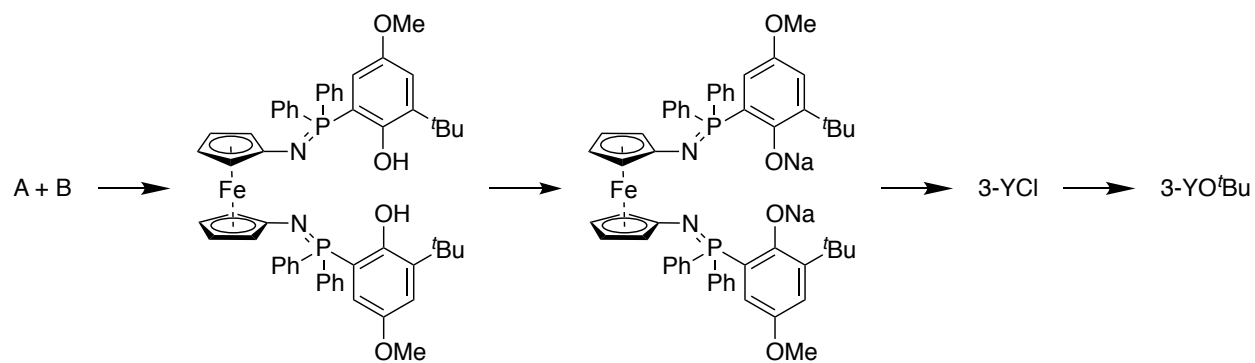
Scheme 2-1: Synthesis of 1,1'-diazidoferrocene



Scheme 2-2: Synthesis of 2-(tert-butyl)-6-(diphenylphosphaneyl)-4-methoxyphenol

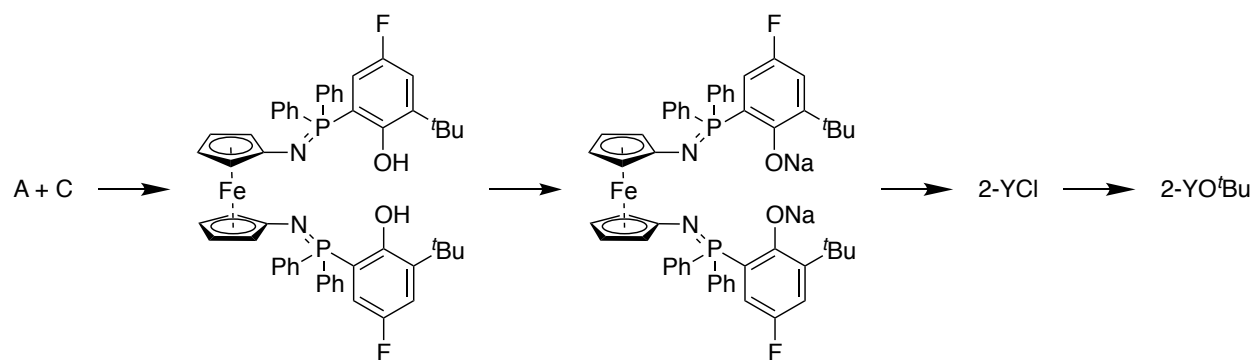


Scheme 2-3: Synthesis of 2-bromo-6-(tert-butyl)-4-fluorophenol



Scheme 2-4: Synthesis of 3-YO^tBu

The synthesis of **2-YO^tBu**, is shown in Scheme 2-5. Although **2-(tert-butyl)-6-(diphenylphosphaneyl)-4-fluorophenol (C)** was isolated, the attempted Staudinger reaction resulted in decomposition; the reaction conditions were analogous to the synthesis of **3-YO^tBu**. Moreover, the synthesis of **C** was attempted many times before a product was isolated: addition of ⁿBuLi had to be very slow, otherwise decomposition followed. Presumably, lithiation of fluorine occurred in lieu of bromine; lithium-halogen exchanges are kinetically controlled (March's advanced organic chemistry), and fluorine is less sterically hindered than bromine in 2-bromo-6-(tert-butyl)-4-fluorophenol.



Scheme 2-5: Synthesis of 2-YO^tBu

Subchapter 2 B. Redox Stability of 3-YO'Bu

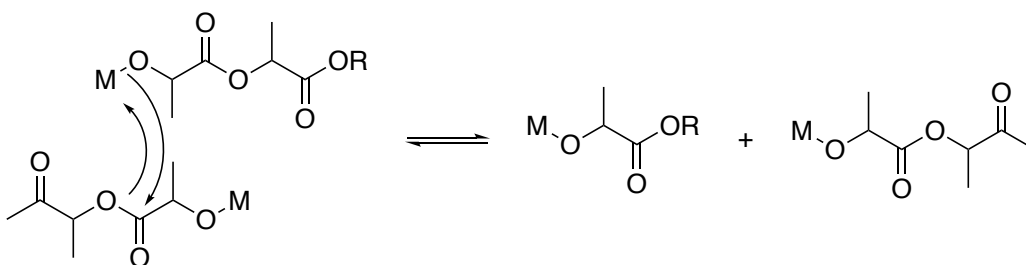
Substitutionally inert, redox-switchable catalysis implies redox stability of the catalysts – reversibility of oxidation and reduction without changes in geometry or adventitious chemical reactions. Cyclic voltammetry provides a means to investigate the reversibility of a redox switch, as well as the stability of a catalysts upon oxidation or reduction. Cyclic voltammetry of 3-YO'Bu is not presented in this work; however, a simple experiment, addressing the stability of 3-YO'Bu upon oxidation with a chemical oxidant was conducted.

By contrasting the ^1H NMR spectrum of 3-YO'Bu to the ^1H NMR spectrum of 3-YO'Bu after the addition of acetylferrocenium BAr^{F} (oxidizing 3-YO'Bu to $[\text{3-YO'Bu}][\text{BAr}^{\text{F}}]$), as well as the ^1H NMR spectrum after addition of cobaltocene (reducing $[\text{3-YO'Bu}][\text{BAr}^{\text{F}}]$ back to 3-YO'Bu), stability can be induced. If the ^1H NMR spectra before oxidation and after reduction contain overlapping peaks of 3-YO'Bu, then the catalyst is redox stable. The ^1H NMR spectrum after the addition acetylferrocenium BAr^{F} to 3-YO'Bu of oxidant showed broad, paramagnetic peaks and the ^1H NMR spectrum after the addition of cobaltocene showed the recovery of the precatalyst. There was, however, a concomitant shift of the ^1H NMR, *tert*-butoxide peak; the cause of this has not been investigated. Evidence for redox stability is imperative to this work. Thus, cyclic voltammetry needs to be performed on 3-YO'Bu, and the shifting of ^1H NMR, *tert*-butoxide peak must be addressed.

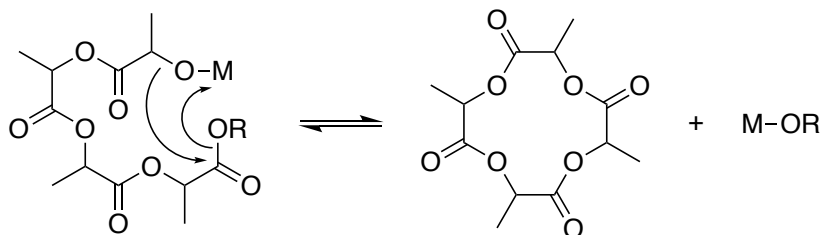
Subchapter 2 C. Depolymerization and Polymer Analysis

Because of the possibility of catalytic depolymerization, reaction time is therefore an important parameter. If reaction times are too long, a transesterification mechanism becomes operative as a result of polymer to monomer concentrations (38). The two possible reaction

coordinates that lead to a decrease in the PDI of a polymer solution are shown below in Scheme 3-2. Either “backbiting” occurs intramolecularly, causing the catalyst to close an oligomeric form of the polymer, or an intermolecular mechanism becomes operative, wherein the catalyst breaks the polymer chains into increasingly smaller polymer chains. Reaction times presented in this work are all restricted to margins wherein no depolymerization occurs and were determined by monitoring the reactions of interest. Also, quenching, which was performed before each aliquot was taken, kills the catalyst; thus, no depolymerization could occur.



Scheme 2-6: Intermolecular transesterification



Scheme 2-7 Intramolecular transesterification

Gel permeation chromatography (GPC) is an effective means to ascertain the distribution of the polymer products. A chromatographic column filled with porous beads is used to separate macromolecules based on their hydrodynamic volume – an ensemble average, corresponding roughly to the volume of a polymer in solution. The pores within the beads trap smaller species,

thereby slowing their elution from the column. Thus, the larger the macromolecule, the quicker it elutes from the GPC. The eluted macromolecules are subsequently analyzed via spectroscopic scattering techniques. The readout from such an experiment provides a graph of intensity versus retention time; the width of this distribution corresponds to the PDI of the sample. Molecular weights can be ascertained based on retention times. By comparing species of known molecular weights – usually polystyrene with a PDI of essentially one, empirical molecular weights can be inferred.

With respect to back-biting, mentioned above, the width of the molecular mass distribution is also an indicator for depolymerization. If polymer chains are broken into consecutively smaller oligomeric species, then the distribution spreads out. Information regarding block copolymerization can also be inferred from GPC. The modality provides evidence for the existence of a block copolymer. If a distribution is bimodal (Figure 2-2), then it is possible that the distributions correlate to different homopolymers – polymers of only one type of monomer. If, however, after block copolymerization only one distribution is present in the GPC trace, then the existence of a block copolymer is corroborated (Figure 2-1). 2D NMR experiments provide more evidence in determining the microstructure of a polymer. All of these experiments will need to be conducted before a convincing argument regarding the block copolymerization can be made.

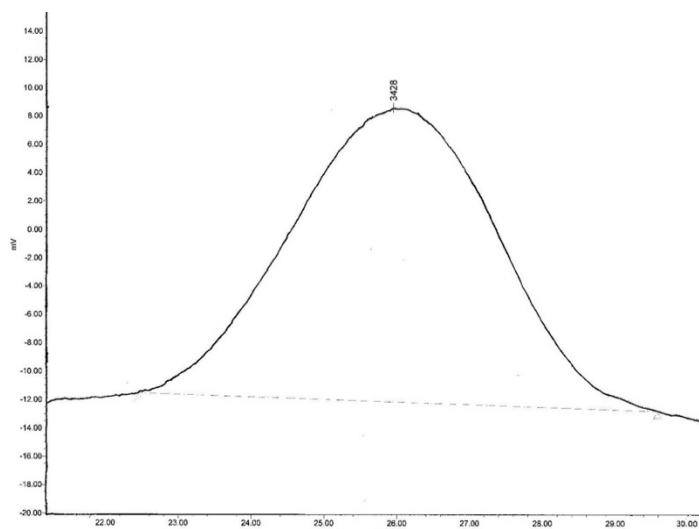


Figure 2-1: Example of a monomodal GPC trace (reprinted with permission (45))

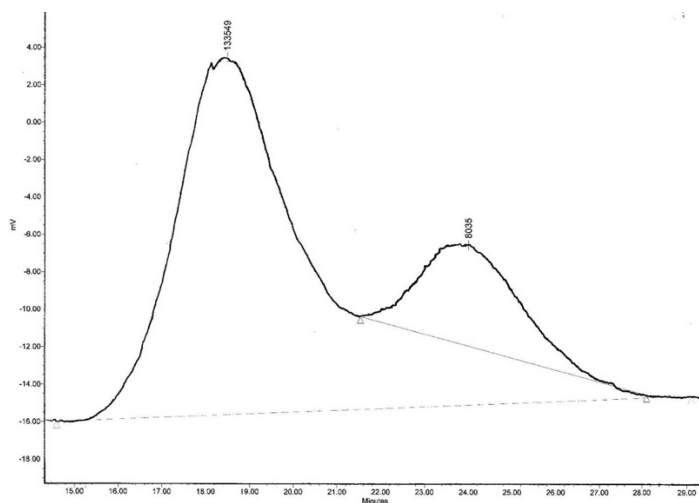


Figure 2-2: Example of a bimodal GPC trace (reprinted with permission (45))

Subchapter 2 D. Solvent Effects

The effects of changing the solvent on polymerization rates were investigated. Polymerizations of LA using **3-YO'Bu** were performed in THF and benzene; Chart 2-1 and Chart 2-2 contrast time versus percent conversion plots of the different systems. Polymerizations of LA were faster in benzene than in THF: conversion is complete in benzene by the time 50% conversion

is reached in THF. To conduct research more efficiently, benzene was therefore chosen as the solvent for all other polymerizations.

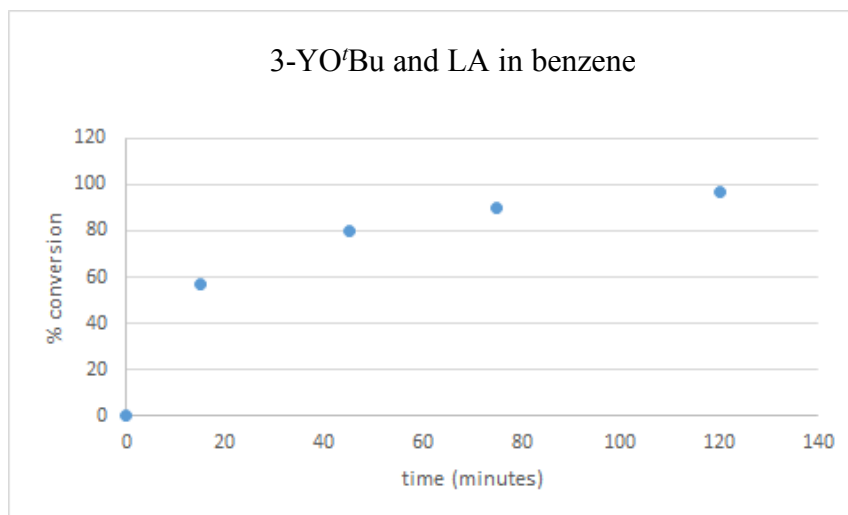


Chart 2-1: Lactide polymerization in benzene

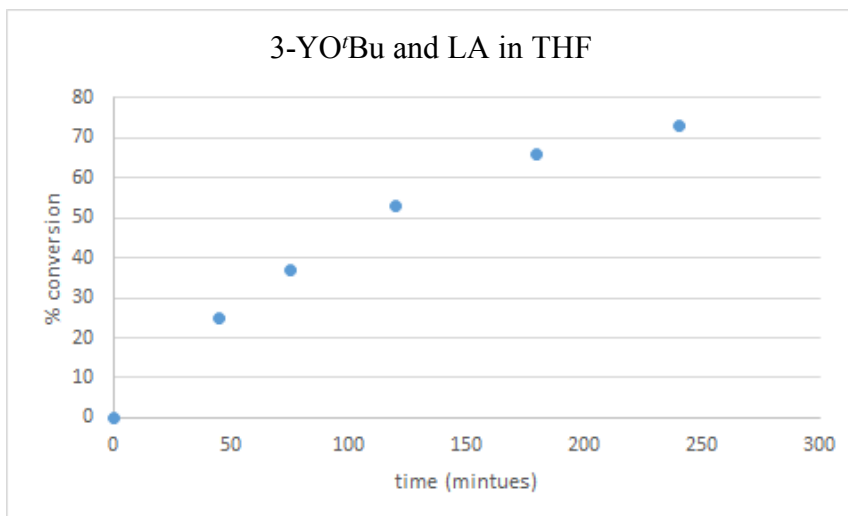


Chart 2-2: Lactide polymerization in THF

Subchapter 2 E. Polymerizations with 3-YO'Bu

Experiments regarding the activity of **3-YO'Bu** in ROP catalysis were performed towards an assay of monomers in both the reduced and oxidized states of the catalyst: *l*-lactide (LA), cyclohexene oxide (CHO), trimethylene carbonate (TMC), ϵ -caprolactone (CL), β -butyrolactone

(BBL), styrene oxide (SO), and propylene oxide (PO). LA, TMC, CL, and CHO were polymerized by either the reduced or oxidized **3-YO'Bu**. Table 2-1 below summarizes the activities of both **3-YO'Bu** and **[3-YO'Bu][BAr^F]**.

Monomer	LA 	TMC 	CL 	CHO 	PO 	BBL 	SO
3-YO'Bu	99% 2 h.	99% 5 min.	10% 30 h.	0% 24 h.	NR	NR	NR
[3-YO'Bu][BAr^F]	0% 2 h.	99% 5 min.	0% 30 h.	100% 2 h.	NR	No data	NR

Table 2-1: Polymerization assay

As stated previously, benzene was chosen as the solvent for all polymerizations, because of efficiency. Thus, all of the polymerizations shown in Table 2-1 were conducted in benzene. However, polymerization data collected in the original 2011 Diaconescu work was collected in THF. Thus, in order to correctly contrast the activities of **1-YO'Bu** and **3-YO'Bu**, polymerizations needed to be conducted in THF as well. Table 2-1 juxtaposes results of polymerizations in THF gathered in this work with the results found with **1-YO'Bu** and **[1-YO'Bu][BAr^F]**. (26).

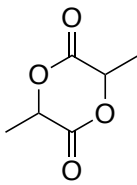
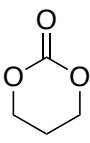
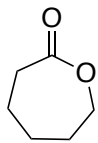
Monomer	LA 	TMC 	CL 
1-YO^tBu	74% 3 h.	99% 5 min.	Not reported “slow”
[1-YO^tBu][BAr^F]	0% 1h.	99% 5 min.	Not reported “slow”
3-YO^tBu	68% 2 h.	99% 5 min.	10% 30 h.
[3-YO^tBu][BAr^F]	0% 2 h.	99% 5 min.	0% 30 h.

Table 2-1: Contrasting polymerization rates

The polymerization results gathered suggest that modulation of ROP catalysis via ligand substitution in the ferrocene phosphinimine system is nil. The activities of **1-YO^tBu** and **3-YO^tBu** towards TMC and LA are essentially the same. These negligible differences allude to the robust electronic properties of these catalysts, in particular the strength of the metal-ligand interaction. This interaction may be too strong for electronegativity perturbations from the ligand to have any effect.

Although the reactivities of both catalysts are similar, orthogonality was shown between lactide and ϵ -caprolactone. Thus, the synthesis of block copolymers is feasible with the **3-YO^tBu** system. As can be observed in Table 3, the amount of time associated with the inactivity of CHO

is sufficient for LA to be polymerized. Therefore, it is feasible that the polymerization of LA could run to completion before the catalysts is switched and CHO polymerized, resulting in block copolymerization. It is likely that **1-YO'Bu** would also exhibit this orthogonality as well, since a small perturbation in activity was found with alterations in the ligand scaffold. Although the ligand scaffold used in these experiments seemingly disallowed ligand substitution as a modality of ROP control, nonetheless, alternative modifications may have an effect on ROP kinetics.

Subchapter 2 F. Lewis Acidity

In the 2011 Diaconescu paper, **1-InOPh** was synthesized (Figure 9) and its activity towards ROP catalysis was shown to be less than **1-YO'Bu**. However, as mentioned previously, **1-InOPh** exhibited obverse modulation of reactivity upon oxidation. It was hypothesized that for **1-YO'Bu** the activation barrier for alkoxide migration and ring-opening (steps i and ii in Figure 3) increase upon oxidation, a consequence of increasing the electrophilicity of the metal center (26). On the other hand, the activation barrier corresponding to the coordination of LA was hypothesized to decrease upon oxidation. This posits a scenario in which oxidation causes LA to coordinate strongly with [**1-YO'Bu**][**BAr^F**], whereupon the system ceases in this static state. The reactivity of **1-YO'Bu** and [**1-YO'Bu**][**BAr^F**] with TMC parallels the reactivity with LA; the modulation of the kinetics as a result of oxidation are in the same direction. With **1-InOPh**, the dynamic is hypothesized to be the obverse of **1-YO'Bu**: the increase in electrophilicity affects stronger coordination to TMC, in addition to lowered energy barriers for migration and ring-opening. These findings allude to optimal regimes of Lewis acidity – i.e. switch domains. In regard to this work, an investigation into ligand substitution effects would provide an additional handle to understand the spectrum of Lewis acidity that ROP catalysis operates within.

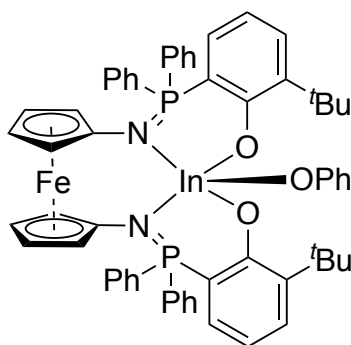


Figure 3-1: 1-InOPh

The effects of ligand substitutions have been conducted regarding aluminum complexes towards ROP of CL (46). Tolman *et al.* suggested that such modulation is case-dependent. Both an increase and decrease in electron density resulted in a decrease of reactivity. The unexpected substituent effects found in this study also allude to the small margins – switch domains – of Lewis acidity that are operative during ROP. Moreover, these findings provide additional evidence that “off” regions on a Lewis acidity spectrum can lie to the left of “on” regions. The aim of the work presented in this thesis, in principle, could provide additional evidence for the findings in the Tolman paper.

Discovering similar directionality in the phosfen-based systems would allude to the existence of an optimized Lewis acidity at the metal center. Modulation of this sort, however, has yet to be observed in the **1-YO’Bu** and **3-YO’Bu** systems. Although no substituent effects have been observed thus far, ascertaining a contrast between more and less electronegative ligand environments – corroborated by computational studies and redox potentials via cyclic voltammetry – would provide an experimental handle to probe these energy barriers; specifically, if ligand substitution can shift these catalysts along the spectrum of Lewis acidity, then switch domains can

be qualitatively surmised. The purported hypothesis of the original yttrium phosfen work can be corroborated by such an investigation. Unfortunately, evidence suggests that ligand substitution cannot impart enough change in the Lewis acidity of the catalysts.

Subchapter 2 G. Alkoxide Ligand

In comparing the metal dependence of redox control over ROP, the choice of alkoxide ligand would ideally remain unchanged. However, some alkoxide ligands are restricted due to synthetic inaccessibility. Nonetheless, an investigation into the effects of altering the alkoxide ligand on polymerization kinetics is important, because the alkoxide ligands is an extraneous parameter when considering the metal-dependence of the polymerization rates found by Diaconescu *et al.*

A computational study of tin(IV) alkoxide systems was conducted by Nawee Kungwan *et al.* (47). Their findings indicate that the nucleophilicity of the bound alkoxide ligand parameterizes the reactivity of their catalysts. The nucleophilicity of the alkoxide would feasible decrease the energy barrier corresponding to the alkoxide attack at the carbonyl, thereby decreasing the rate of initiation. Thus, the effects of alkoxide on initiation kinetics need to be addressed as well, especially since different alkoxides are used in the yttrium and indium phosfen systems. This could be accomplished by synthesizing both phenoxide and *tert*-butoxide variants of the yttrium and indium phosfen complexes and contrasting the resulting activities.

Chapter 3. Experimental Section

Most air-sensitive reactions were carried out within an MBraun drybox, achieving an atmosphere with less than 1 ppm of O₂ and H₂O. Air-sensitive reactions that required heating were performed using standard Schlenk techniques. If not otherwise stated, reactions were thus carried out within a drybox. Solvents were purified via Grubbs method – two-column solid-phase purification, then subsequently transferred to the drybox within an air-free bomb (27). All glassware used inside the box had previously been stored within an oven at least at 425 K for a minimum time of 2 hours. All chemicals, unless explicitly described herein, were purchased from commercial sources and used as received (excluding the drying of NMR, Cambridge Isotope Laboratories' solvents, which were dried and stored over activated molecular sieves). NMR experiments were performed at ambient conditions with Bruker AV-300.

Subchapter 3 A. Synthesis of 1,1'-diazidoferrocene (A)

1,1'-dilithioferrocene (28)

Tetramethylethylenediamine (TMEDA, 7.500 g, 64.52 mmol) was solubilized, along with ferrocene (10.000 g; 53.7 mmol), in hexanes (250 mL) and stirred. Subsequently, ⁿBuLi (2.0 M solution in hexanes, 56 mL, 113 mmol) was added dropwise over an hour. The reaction was allowed to stir overnight. Thereafter, the slurry was filtered over a medium frit, resulting in the isolated, orange solid (13.640 g, 80%).

1,1'-dibromoferrocene (29)

Inside the drybox, 1,1'-dilithioferrocene (10.690g, 34.1 mmol) was solubilized and stirred in diethyl ether. An addition funnel loaded with a mixture of 1,1,2,2-tetrabromoethane (25.90g, 74.9mmol) was mounted onto the round bottom flask containing the 1,1'-dilithioferrocene/ether mixture, inside the drybox. This setup was taken out of the drybox and cooled to -78 °C over the course of 3 hours, whereupon the reaction was warmed to room temperature and allowed to stir overnight. The reaction was quenched with water and stirred for 30 minutes. The resultant biphasic slurry was extracted three times with diethyl ether (50 mL), dried with anhydrous magnesium sulfate and filtered over Celite using a frit. The solvent was, thereafter, removed via reduced pressure, resulting in brown precipitate. Recrystallization was performed in methanol to purify the product (8.823g, 75.3%): ¹H NMR (CDCl₃, 300 MHz, ppm): δ 4.42 (t, *J* = 1.3 Hz, 4H, CpH), 4.17 (t, *J* = 1.3 Hz, 4H, CpH).

1,1'-diazidoferrocene (30)

In the dark, 1,1'-dibromoferrocene (5.2200 g, 19.68 mmol) was mixed with copper (I) chloride (2.283 g, 23.06 mmol), ethanol (150 mL), and sodium azide (2.9607 g, 45.52 mmol) in 50 mL of water. The reaction flask was wrapped with foil to prevent light exposure. The reaction was allowed to run for 72 hours. Afterwards, quenching was accomplished with the addition of water 150 mL; this solution was then extracted with diethyl ether (100 mL) three times. The extracted mixture was then dried with magnesium sulfate and filtered through Celite on a frit. Diethyl ether was removed via reduced pressure and the resultant crystals were recrystallized in pentane, isolating the product (2.337 g, 68%): ¹H NMR (CDCl₃, 300 MHz, ppm): δ 4.35 (t, *J* = 1.3 Hz, 4H, CpH), 4.16 (t, *J* = 1.8 Hz, 4H, CpH).

Subchapter 3 B. 2-(*tert*-butyl)-6-(diphenylphosphaneyl)-4-methoxyphenol (B)

2-bromo-6-(*tert*-butyl)-4-methoxyphenol (31)

2-*tert*-butyl-4-methoxyphenol (2.0072 g, 11.09 mmol) was solubilized in dichloromethane (200 mL), cooled to 0 °C, then bromine (0.57 mL, 11.09 mmol) was added dropwise over the course of 2 hours. This mixture was allowed to stir for two days. Dichloromethane was then removed via reduced pressure and the product mixture was dissolved in diethyl ether (100 mL) and neutralized with an aqueous, saturated sodium bicarbonate solution (100 mL). The organic layer was isolated, and the aqueous layer was extracted with ether (50 mL). Anhydrous magnesium sulfate was then used to dry the ether solution. Reduced pressure removed diethyl ether and chromatography (97.5/2.5 = Petroleum Ether/Et₂O) was used to isolate the product (1.010 g, 35%): ¹H NMR (300 MHz, CDCl₃, δ (ppm)): 6.88 (d, *J* = 3.0 Hz, 1H, *CH*), 6.85 (d, *J* = 3.0 Hz, 1H, *CH*), 5.44 (s, 1H, *OH*), 3.75 (s, 3H, *OCH*₃), 1.39 (s, 9H, C(*CH*₃)₃).

2-(*tert*-butyl)-6-(diphenylphosphaneyl)-4-methoxyphenol (31)

2-bromo-6-(*tert*-butyl)-4-methoxyphenol (1.1002 g, 4.25 mmol) was solubilized in ether (5 mL) and cooled to -78 C; afterwards, ⁿBuLi (2 eq., 1.6 M) was slowly added dropwise. White precipitate formed upon the addition of 1 ⁿBuLi. The solution was allowed to stir for 2 hours, then PPh₂Cl (0.9367 g, 1 eq.) was added dropwise, resulting in a color change. The reaction was allowed to stir overnight. The mixture was filtered over a frit and precipitate was suspended in diethyl ether, taken out of the drybox, and quenched with the addition of 1 M HBF₄ solution. This mixture was then extracted with diethyl ether (50 mL) three times, dried with magnesium sulfate. Diethyl ether was then removed via reduced pressure, resulting in an oil (0.634 g, 48%): ¹H NMR

(300 MHz, CDCl₃, δ (ppm)): 7.39 (m, 10H, CH(PPh₂)), 6.97 (d, $J = 3.0$ Hz, 1H, CH), 6.61 (d, $J = 10.0$ Hz, 1H, OH), 6.36 (dd, $J = 5.0$ Hz, $J = 3.0$ Hz, 1H, CH), 3.59 (s, 3H, OCH₃), 1.41 (s, 9H, C(CH₃)₃); ³¹P NMR (121.5 MHz, CDCl₃, δ (ppm)): -29.2 (s, 2P)

Subchapter 2 C. Synthesis of 2-(*tert*-butyl)-6-(diphenylphosphaneyl)-4-fluorophenol

2-(*tert*-butyl)-4-fluorophenol (32)

Outside the drybox, 4-fluorophenol (4.982 g, 44.44mmol) was dissolved in DCM and *tert*-butanol (5.9 mL, 62.22 mmol) was added along with concentrated sulfuric acid (3.2 mL, 53.33 mmol). The reaction was stirred overnight. The reaction was washed with water, neutralized with NaHCO₃, dried over MgSO₄. The product (2.432g, 30%) was purified by column chromatography (10:90 EtOAc:C6): ¹H NMR (CDCl₃, 300 MHz): δ 6.70 (m, 1H, CH); 6.74 (m, 1H, CH), 6.61 (m, 1H, CH) 5.00 (s, 1H, OH); 1.39 (s, 9H, C(CH₃)₃). ¹⁹F NMR spectrum (CDCl₃, 282 MHz): δ -124.1 (s, 1F).

2-bromo-6-(*tert*-butyl)-4-fluorophenol

Outside the drybox, 2-(*tert*-butyl)-4-fluorophenol (1.734 g, 10.28 mmol) was dissolved in acetonitrile and cooled to 0 °C. N-bromosuccinimide (1.927 g, 1.05 eq) was added portion wise and the reaction was allowed to slowly warm to room temperature and stir for 12 h. The product was extracted with hexanes and filtered through Celite on a frit. Acetonitrile was removed yielding a yellow-brown oil (0.4620 g, 32%). The product (0.967g, 39%) was purified by column chromatography (hexanes/ethyl acetate = 95/5): ¹H NMR (CDCl₃, 300 MHz): δ 7.10 (m, 1H, CH); 7.00 (m, 1H, CH), 5.60 (s, 1H, OH), 1.39 (s, 9H, C(CH₃)₃). ¹⁹F NMR spectrum (CDCl₃, 282 MHz): δ -122.3 (s, 1F).

2-(*tert*-butyl)-6-(diphenylphosphaneyl)-4-fluorophenol

2-bromo-6-(*tert*-butyl)-4-fluorophenol (1.1004 g, 4.45 mmol) was dissolved in diethyl ether and cooled to -78 °C. ⁿBuLi (1.6M, was added dropwise and the solution was allowed to stir for another 1 hour at -78 °C. Chlorodiphenylphosphine was added dropwise and the solution was allowed to slowly warm to room temperature and stir for 16 hours. Saturated NH₄Cl solution and Et₂O were added to the reaction flask. The organic layer was separated, dried over MgSO₄ and the solvent was removed, yielding xxxx: ¹H NMR (C₆D₆, 300 MHz): δ 7.37 (m, 5H, PPhH), 7.52 (m, 5H, PPhH), 7.10 (m, 1H, CH), 7.00 (m, 1H, CH), 5.60 (s, 1H, OH), 1.39 (s, 9H, C(CH₃)₃). ¹⁹F NMR spectrum (CDCl₃, 282 MHz): δ -122.3 (s, 1F), ³¹P NMR (121 MHz, C₆D₆), δ (ppm): -30.5 (s).

Subchapter 2 D. Synthesis of 3-YO'Bu

1,10-di(2-*tert*-butyl-6-diphenylphosphazide-4-methoxyphenol)ferrocene

1,1'-diazidoferrocene (0.6030 g, 2.25 mmol) was added to a stirring solution of 2-(*tert*-butyl)-6-(diphenylphosphaneyl)-4-methoxyphenol (1.6391 g, 4.50 mmol) in 25 mL of toluene. Thereafter, the reaction was allowed to stir for an additional hour, then the solid was collected on a frit and dried yielding an orange-red solid (570 mg; 66%): ¹H NMR (300 MHz, C₆D₆), δ (ppm): 15.53 (s, 2H, OH), 7.80 (m, 8H, P(C₆H₅)₂), 7.27 (m, 2H, C₆H₃), 6.94 (m, 12H, P(C₆H₅)₂), 6.59 (m, 2H, C₆H₃), 4.03 (s, 4H, C₅H₄), 3.65 (s, 4H, C₅H₄), 3.30 (s, 6H, OCH₃), 1.74 (s, 18H, CCH₃), ³¹P NMR (121 MHz, 25 °C, C₆D₆), δ (ppm): -22.7 (s).

3-H₂

1,10-di(2-*tert*-butyl-6-diphenylphosphazide-4-methoxyphenol)ferrocene (570 mg, 0.57 mmol) was dissolved in toluene and added to a Schlenk flask. The reaction was heated to 50 C for 5 hours, then the solvent was removed. The resulting yellow powder was washed with toluene to give the product as a crystalline yellow-orange powder (0.3360 g, 61%): ¹H NMR (300 MHz, C₆D₆), δ (ppm): 15.38 (s, 2H, OH), 7.71 (m, 8H, P(C₆H₅)₂), 7.26 (m, 2H, C₆H₃), 6.94 (m, 12H, P(C₆H₅)₂), 6.48 (m, 2H, C₆H₃), 3.92 (s, 4H, C₅H₄), 3.54 (s, 4H, C₅H₄), 3.20 (s, 6H, OCH₃), 1.74 (s, 18H, CCH₃), ³¹P NMR (121 MHz, 25 C, C₆D₆), δ (ppm): -22.7 (s).

3-Na₂

3-H₂ (0.1003 g, 0.11 mmol) was dissolved in 10 mL of THF and a slurry of excess sodium hydride in THF was added to the reaction while stirring. This reaction was allowed to stir for 2 hours, then filtered and dried, yielding quantitative product (0.1080 g, 0.11 mmol)

3-YCl

3-Na₂ (0.1080g, 0.11mmol) was dissolved in 5 mL of THF. YCl₃·THF_{3.5} (0.0226 g, 0.17 mmol) was then added portion wise. The reaction was allowed to stir for 3 h, filtered through Celite, then the solvent was removed under reduced pressure. The resulting yellow solid (0.0822 g, 73%) was washed with hexanes and extracted with toluene: ¹H NMR (300 MHz, C₆D₆), δ (ppm): 7.76 (m, 8H, P(C₆H₅)₂), 7.36 (d, 2H, C₆H₃), 6.97 (m, 12H, P(C₆H₅)₂), 6.43 (m, 2H, OC₆H₃), 5.05 (s, 2H, C₅H₄), 3.80 (s, 4H, C₅H₄), 3.55 (s, 2H, C₅H₄), 3.29 (s, 6H, OCH₃), 1.54 (s, 18H, CCH₃), ³¹P NMR (121 MHz, 25 C, C₆D₆), δ (ppm): 31.0 (s).

3-YOMe

3-YCl (0.0822 g, 0.08 mmol) was dissolved in 5 mL of THF and cooled to 0 degrees centigrade. KO'Bu (0.0099 g, 0.09 mmol) was dissolved in THF as well. KO'Bu was slowly added to **3-YCl** and stirred for 1.5 hours, yielding **3-YO'Bu** (0.0670 g, 76%): ^1H NMR (300 MHz, C_6D_6), δ (ppm): 8.00 (m, 8H, $\text{P}(\text{C}_6\text{H}_5)_2$), 7.40 (d, 2H, OC_6H_3), 7.31 (m, 12H, $\text{P}(\text{C}_6\text{H}_5)_2$), 6.34 (m, 2H, OC_6H_3), 5.11 (s, 2H, C_5H_4), 3.81 (s, 4H, C_5H_4), 3.53 (s, 2H, C_5H_4), 3.29 (s, 6H, OCH_3), 1.61 (s, 18H, CCH_3), 1.53 (s, 9H, OCCH_3), ^{31}P NMR (121 MHz, 25 °C, C_6D_6), δ (ppm): 32.5 (s).

Subchapter 3 E. Redox Stability

Chemical redox stability was tested by adding 4.000 micromoles of **3-YO'Bu** (4.400 mg, 4.00 micromoles) to acetylferrocenium BAr^{F} (1 equivalent, 4.364 mg) in 2.0 mL of deuterated benzene. This mixture was stirred for one hour. ^1H NMR spectra were taken before addition and after 1 h. of stirring. Subsequently, excess cobaltocene was added to reduce $[\text{3-YO'Bu}][\text{BAr}^{\text{F}}]$ and a ^1H NMR spectrum was taken thereafter. All spectra can be found in the Appendix.

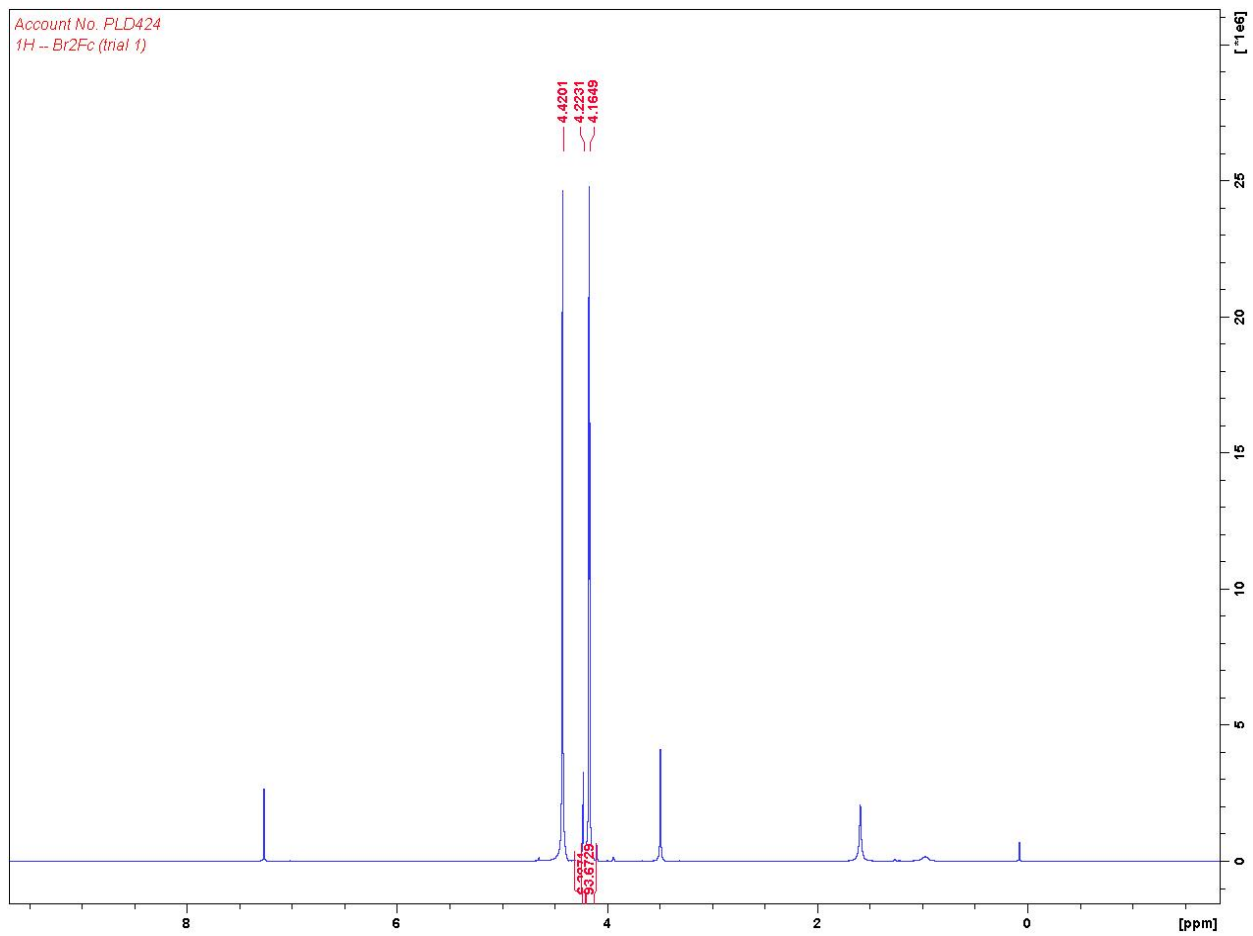
Subchapter 3 F. Polymerizations with 3-YO'Bu

All polymerizations were performed inside a 20 mL vial inside a drybox at 0.200 molar concentration of monomer (100 equivalents), 0.002 molar catalysts (1 equivalent, 4.404 mg, 4.00 micromoles), within 2.00 mL of solvent. 1,3,5-trimethoxybenzene (TMB) was used as an internal standard (13.455mg, 20 equivalents). Aliquots were taken at various times, quenched with hexanes (~1mL). After the addition of hexanes, both solvent and hexanes were removed under reduced

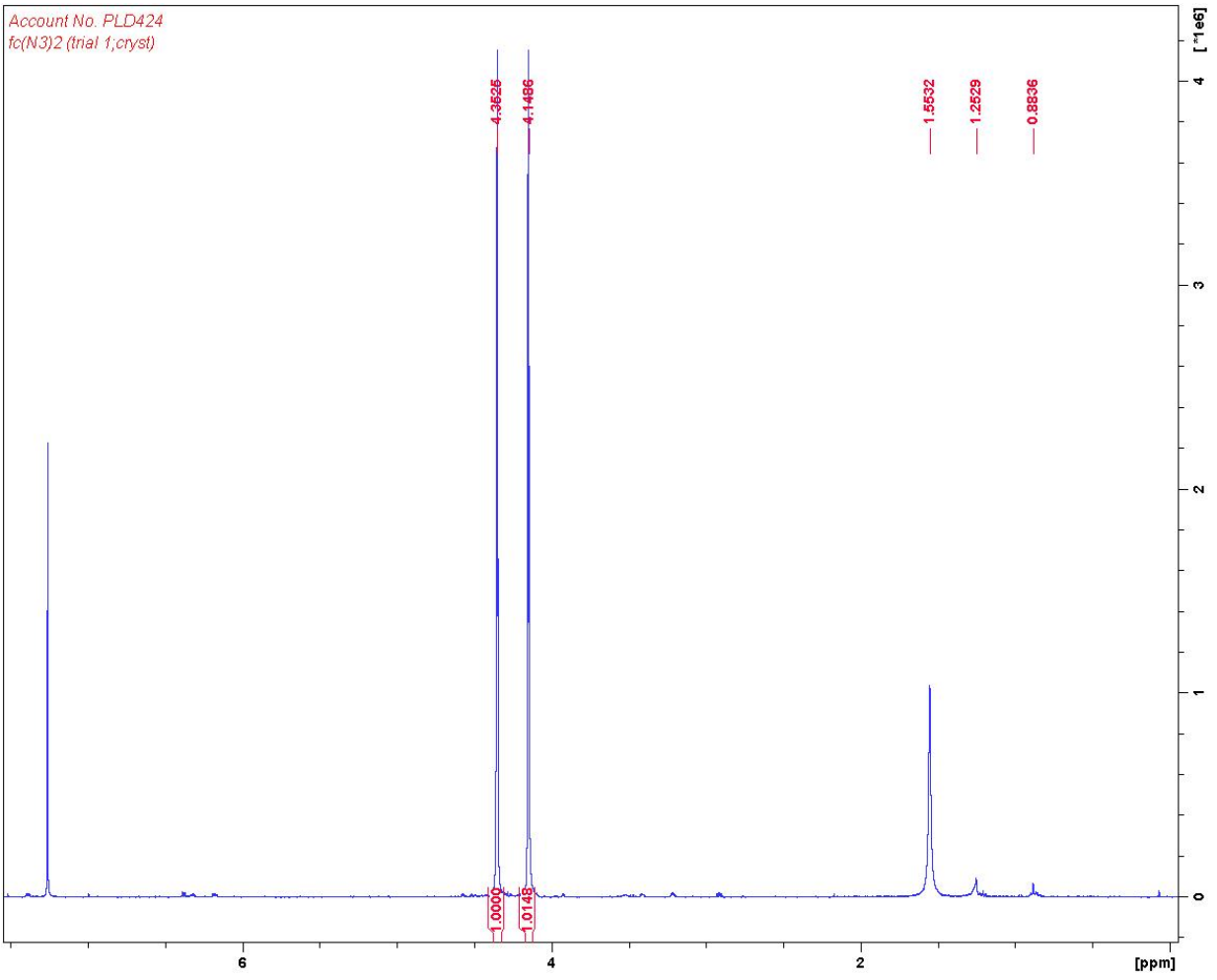
pressure. Acetylferrocenium BAr^{F} was used to oxidize **3-YO'Bu**. 1 equivalent of oxidant was mixed with **3-Y O'Bu** prior to the addition of both TMB and . Oxidation was given 30 minutes to occur while mixing in 1 mL of solvent, then TMB and the monomer were added.

Appendix

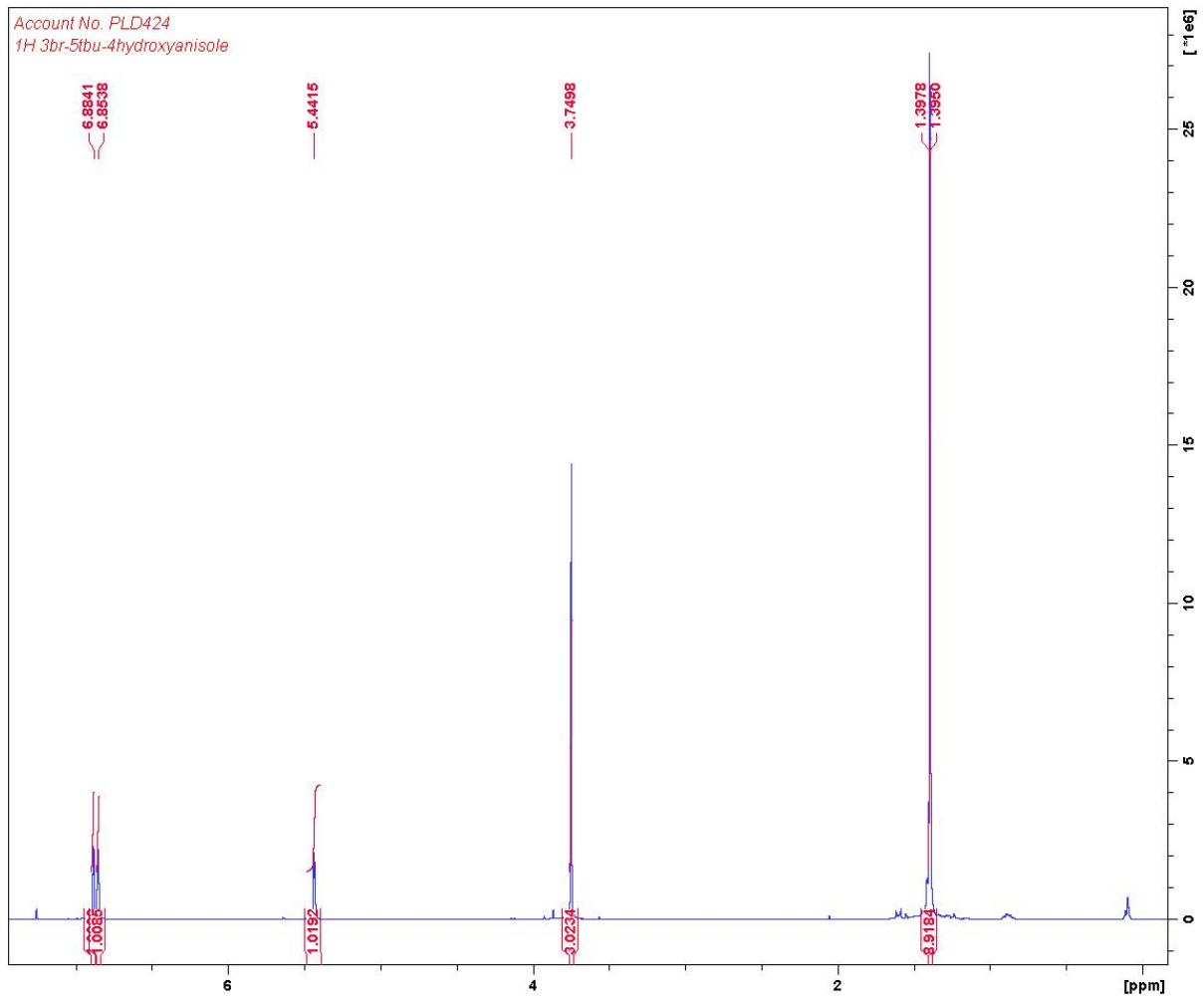
^1H NMR spectrum of 1,1'-dibromoferrocene



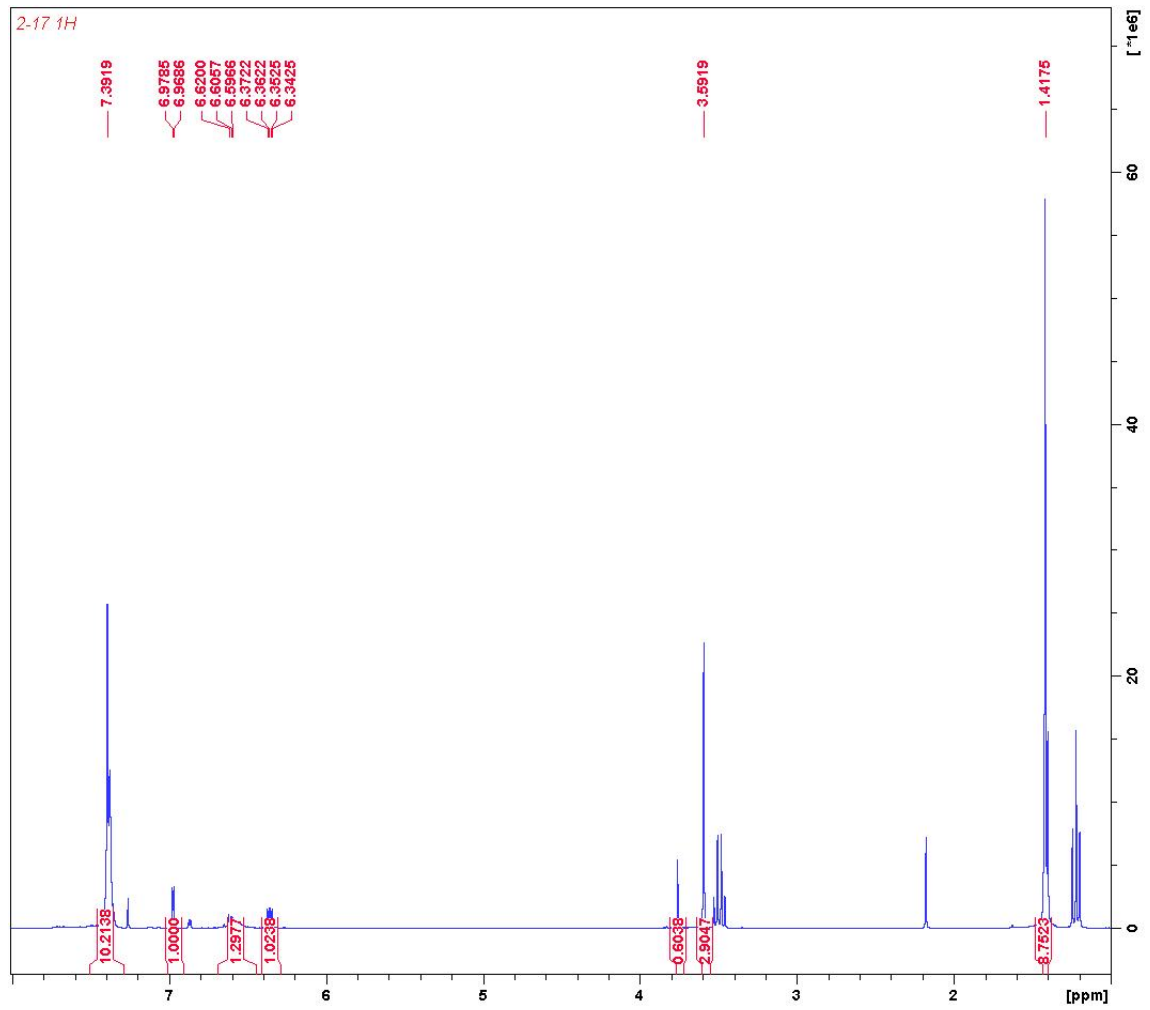
¹H NMR spectrum of 1,1'-diazidoferrocene



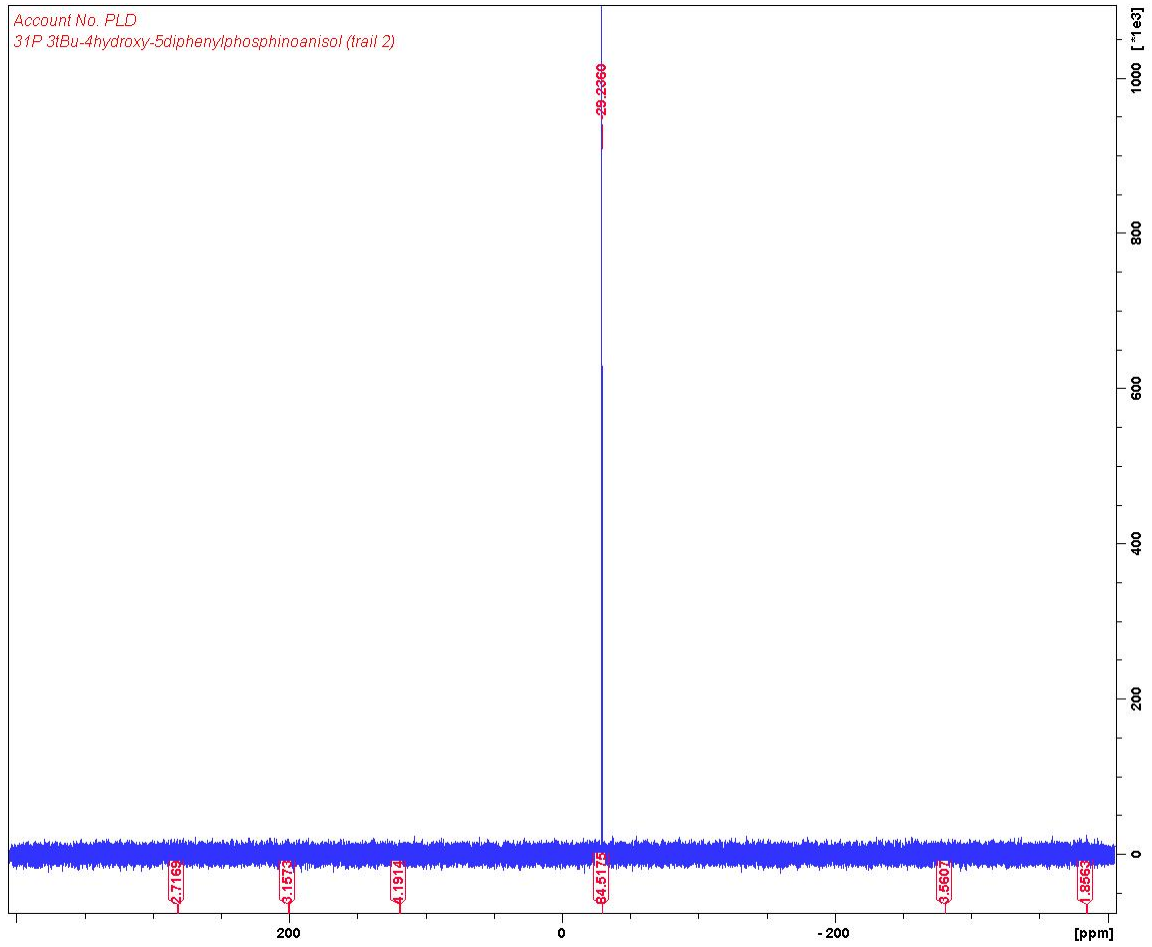
¹H NMR spectrum of 2-bromo-6-(*tert*-butyl)-4-methoxyphenol



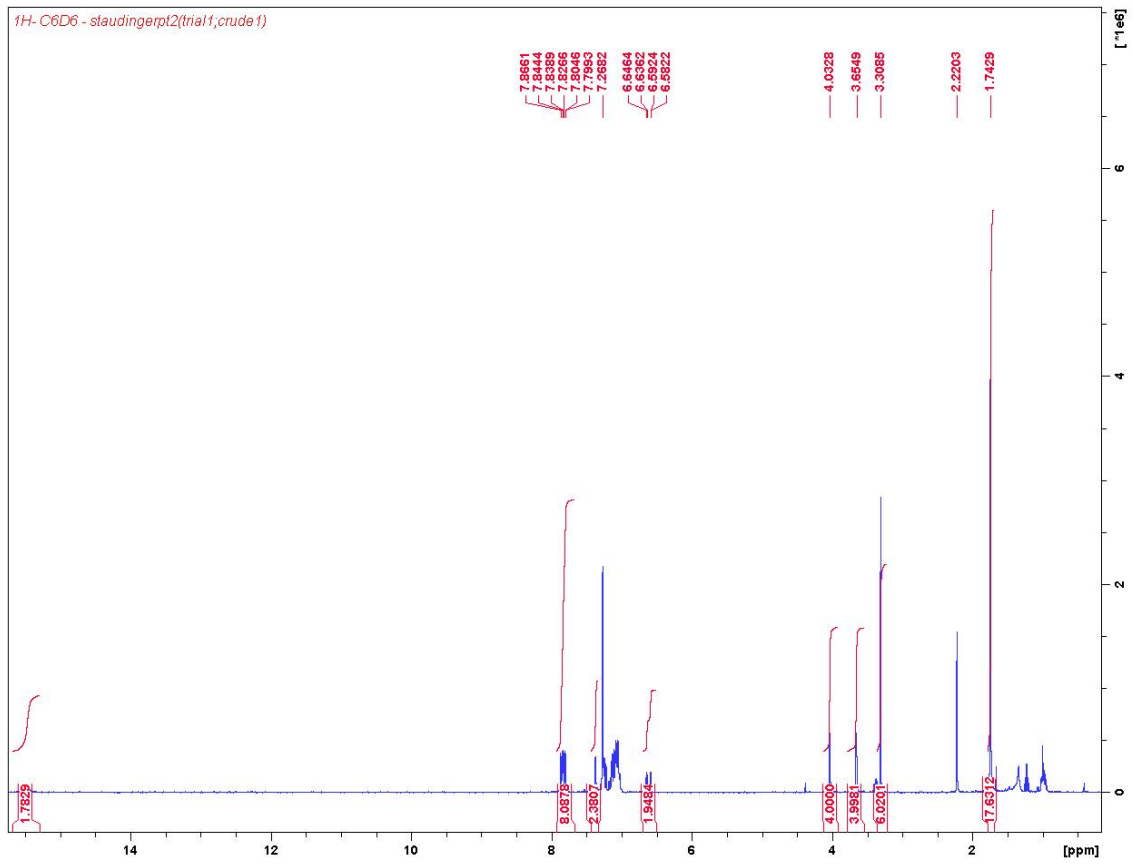
¹H NMR spectrum of 2-(*tert*-butyl)-6-(diphenylphosphaneyl)-4-methoxyphenol



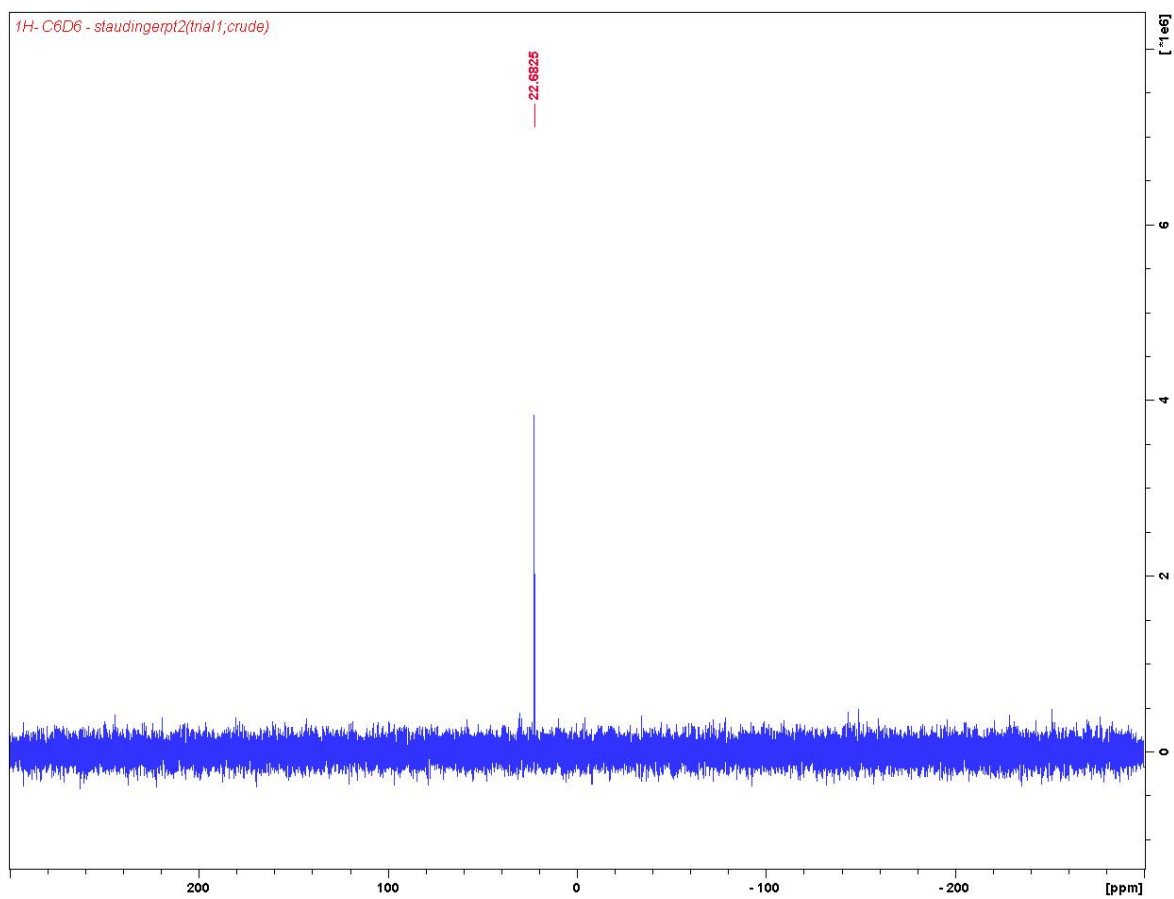
³¹P NMR spectrum of 2-(*tert*-butyl)-6-(diphenylphosphaneyl)-4-methoxyphenol



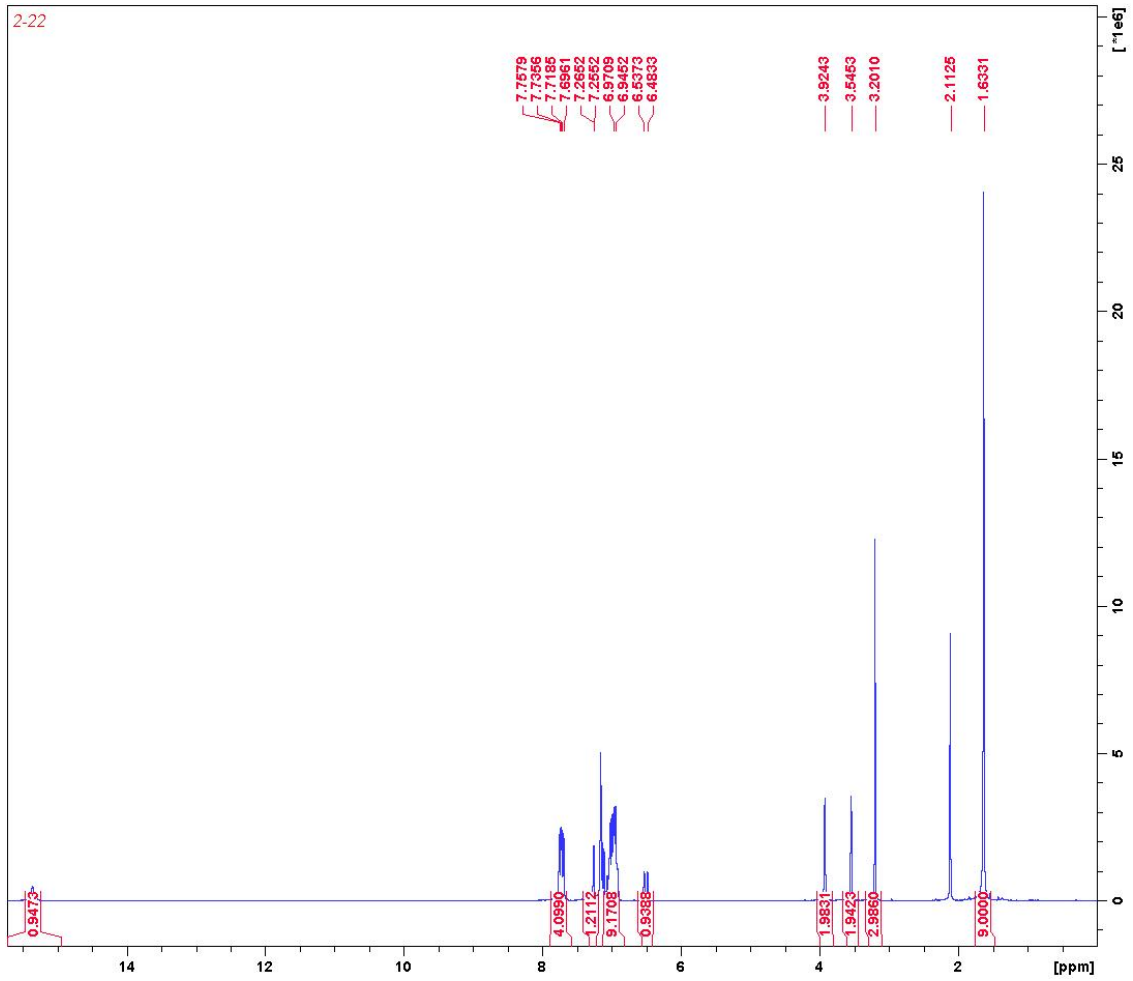
¹H NMR spectrum of 10-di(2-*tert*-butyl-6-diphenylphosphazide-4-methoxyphenyl)ferrocene



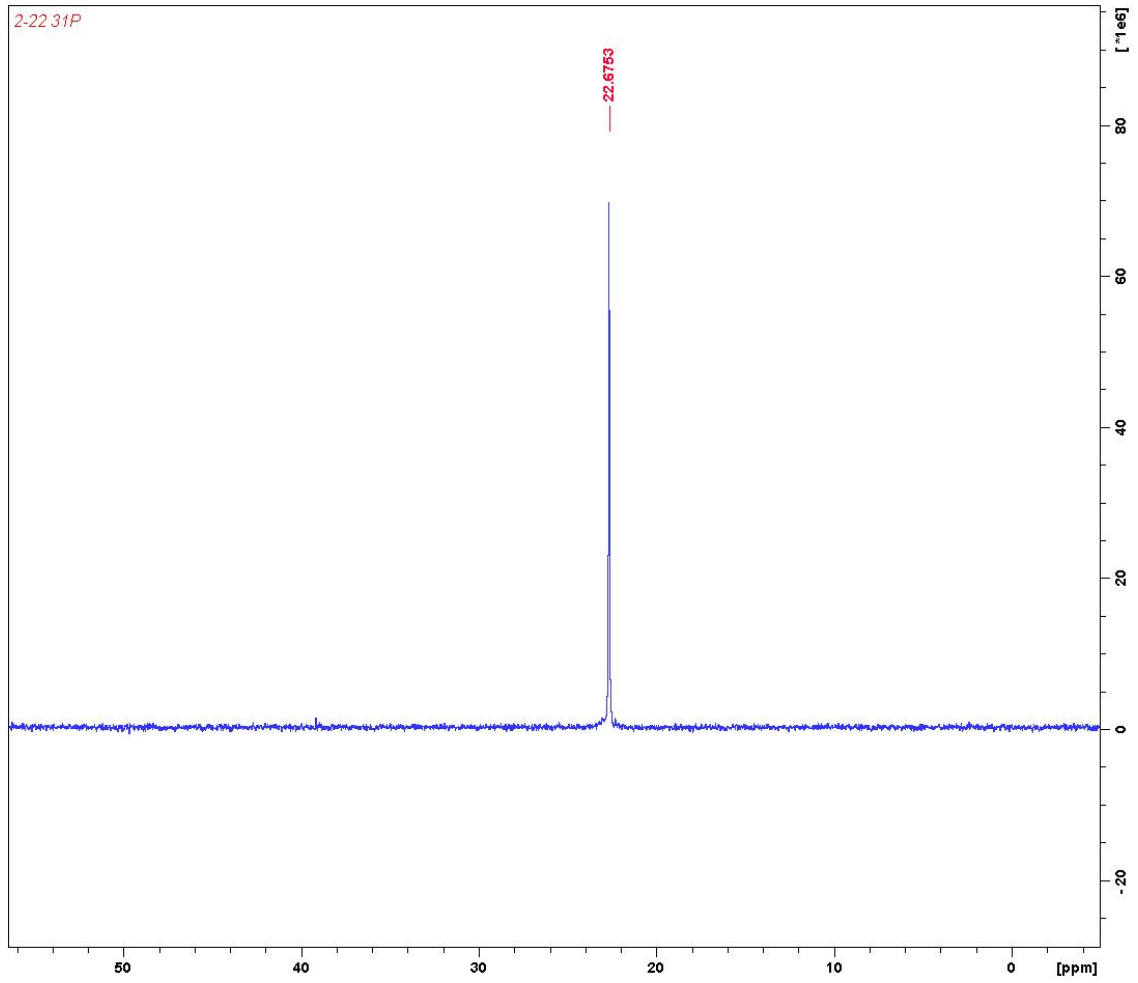
^{31}P NMR spectrum of 10-di(2-*tert*-butyl-6-diphenylphosphazide-4-methoxyphenol)ferrocene



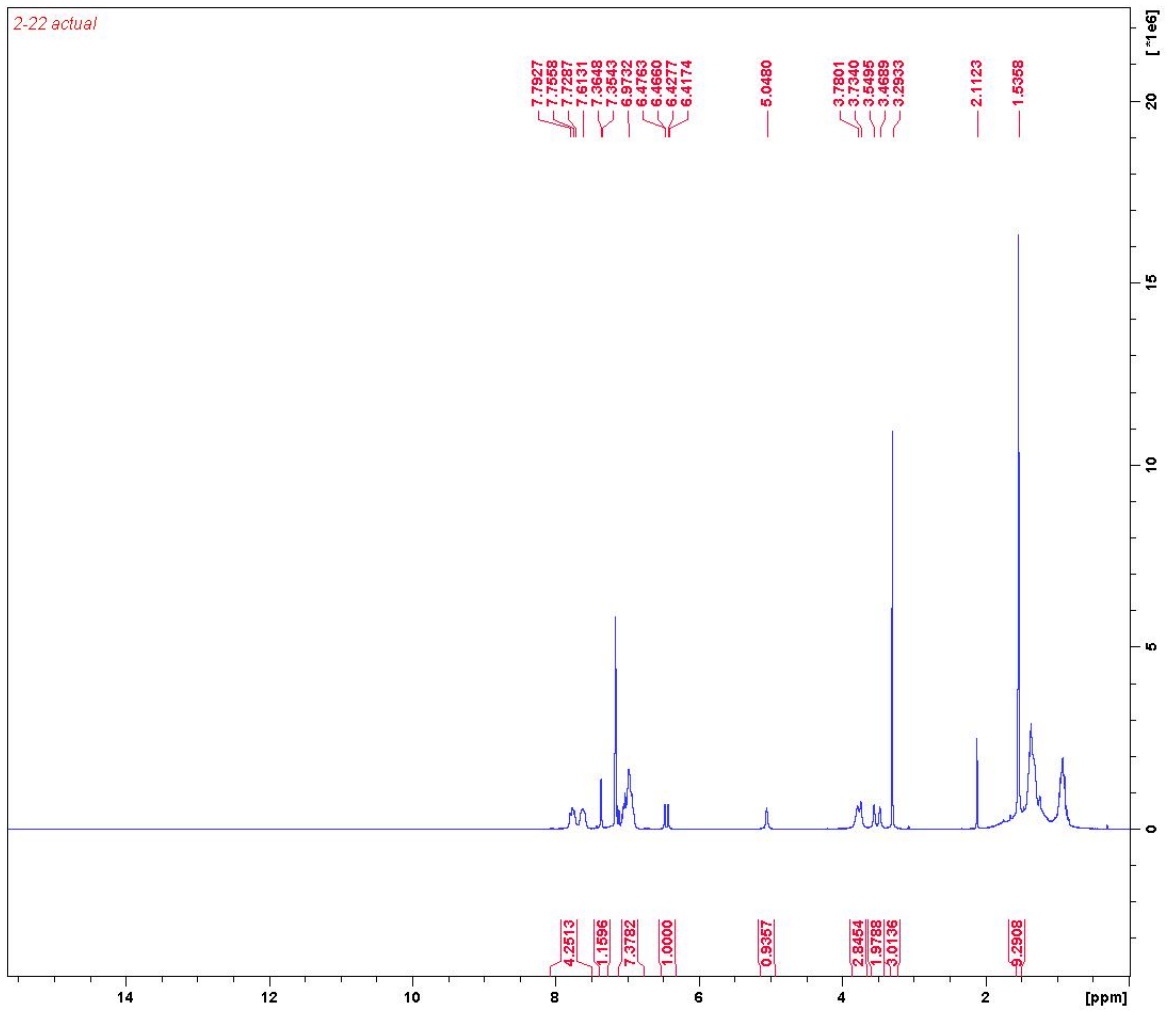
¹H NMR spectrum of 3-H2



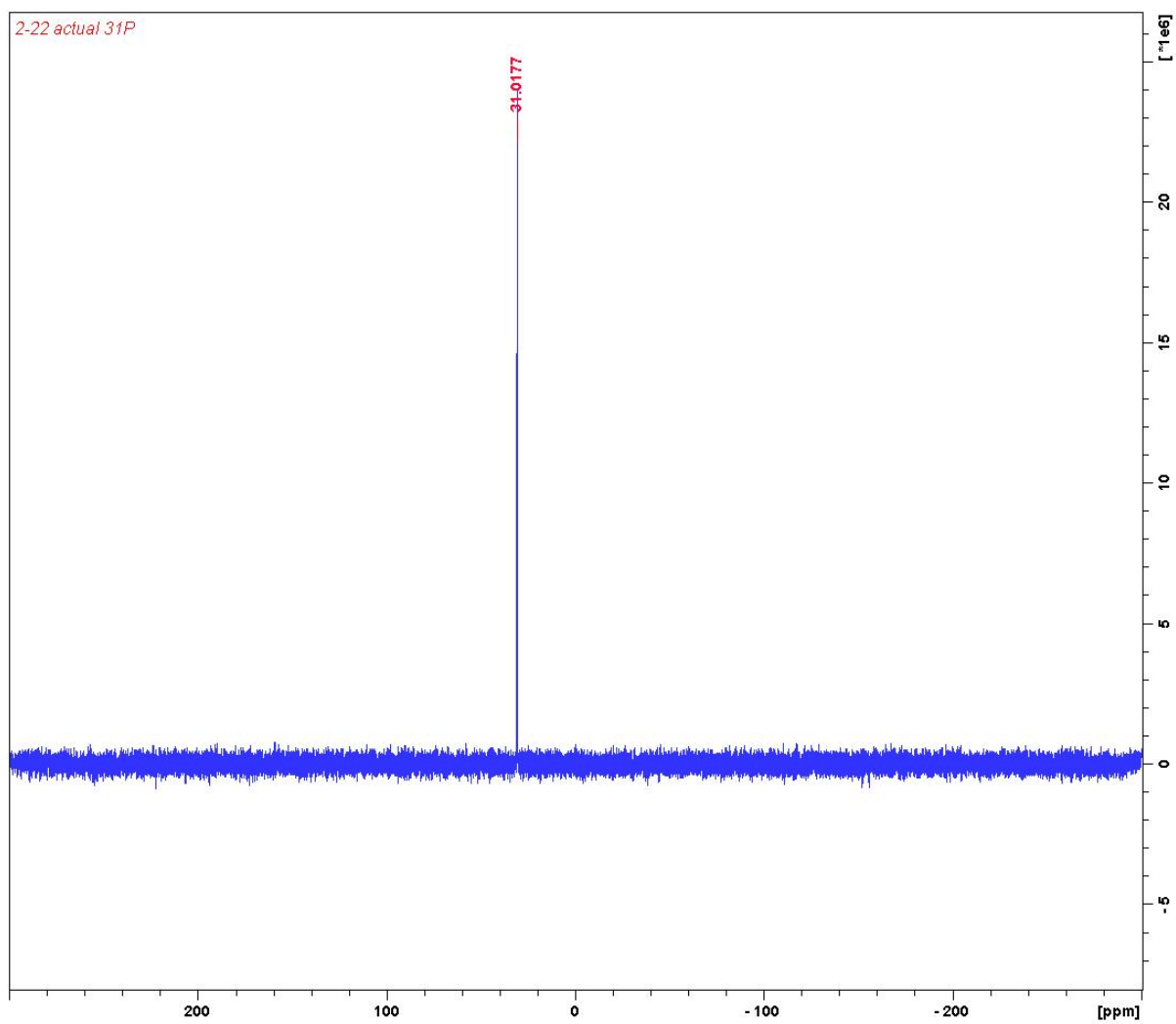
^{31}P NMR spectrum of 3-H2



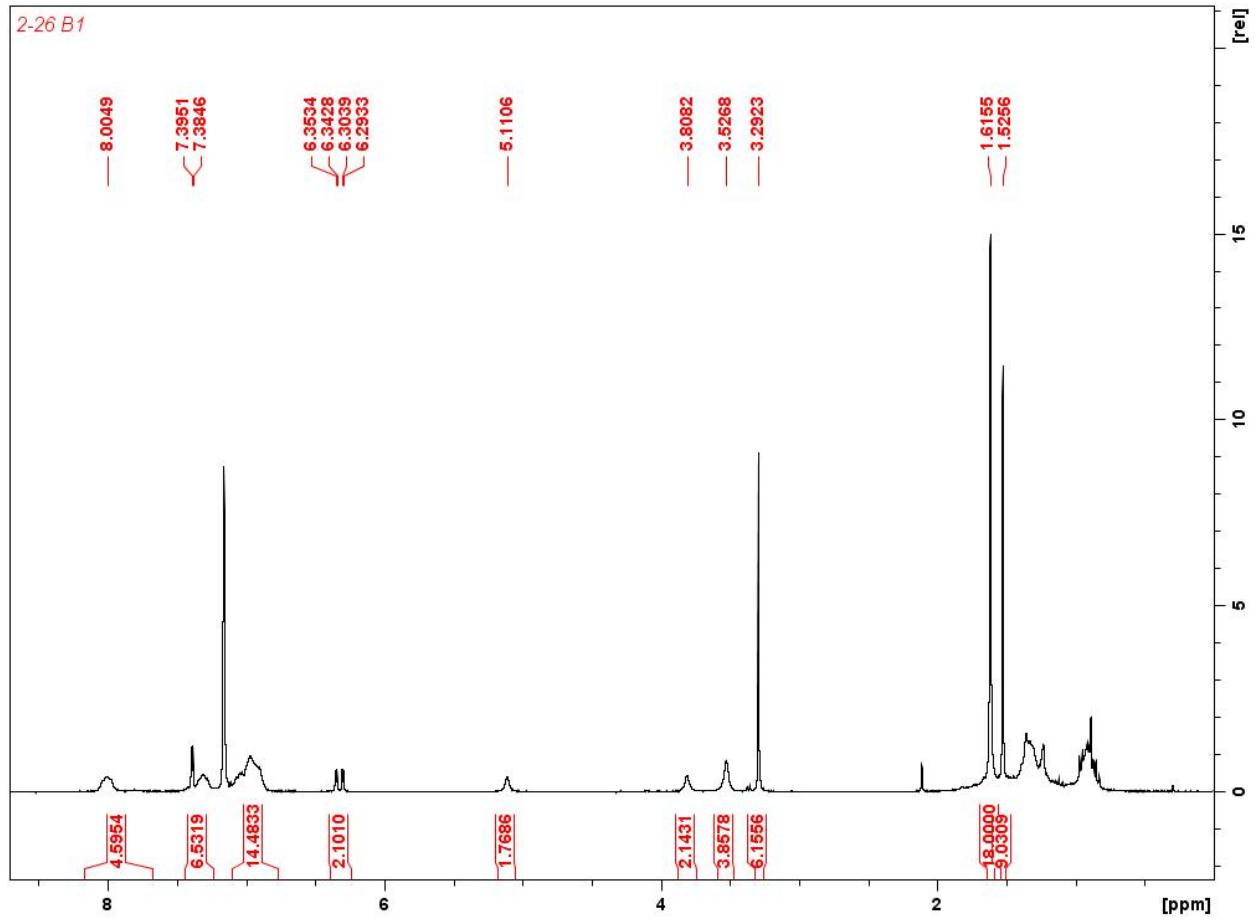
¹H NMR spectrum of 3-YCI



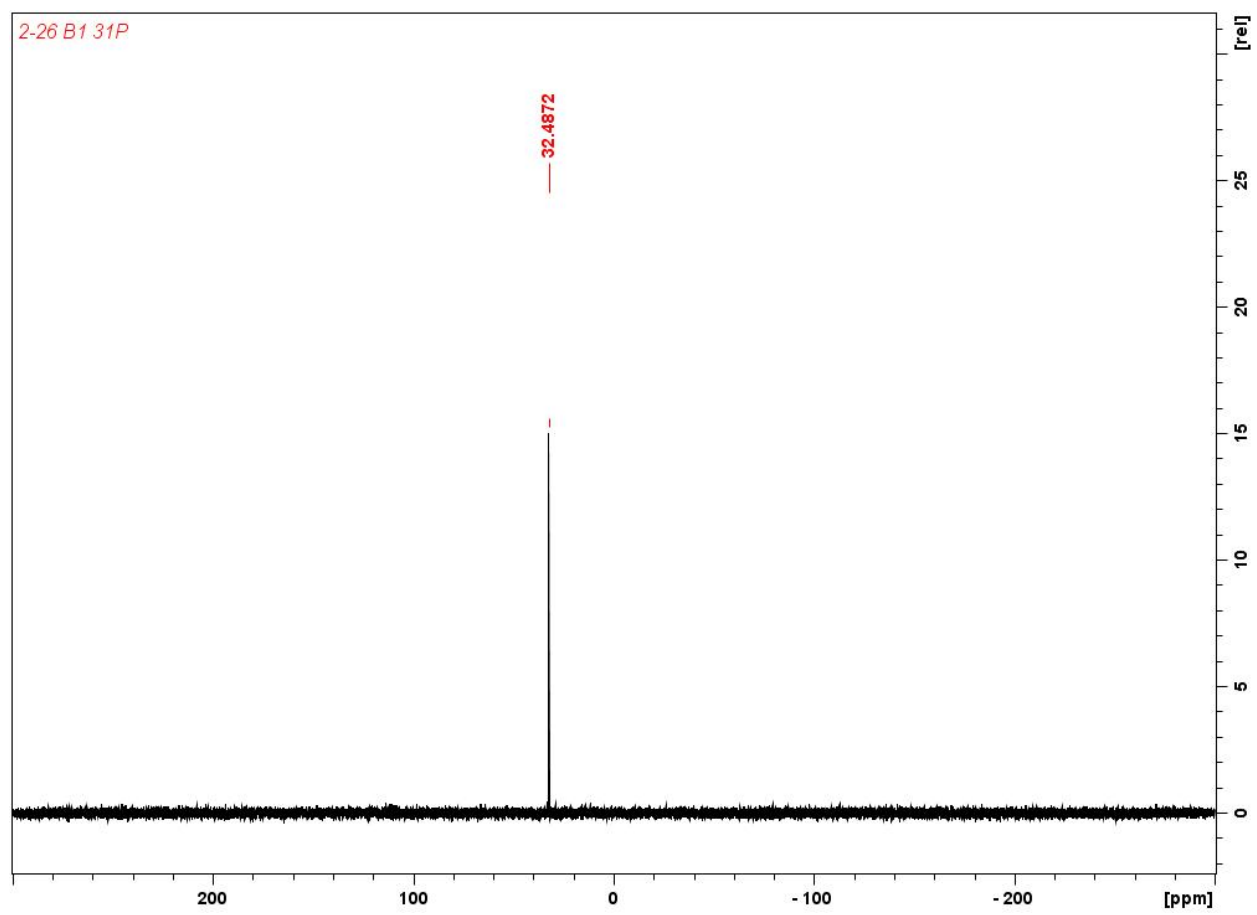
^{31}P NMR spectrum of **3-YCI**



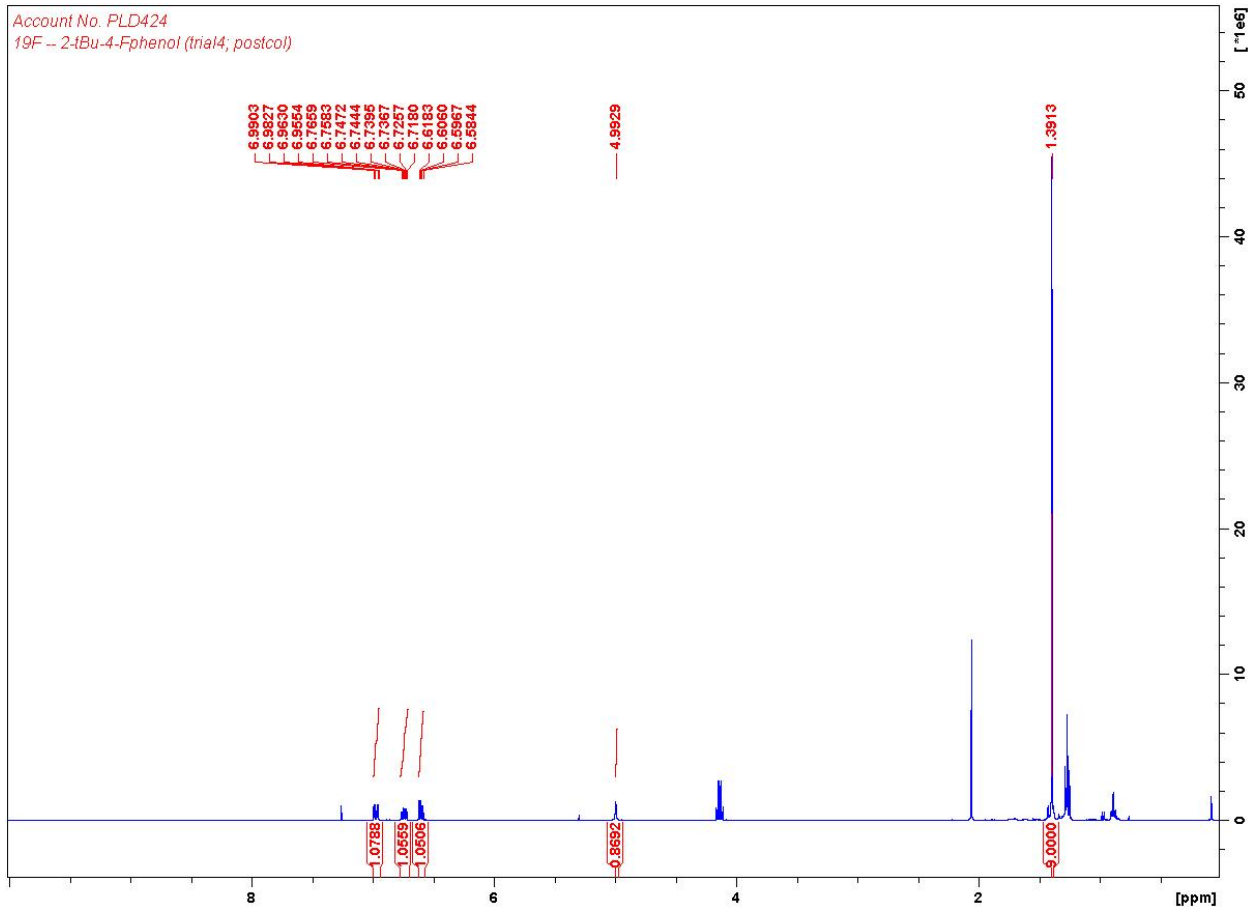
¹H NMR spectrum of 3-YOMe



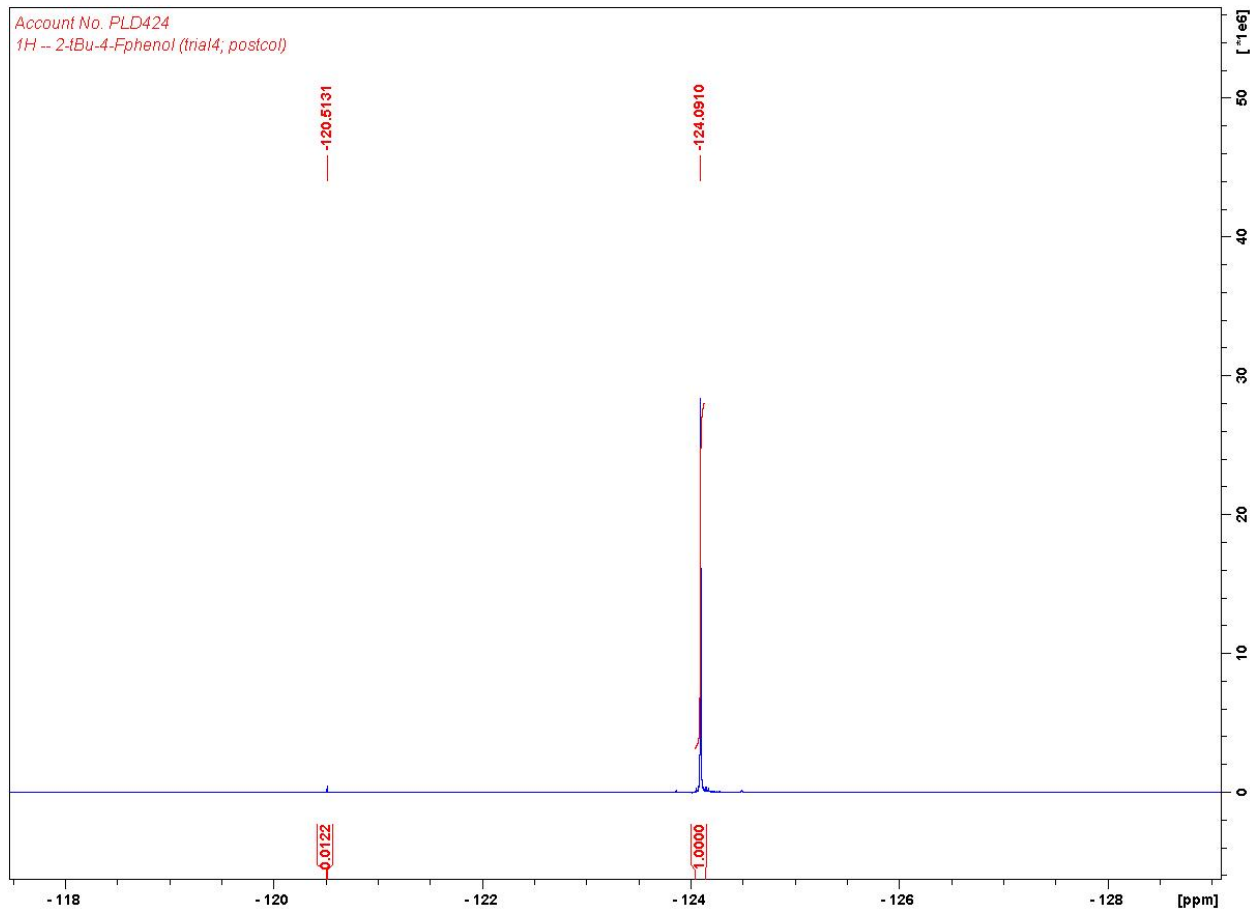
^{31}P NMR spectrum of 3-YOMe



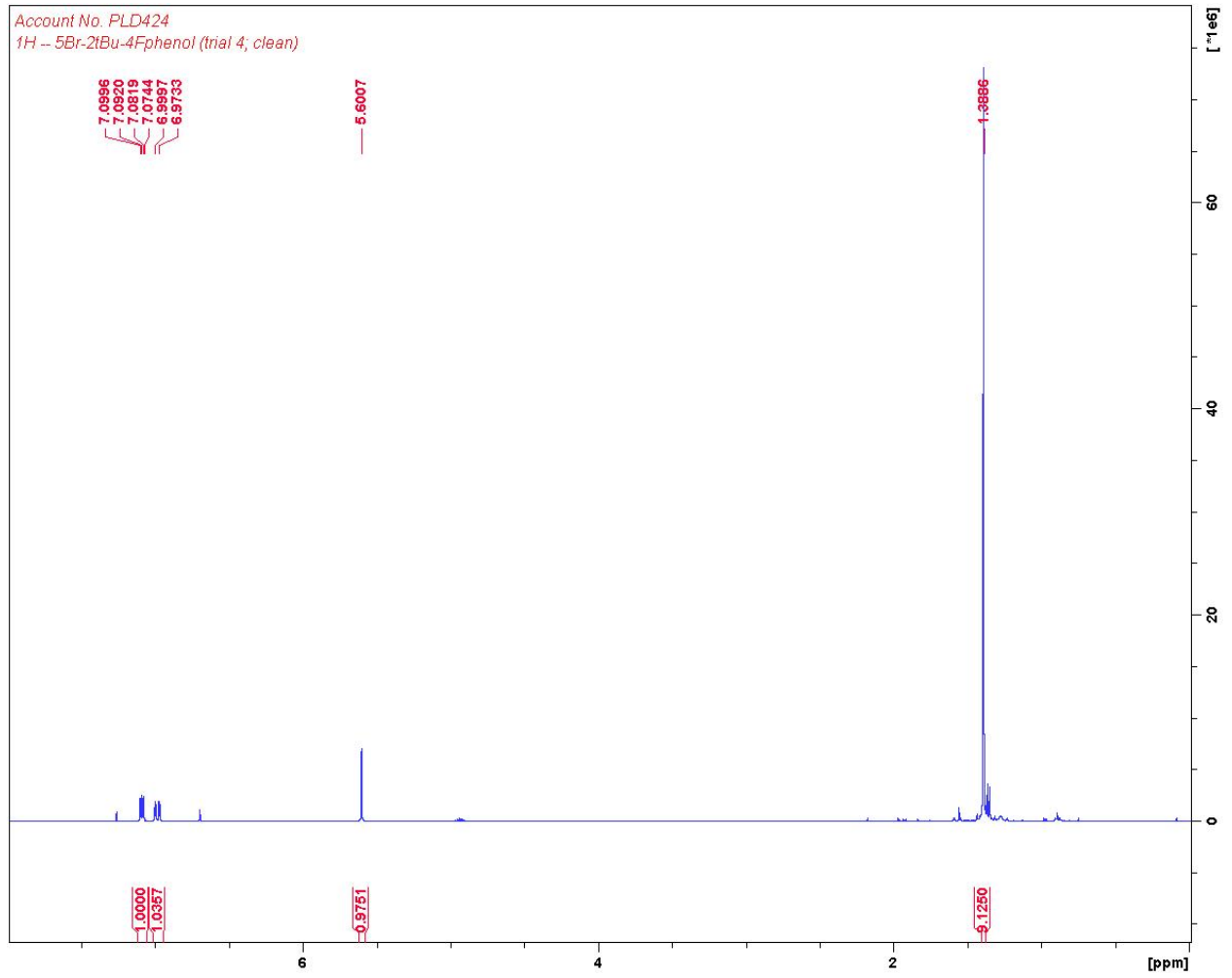
¹H NMR spectrum of 2-(*tert*-butyl)-4-fluorophenol



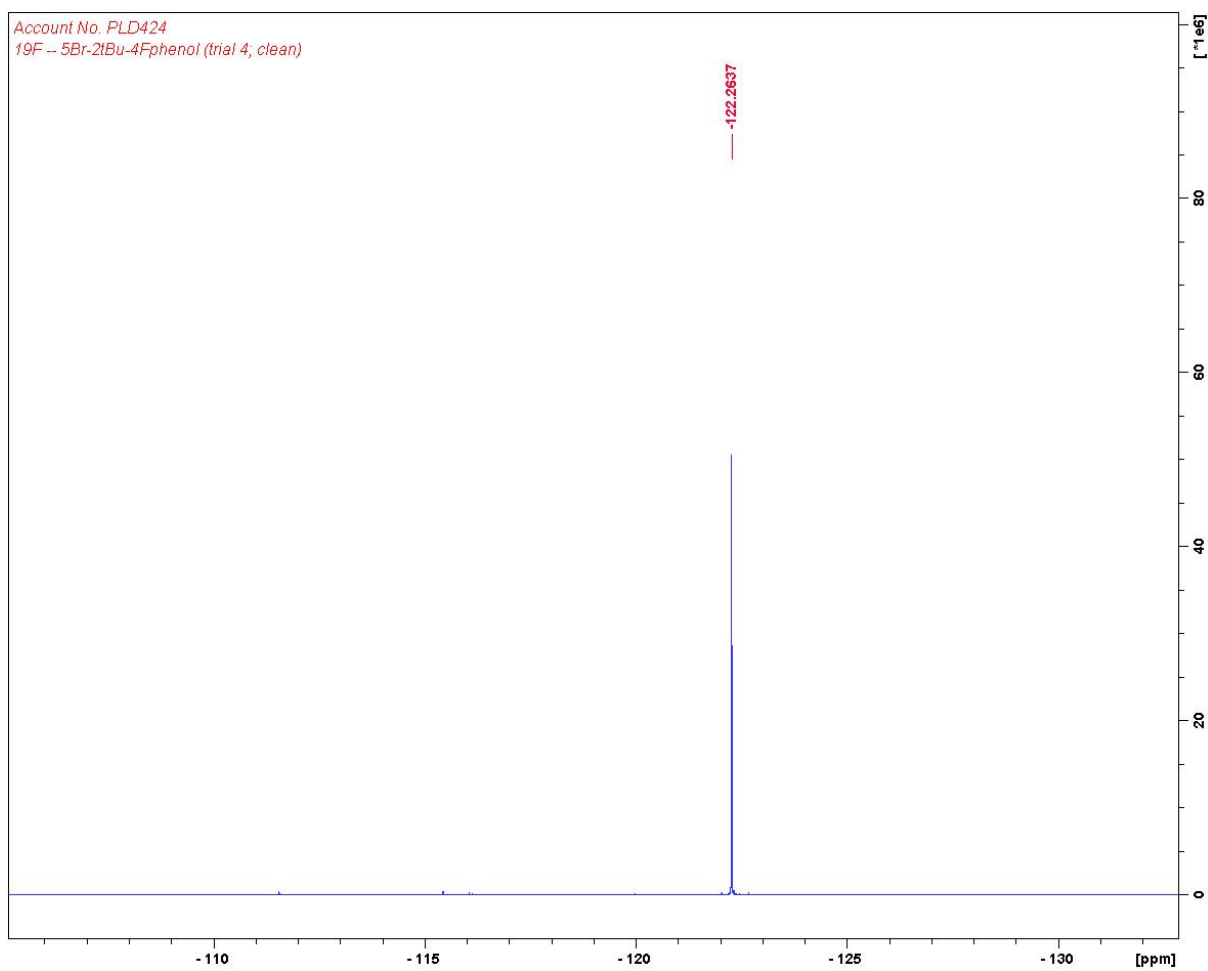
¹H NMR spectrum of 2-bromo-6-(*tert*-butyl)-4-fluorophenol



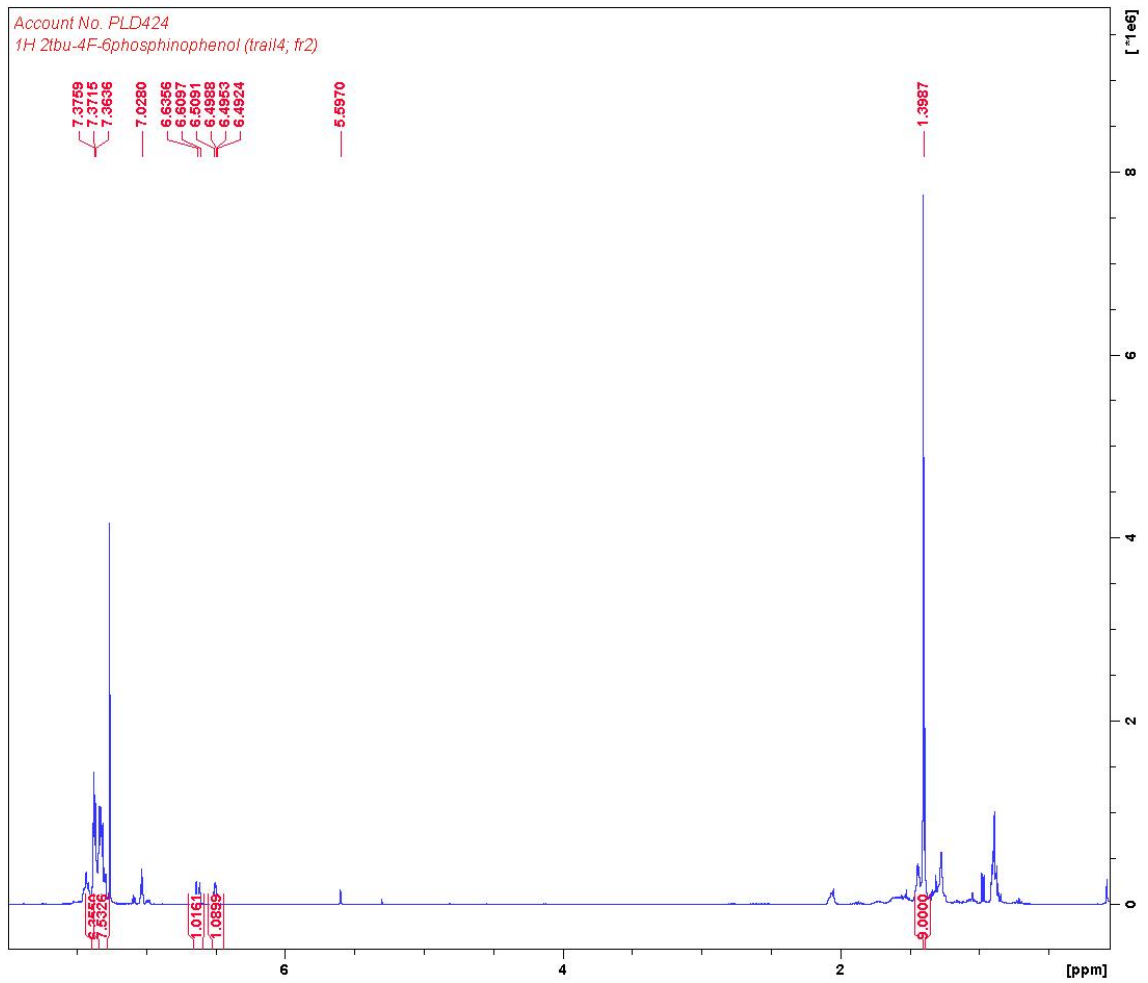
¹H NMR spectrum of 2-bromo-6-(*tert*-butyl)-4-fluorophenol



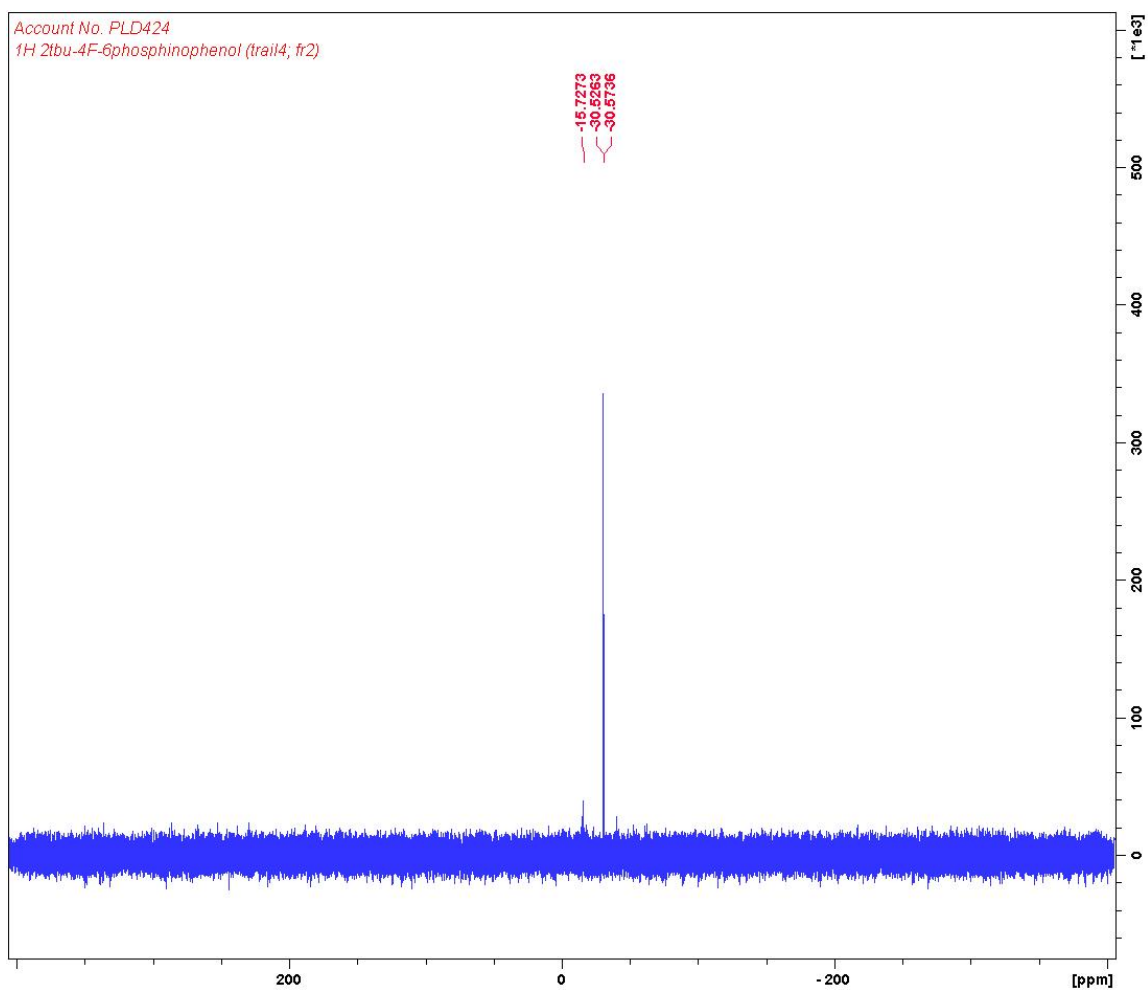
^{31}P NMR spectrum of 2-bromo-6-(*tert*-butyl)-4-fluorophenol



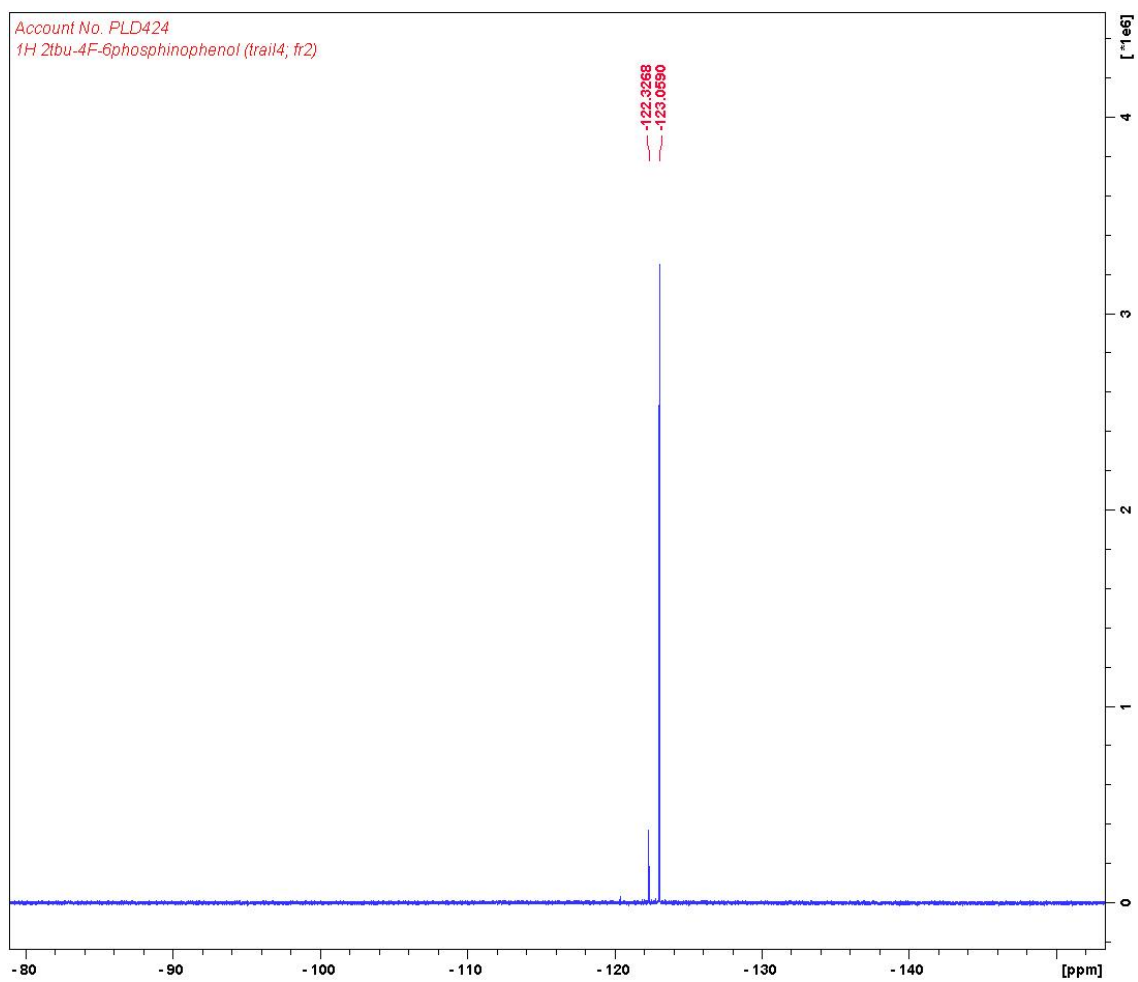
¹H NMR spectrum of 2-diphenylphosphino-4-fluoro-6-*tert*-butylphenol



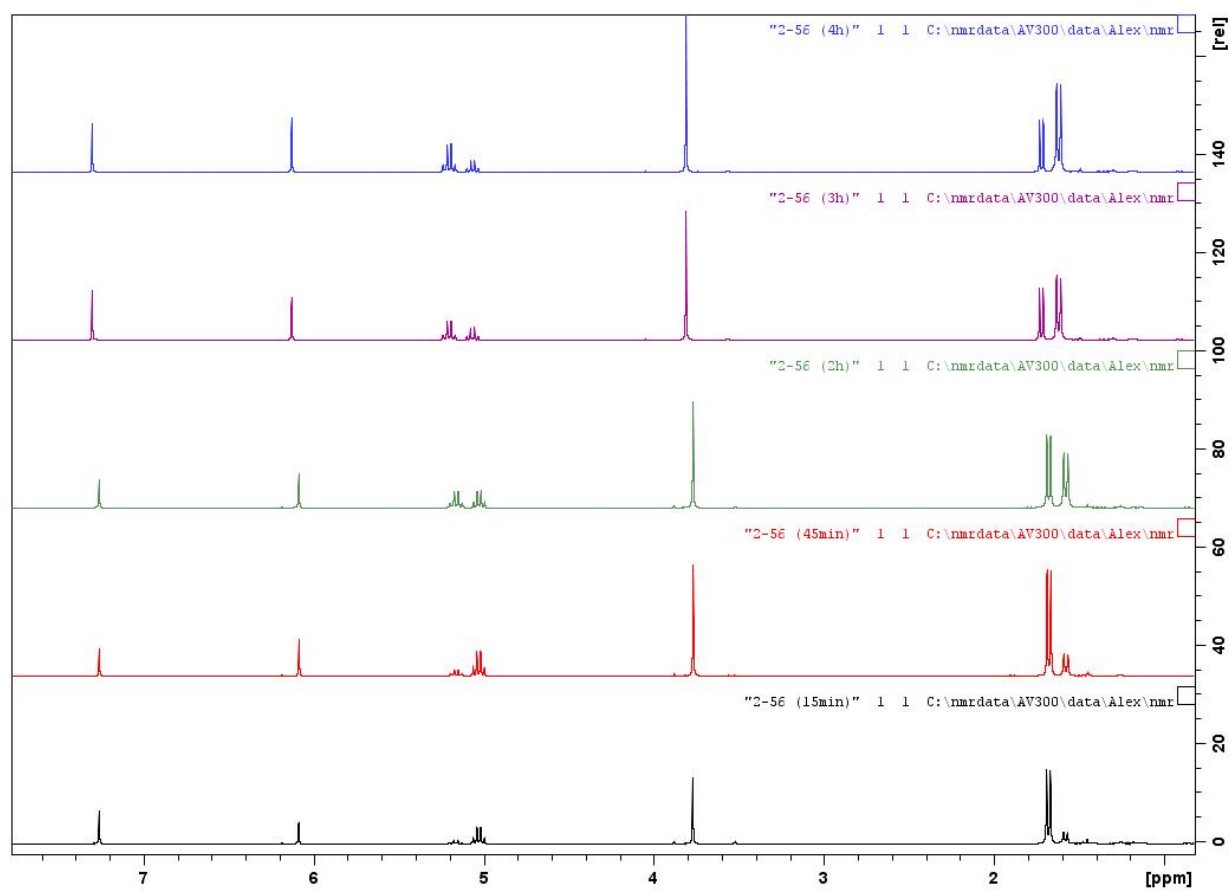
³¹P NMR spectrum of 2-diphenylphosphino-4-fluoro-6-*tert*-butylphenol



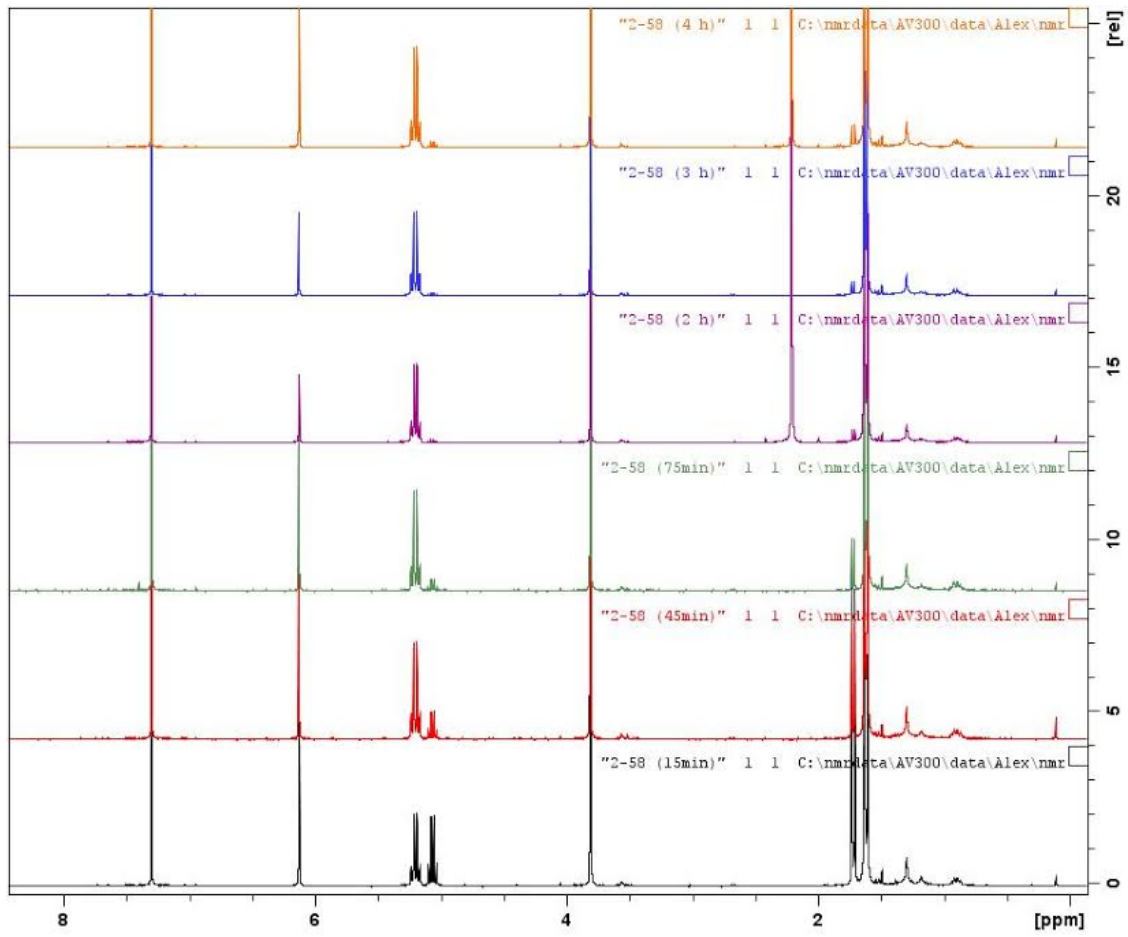
^{19}F NMR spectrum of 2-diphenylphosphino-4-fluoro-6-*tert*-butylphenol



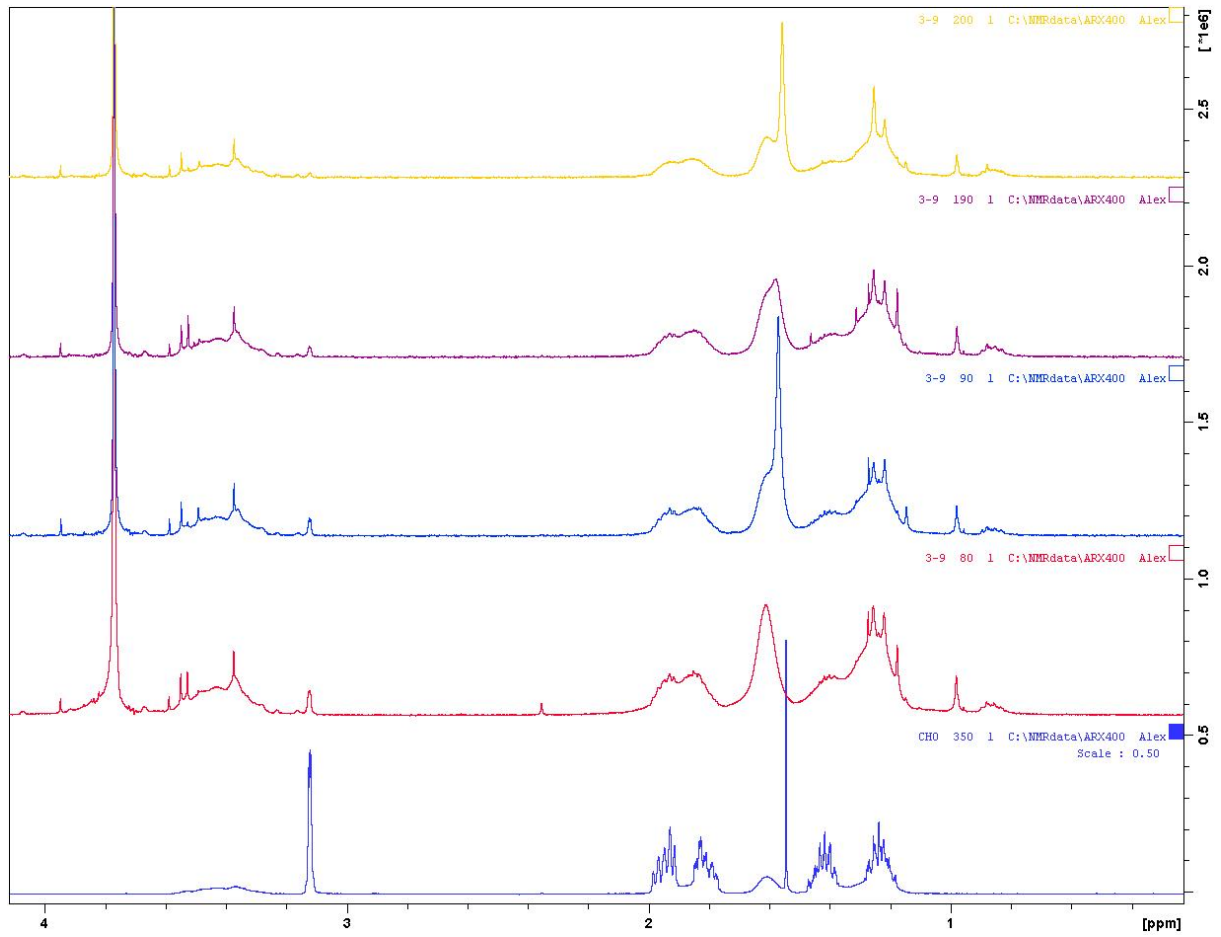
^1H NMR spectrum of Polymerization of LA with **3-YO'BU** in THF



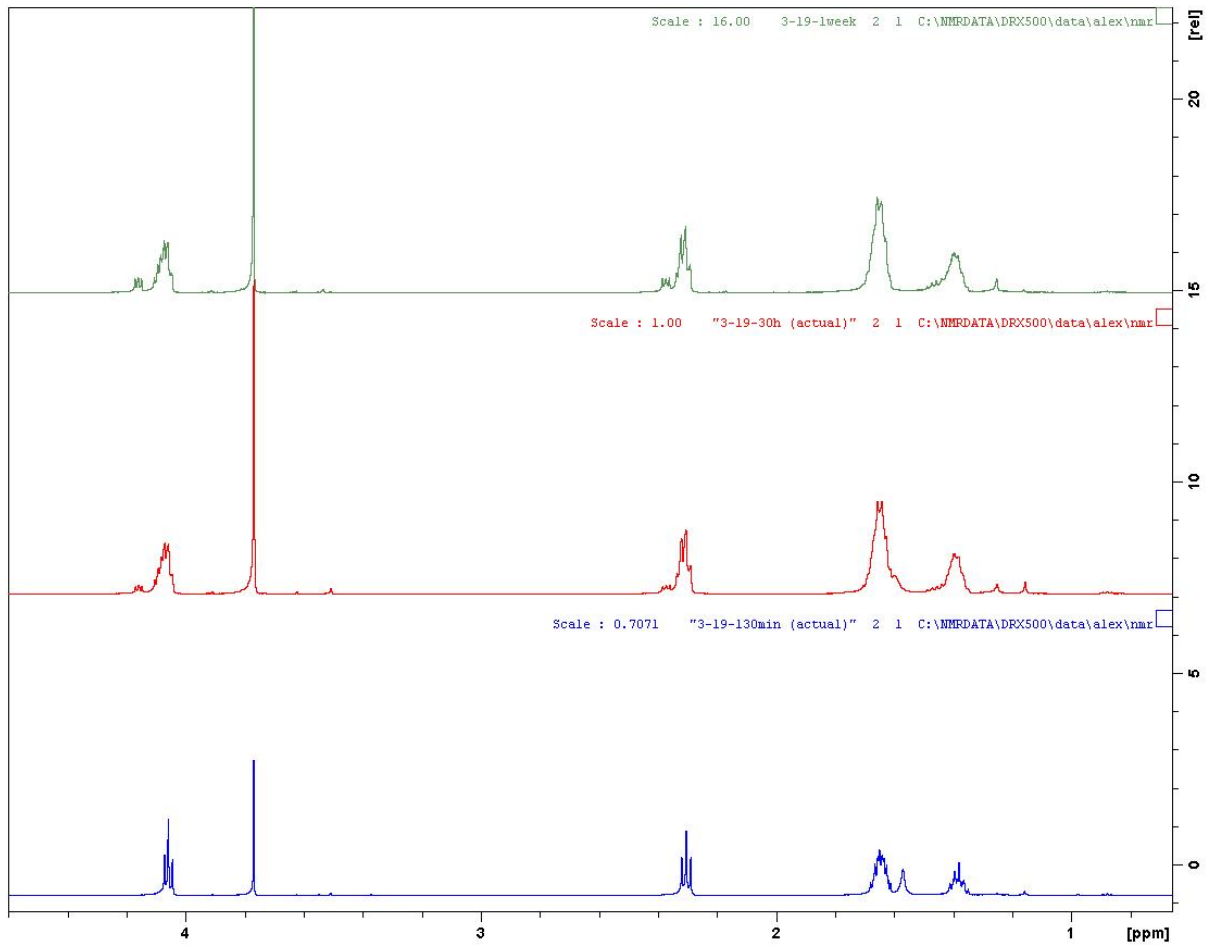
^1H NMR spectrum of Polymerization of LA with **3-YO'BU** in benzene



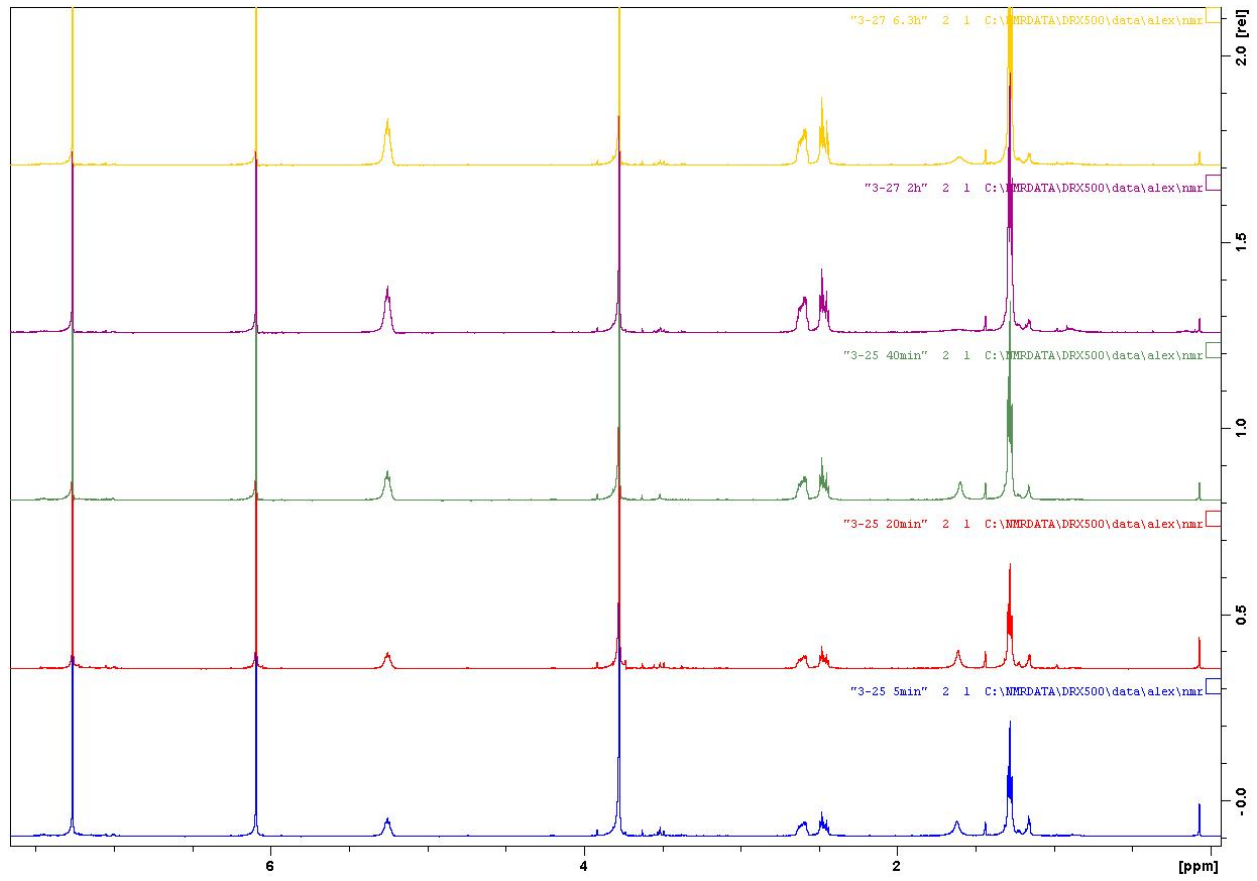
^1H NMR spectrum of Polymerization of CHO with 3-YO'BU in benzene



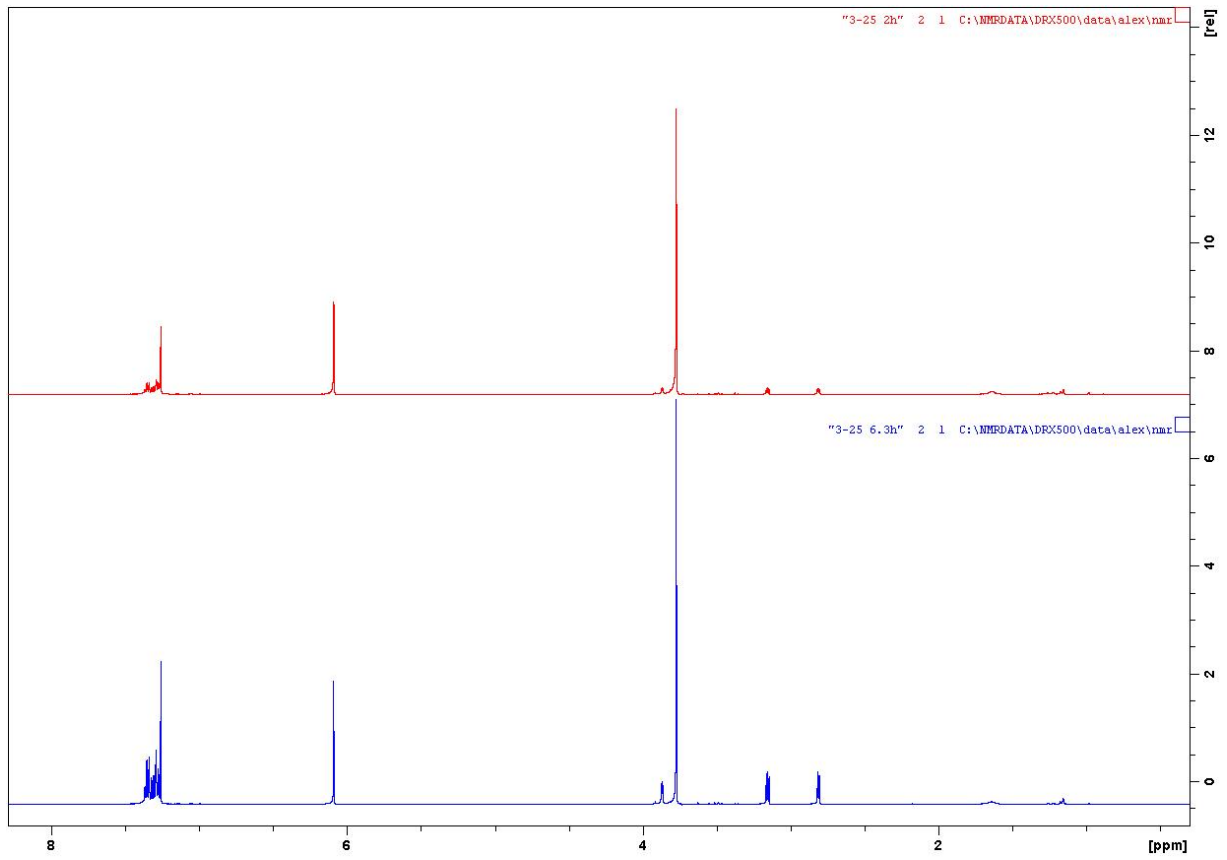
^1H NMR spectrum of Polymerization of CL with **3-YO'BU** in benzene



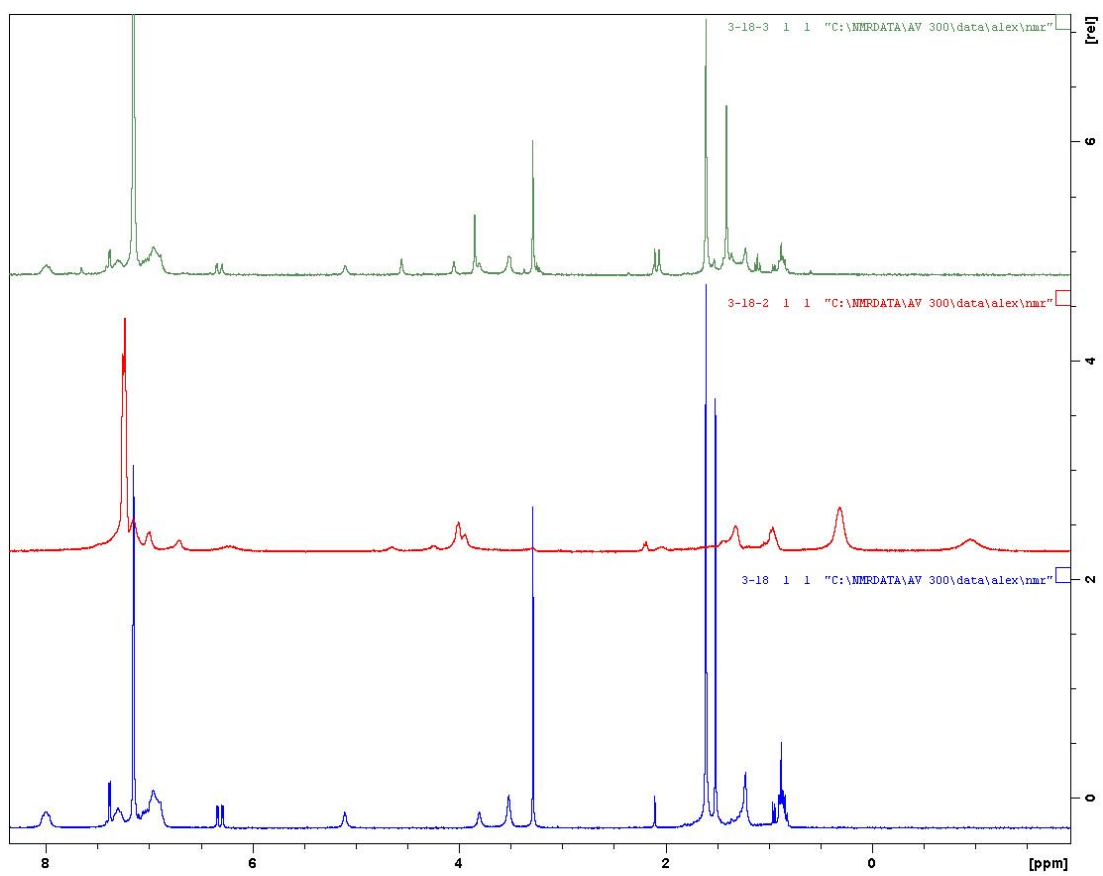
^1H NMR spectrum of Polymerization of BBL with 3-YO'BU in benzene



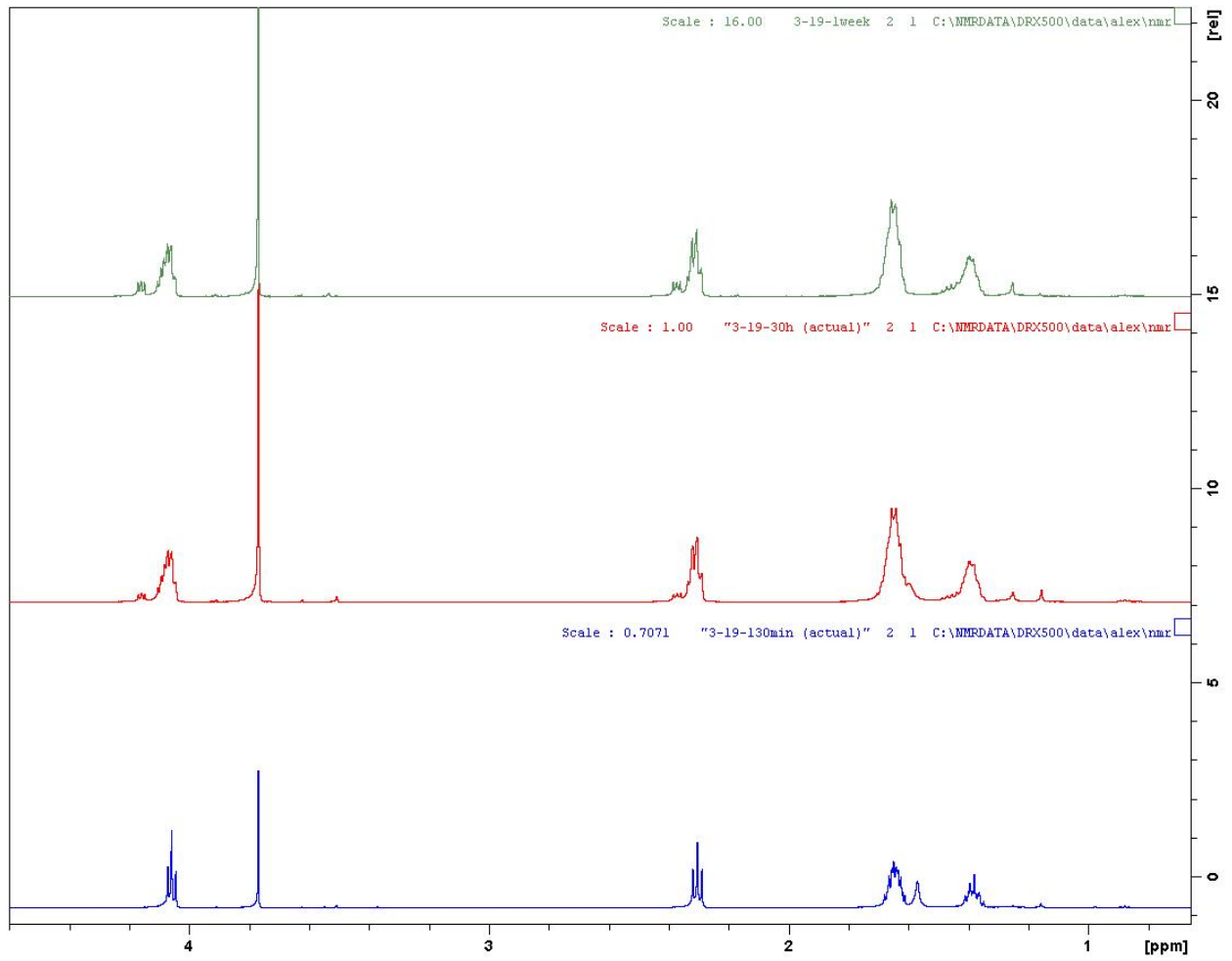
^1H NMR spectrum of Polymerization of SO with **3-YO'BU** in benzene



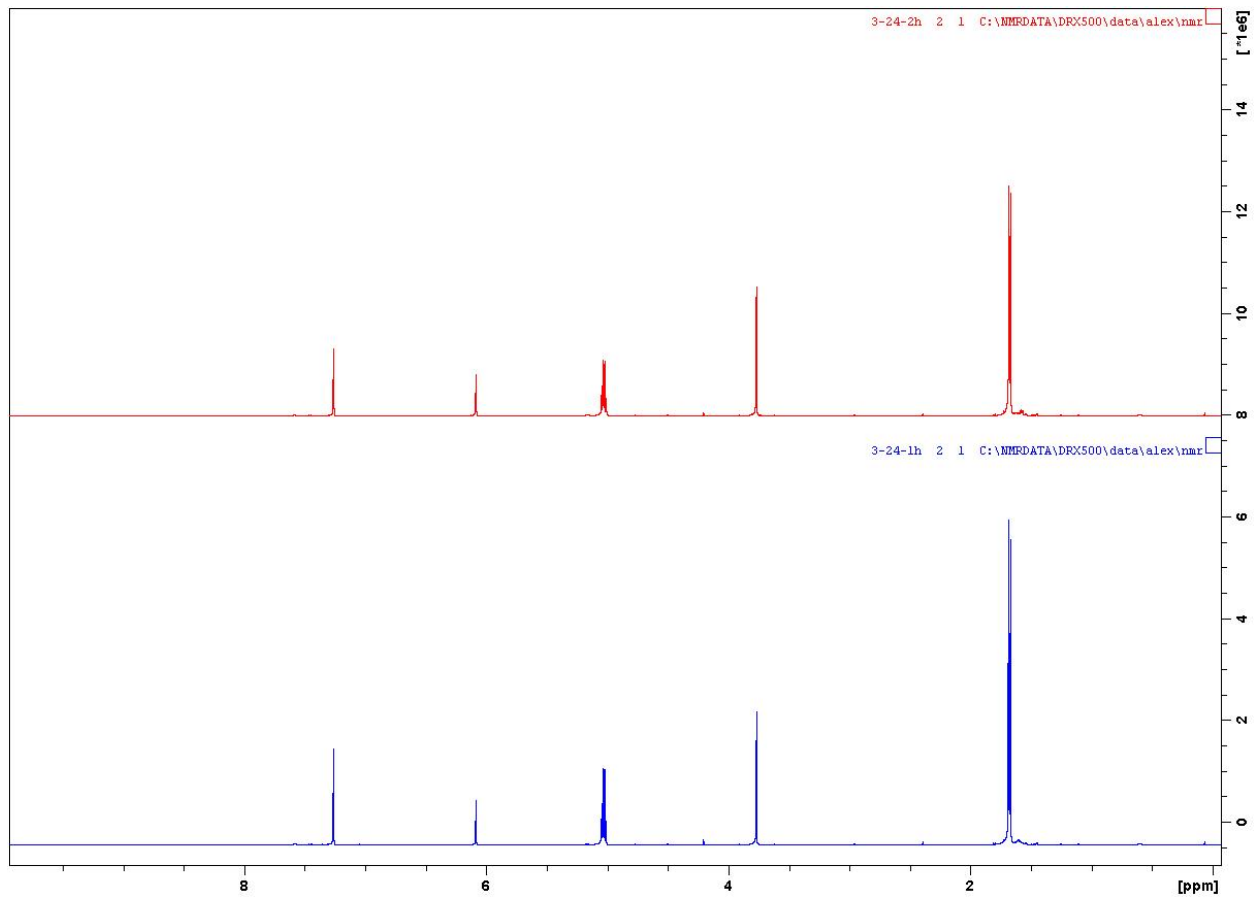
¹H NMR spectrum of Chemical Redox Stability



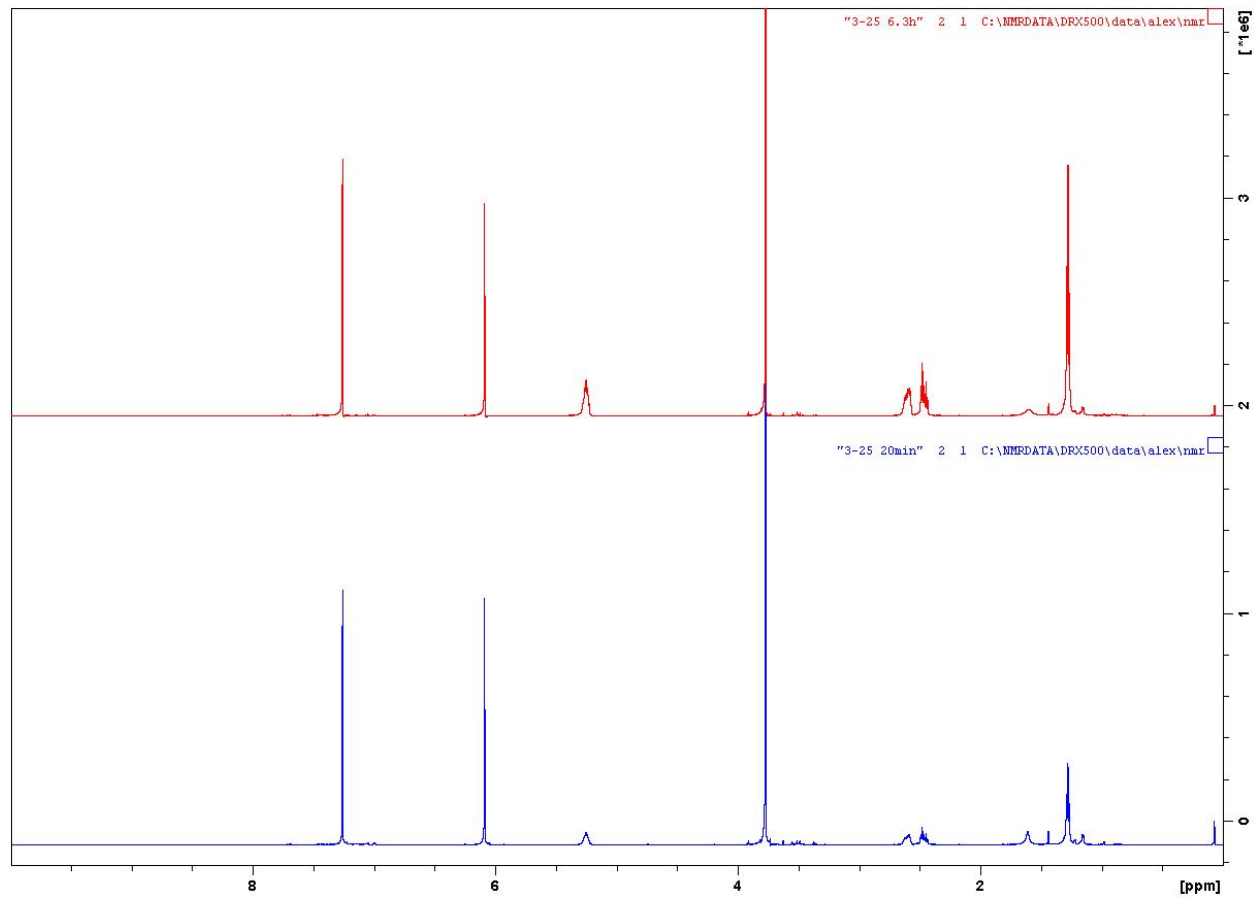
¹H NMR spectrum of Polymerization of CL with **3-YO'BU** in benzene



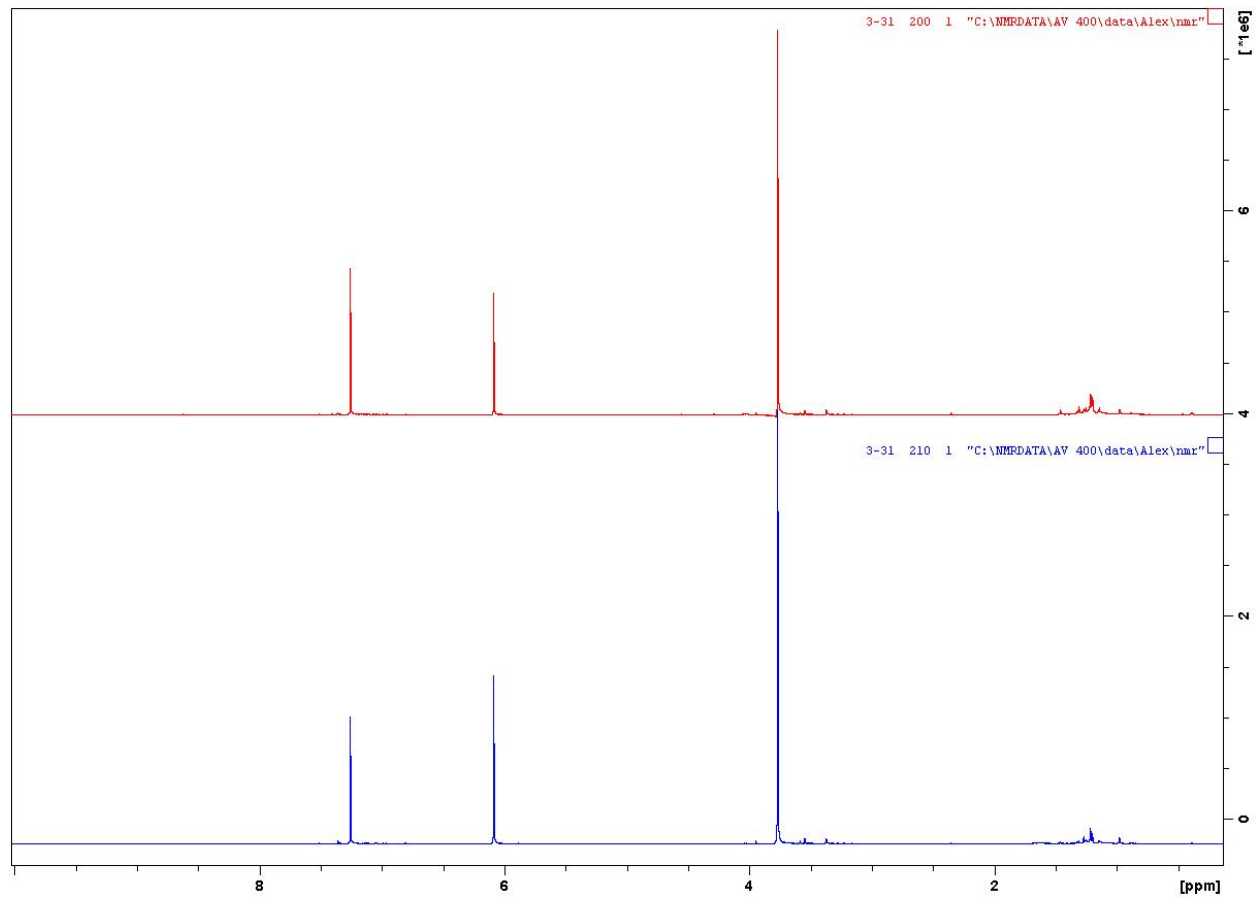
^1H NMR spectrum of Polymerization of LA with [3-YO'BU][BAr^F] in benzene



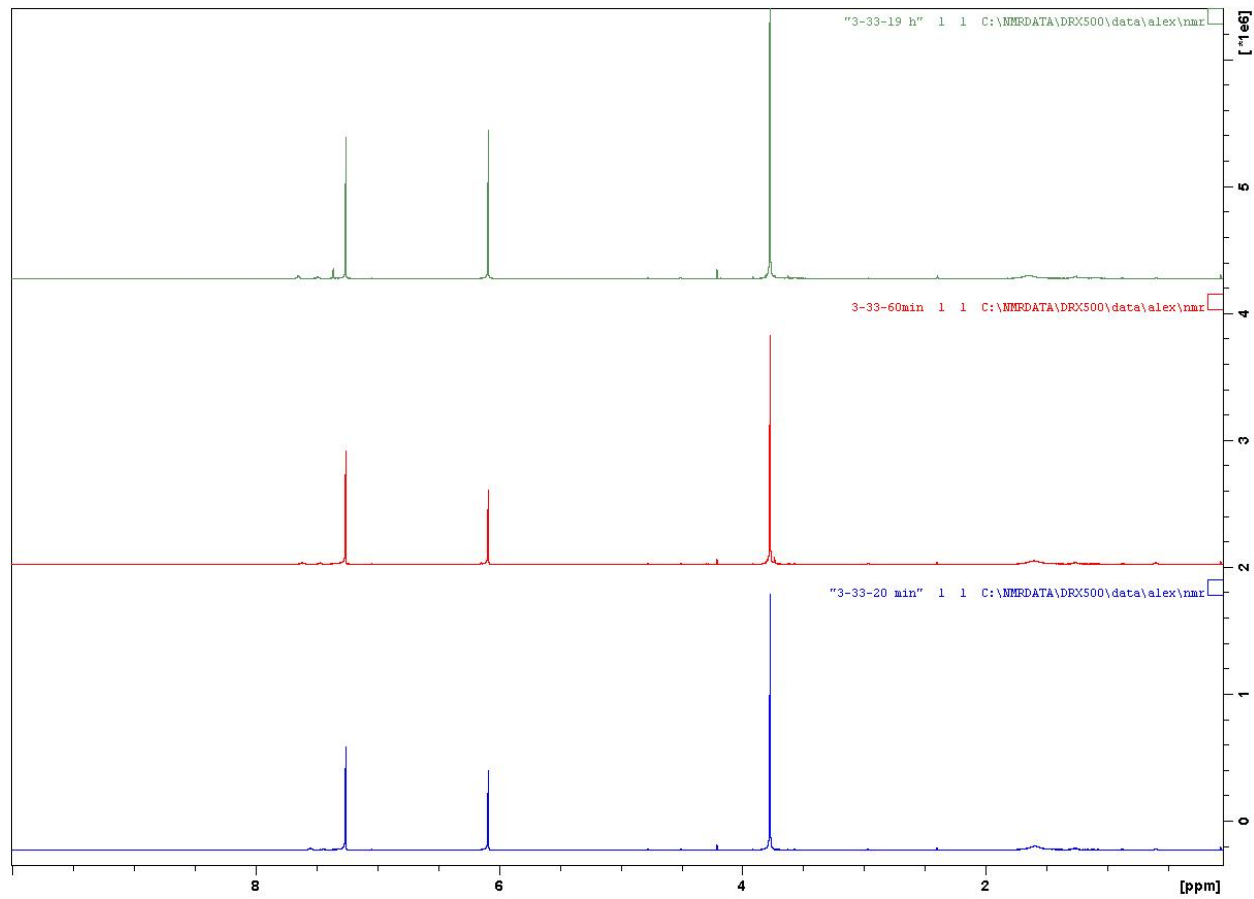
^1H NMR spectrum of Polymerization of BBL with **3-YO'BU** in benzene



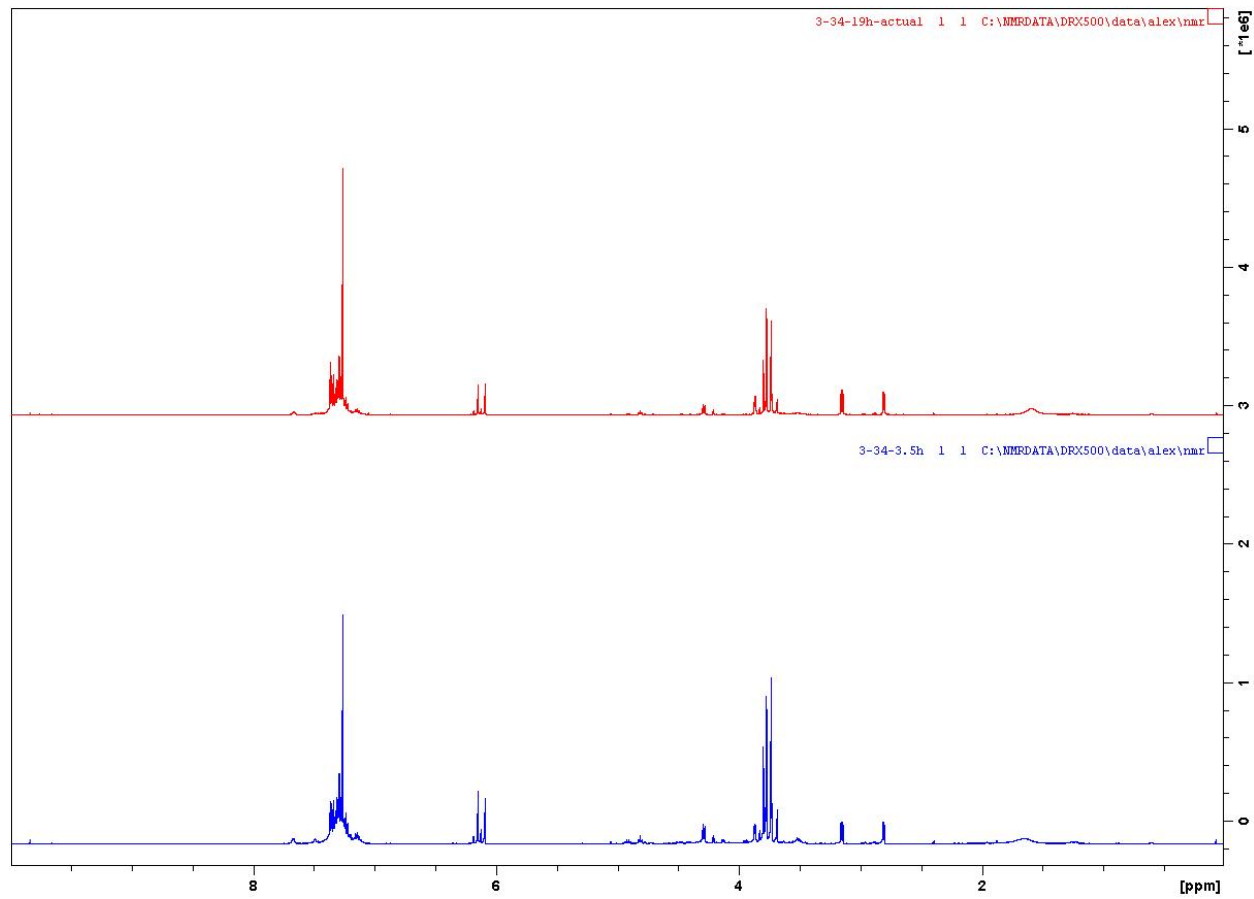
^1H NMR spectrum of Polymerization of PO with **3-YO'BU** in benzene



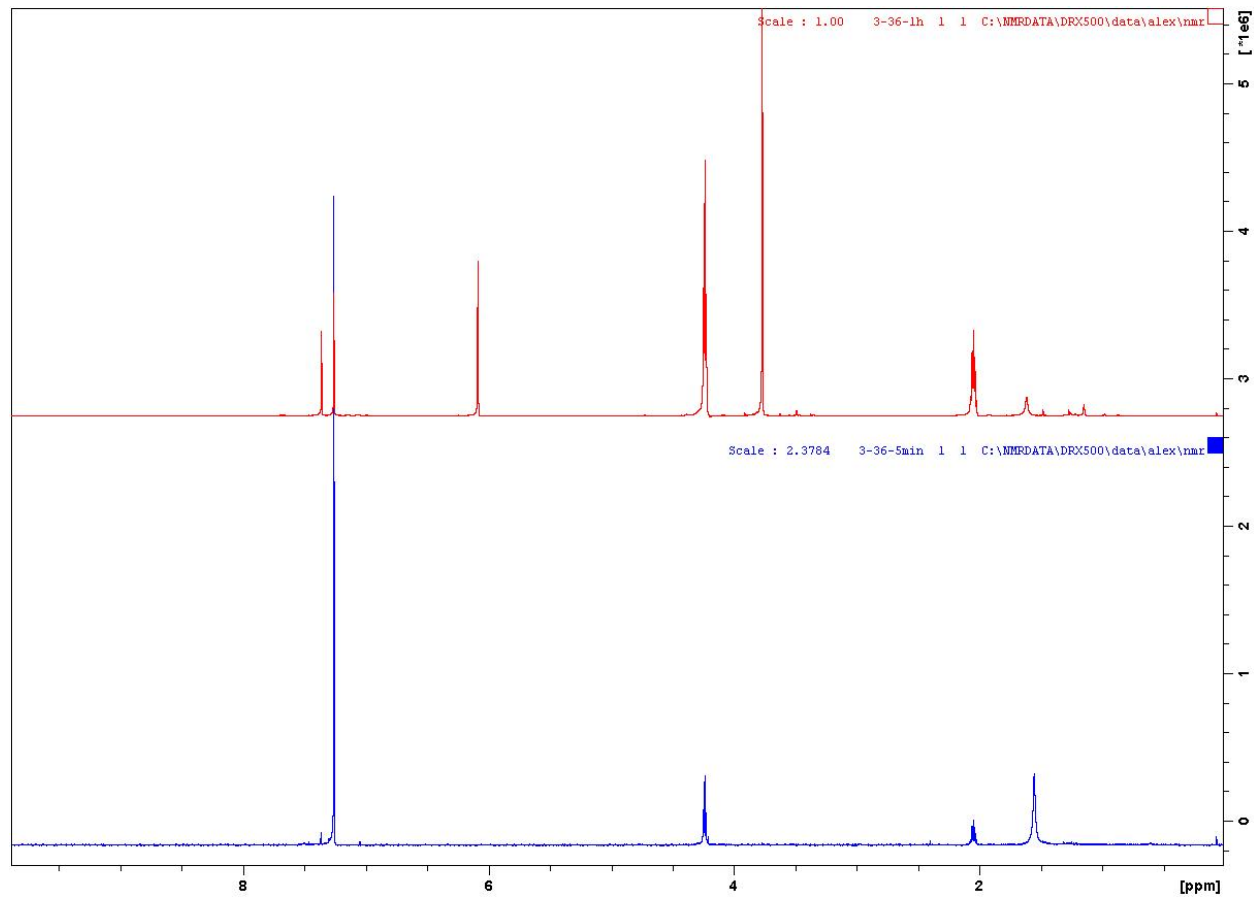
^1H NMR spectrum of Polymerization of PO with [3-YO'BU][BAr^F] in benzene



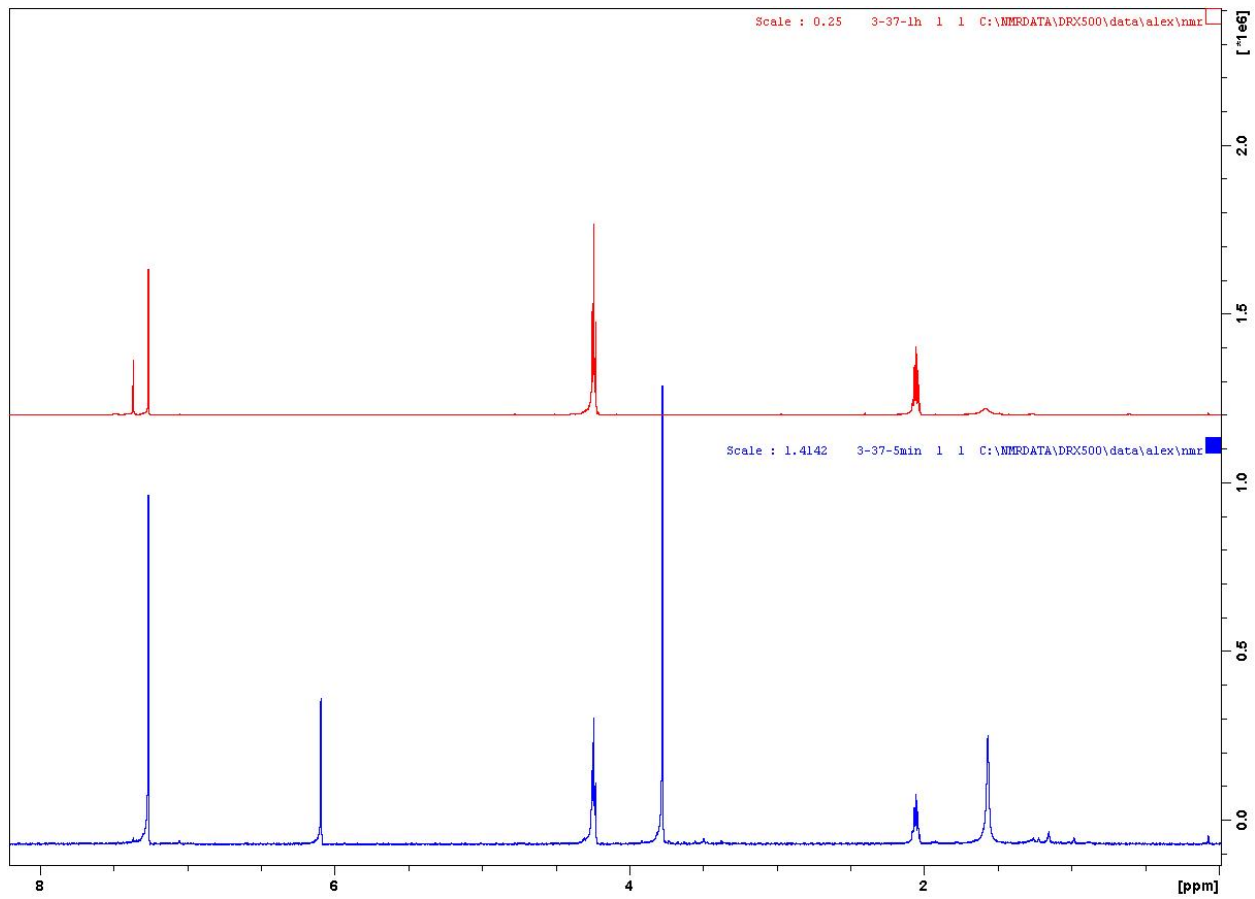
^1H NMR spectrum of Polymerization of SO with [3-YO'BU][BAr^F] in benzene

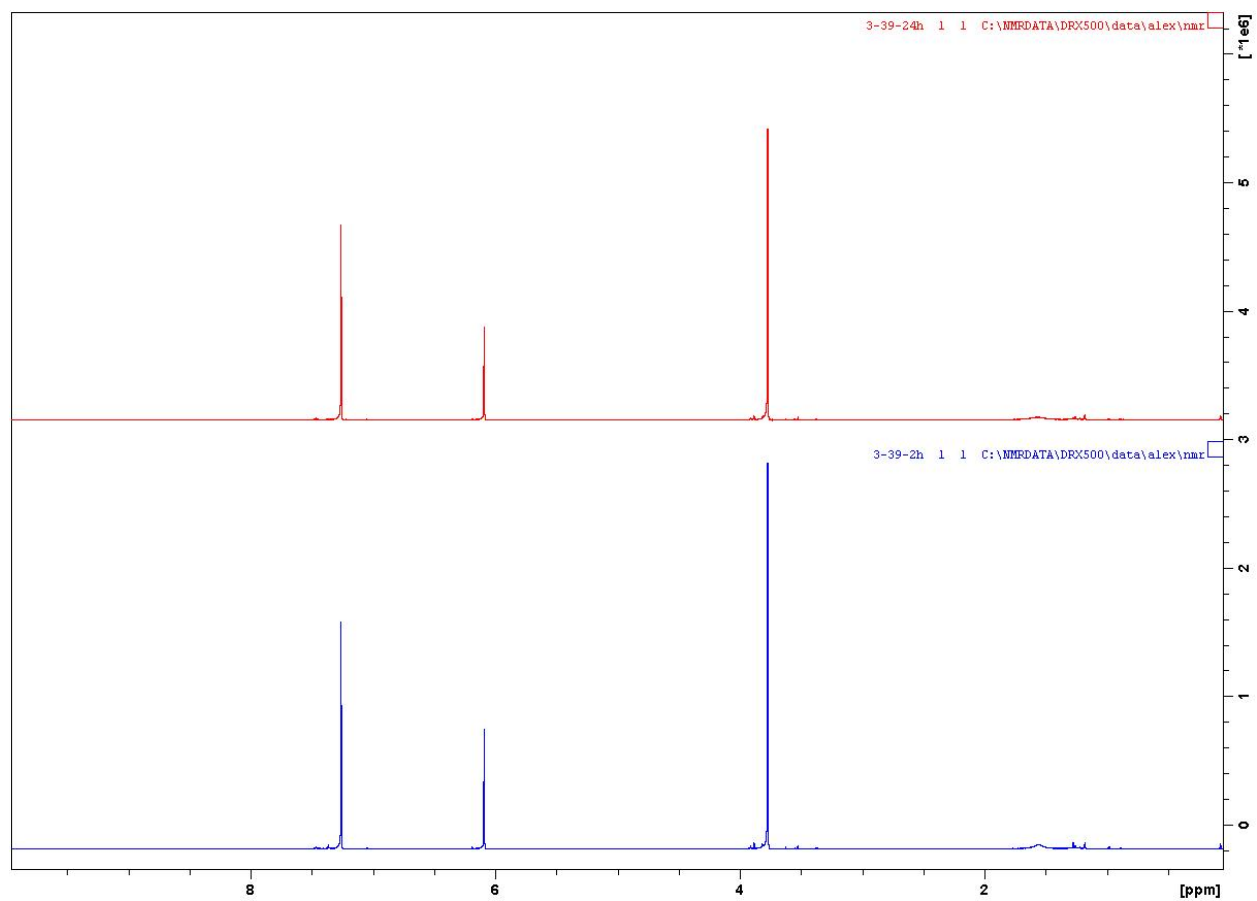


¹H NMR spectrum of Polymerization of TMC with **3-YO'BU** in benzene



¹H NMR spectrum of Polymerization of TMC with [3-YO'BU][BAr^F] in benzene





References

- 1) Ellen MacArthur Foundation. *The New Plastic Economy: Rethinking the Future of Plastic*; Ellen MacArthur Foundation, 2016.
- 2) Gregory, M. R. *Philosophical Transactions of the Royal Society B: Biological Sciences* **2009**, *364*(1526), 2013
- 3) Geyer, R.; Jambeck, J. R.; Law, K. L. *Science Advances* **2017**, *3* (7).
- 4) Industry Agenda The New Plastics Economy <http://www3.weforum.org> (accessed Jun 11, 2018).
- 5) Crawford, C. B.; Quinn, B. *Microplastic pollutants*; Elsevier: Amsterdam, 2017.
- 6) Lebreton, L.; Slat, B.; Ferrari, F.; Sainte-Rose, B.; Aitken, J.; Marthouse, R.; Hajbane, S.; Cunsolo, S.; Schwarz, A.; Levivier, A.; Noble, K.; Debeljak, P.; Maral, H.; Schoeneich-Argent, R.; Brambini, R.; Reisser, J. *Scientific Reports***2018**, *8*(1).
- 7) McConnaughey, B. H.; Zottoli, R. *Introduction to marine biology*; Waveland Press: Prospect Heights, IL, 1989.
- 8) Bouwmeester, H.; Hollman, P. C. H.; Peters, R. J. B. *Environmental Science & Technology***2015**, *49*(15), 8932.
- 9) *Chemistry International -- Newsmagazine for IUPAC* **2012**, *34*(3).
- 10) Tokiwa, Y.; Calabia, B.; Ugwu, C.; Aiba, S. *International Journal of Molecular Sciences***2009**, *10*(9), 3722.
- 11) Chen, G.-Q.; Patel, M. K. *Chemical Reviews***2011**, *112*(4), 2082.
- 12) Maul, J.; Frushour, B. G.; Kontoff, J. R.; Eichenauer, H.; Ott, K.-H. *Ullmanns Encyclopedia of Industrial Chemistry***2000**.

- 13) Qi, X.; Ren, Y.; Wang, X. *International Biodeterioration & Biodegradation***2017**, *117*, 215.
- 14) Zhu, Y.; Romain, C.; Williams, C. K. *Nature***2016**, *540*(7633), 354.
- 15) Carraher, C. E. *Carrahers polymer chemistry*; CRC Press, Taylor & Francis Group: Boca Raton, FL, 2018.
- 16) Mezzasalma, L.; Dove, A. P.; Coulembier, O. *European Polymer Journal***2017**, *95*, 628.
- 17) Fiore, G. L.; Jing, F.; Young, J. V. G.; Cramer, C. J.; Hillmyer, M. A. *Polymer Chemistry***2010**, *1*(6), 870.
- 18) Mehta, R.; Kumar, V.; Bhunia, H.; Upadhyay, S. N. *Journal of Macromolecular Science, Part C: Polymer Reviews***2005**, *45*(4), 325.
- 19) Wanamaker, C. L.; Bluemle, M. J.; Pitet, L. M.; O'Leary, L. E.; Tolman, W. B.; Hillmyer, M. A. *Biomacromolecules***2009**, *10*(10), 2904.
- 20) Martello, M. T.; Hillmyer, M. A. *Macromolecules***2011**, *44*(21), 8537.
- 21) Ruzette, A.-V.; Leibler, L. *Nature Materials***2005**, *4*(1), 19.
- 22) Dechy-Cabaret, O.; Martin-Vaca, B.; Bourissou, D. *ChemInform***2005**, *36*(14).
- 23) Hillmyer, M. *Encyclopedia of Materials: Science and Technology***2001**, 667.
- 24) Teator, A. J.; Lastovickova, D. N.; Bielawski, C. W. *Chemical Reviews***2015**, *116*(4), 1969.
- 25) Gregson, C. K. A.; Gibson, V. C.; Long, N. J.; Marshall, E. L.; Oxford, P. J.; White, A. J. *P. Journal of the American Chemical Society***2006**, *128*(23), 7410.
- 26) Broderick, E. M.; Guo, N.; Vogel, C. S.; Xu, C.; Sutter, J.; Miller, J. T.; Meyer, K.; Mehrkhodavandi, P.; Diaconescu, P. L. *Journal of the American Chemical Society***2011**, *133*(24), 9278.

- 27) Pangborn, A. B.; Giardello, M. A.; Grubbs, R. H.; Rosen, R. K.; Timmers, F.
J. Organometallics **1996**, *15*(5), 1518.
- 28) Lee, J. A.; Williams, B. N.; Ogilby, K. R.; Miller, K. L.; Diaconescu, P. L. *Journal of Organometallic Chemistry* **2011**, *696*(25), 4090.
- 29) Bishop, J. J.; Davison, A.; Katcher, M. L.; Lichtenberg, D. W.; Merrill, R. E.; Smart, J.
C. J. Organomet. Chem. 1971, *27*, 241.
- 30) Shafir, A.; Power, M. P.; Whitener, G. D.; J. Arnold. *Organometallics* **2000**, *19*, 3978–3982.
- 31) Tennyson, A. G.; Khramov, D. M.; Jr., C. D. V.; Creswell, P. T.; Kamplain, J. W.; Lynch, V. M.; Bielawski, C. W. *Organometallics* **2009**, *28*, 5142–5147
- 32) Bakewell, C.; Cao, T.-P.-A.; Long, N.; Goff, X. F. L.; Auffrant, A.; Williams, C.
K. Journal of the American Chemical Society **2012**, *134*(51), 20577.
- 33) Housecroft, C. E. *Inorganic chemistry*; Pearson: Harlow, England, 2018.
- 34) Diccio, A. M.; Longo, J. M.; Rodríguez-Calero, G. G.; Coates, G. W. *Journal of the American Chemical Society* **2016**, *138*(22), 7107.
- 35) Sumerlin, B. S.; Lowe, A. B.; Stroud, P. A.; Zhang, P.; Urban, M. W.; McCormick, C. L. *Langmuir* **2003**, *19*(14), 5559.
- 36) Bakelite First Synthetic Plastic - National Historic Chemical Landmark
<https://www.acs.org/content/acs/en/education/whatischemistry/landmarks/bakelite.html>
(accessed Jun 11, 2018).
- 37) Crabtree, R. H. *The organometallic chemistry of the transition metals*; Wiley: Hoboken, NJ, 2014.
- 38) Platel, R.; Hodgson, L.; Williams, C. *Polymer Reviews* **2008**, *48*(1), 11.

- 39) Tsuji, H.; Ikada, Y. *Biodegradable Polymer Blends and Composites from Renewable Resources* **2009**, 163.
- 40) Buchmeiser, M. R. *Handbook of Ring-Opening Polymerization* 197.
- 41) Allgeier, A. M.; Mirkin, C. A. *Angewandte Chemie International Edition* **1998**, 37(7), 894.
- 42) Koepp, H. M.; Wendt, H.; Strehlow, H. Z. *Electrochem.* **1960**, 64, 483.
- 43) Gritzner, G.; Kuta, J. *Pure Appl. Chem.* **1984**, 56, 461.
- 44) Tong, L.; Liu, X.; Deng, J.; Yang, W. *Polymer Chemistry* **2010**, 1(10), 1633.
- 45) Public Domain
- 46) Alcazar-Roman, L.M.; O'Keefe, B.J.; Hillmyer, M.A.; Tolman, W. B. *Dalton Trans.* 2003, 3082.
- 47) Sattayanon, C.; Sontising, W.; Limwanich, W.; Meepowpan, P.; Punyodom, W.; Kungwan, N. *Structural Chemistry* **2014**, 26(3), 695.